ALMA Mater Studiorum
Università degli studi di Bologna

Scuola di scienze

Corso di Laurea Magistrale in Fisica

Dipartimento di Fisica e Astronomia

Initial Conditions for Cosmological Perturbations in Scalar-Tensor Dark-Energy Models

Tesi di laurea Magistrale

Candidato:
Matteo Braglia

Relatore:
Chiar.mo Prof.
Roberto Balbinot

Co-relatori:
Dott. Fabio Finelli
Dott. Daniela Paoletti

Sessione I

Anno Accademico 2016/2017

Questo lavoro è dedicato a mia nonna, Siria.

Abstract

In questa tesi, studiamo in dettaglio le condizioni iniziali per le perturbazioni cosmologiche in teorie scalari-tensoriali della gravitazione ed il loro impatto sulle anisotropie della radiazione cosmica di fondo a microonde (CMB). Consideriamo due semplici teorie scalari-tensoriali quali quella di gravità indotta (IG, che può essere riformulato come teoria estesa di Jordan-Brans-Dicke con una ridefinizione del campo scalare) e la teoria di campo scalare con accoppiamento non minimale (NMC). Entrambe sono modelli di energia oscura in cui l'accelerazione dell'Universo è connessa alla variazione nel tempo della massa di Planck effettiva. Dopo aver introdotto le idee alla base della teoria delle perturbazioni cosmologiche e delle teorie scalari-tensoriali della gravità, studiamo in dettaglio le equazioni per le perturbazioni alla metrica, alla materia ed al campo scalare, con attenzione particolare al gauge sincrono, nel quale sono scritti i codici Einstein-Boltzmann per le predizioni delle anisotropie della CMB. Usiamo queste equazioni per trovare, oltre alle generalizzazioni dei noti modi di isocurvatura in relatività generale, una nuova soluzione di isocurvatura peculiare dei modelli scalari tensoriali in cui il campo scalare è quasi statico ed il suo potenziale è trascurabile durante l'era relativistica dopo il disaccoppiamento dei neutrini. In questa soluzione, le fluttuazioni del campo scalare si compensano con quelle delle componenti relativistiche. Questa è una nuova soluzione regolare e valida nel regime di grandi lunghezze d'onda per le due classi di teorie scalari tensoriali considerate in questa tesi. Mostriamo poi la differente evoluzione delle fluttuazioni cosmologiche per le condizioni iniziali di isocurvatura in queste due teorie

scalari-tensoriali, rispetto al modo adiabatico standard con particolare enfasi per il nuovo modo originale. Studiamo quindi le implicazioni cosmologiche di differenti condizioni iniziali derivando lo spettro angolare della CMB per le nuove soluzioni nel contesto del modello di IG, mediante una estensione del codice pubblico Einstein-Boltzmann CLASS, realizzata appositamente per questo modello. In particolare lo spettro di potenza della CMB è stato calcolato separatamente per condizioni iniziali adiabatiche e di isocurvatura, ovvero per modi totalmente non correlati, e per correlazioni arbitrarie. Esattamente come per gli usuali modi di isocurvatura, anche il nuovo modo non può essere da solo responsabile della formazione delle strutture osservate, ma può essere una componente non trascurabile. Inoltre, sottolineamo il suo potenziale interesse mostrando come la correlazione tra quest'ultimo e il modo adiabatico possa portare ad una diminuzione dell'ampiezza dello spettro della CMB a bassi multipoli, come le osservazioni di WMAP e Planck sembrano indicare.

Concludiamo mostrando come precedenti studi confermino la presenza di perturbazioni di isocurvatura in modelli inflazionari a due campi collegati alla cosmologia che abbiamo studiato in questa tesi.

Contents

Introduction

The current cosmic concordance model is the ΛCDM model which gives a satisfactory explanation of the observed accelerated expansion of the Universe. This model is formulated within the the framework of Einstein General Relativity with dark energy in the form of a cosmological constant.

However this model alone cannot solve some important results of observations as the spatial flatness and the high level of isotropy of the cosmic microwave background (CMB). In order to solve these problems, it is usually assumed that the Universe undergoes a period of accelerated expansion in the early stage of its evolution, called inflation. In the simplest model of inflation this acceleration is driven by a scalar field, called inflaton, slowly rolling toward the minimum of its potential. The quantum fluctuations of the inflaton produced during inflation seed the inhomogeneities in the matter density that then may grow by gravitational instability and eventually form the large structures observed today. Such a simple model can produce an adiabatic spectrum of quantum fluctuations, which is in great agreement with the observations.

However, inflation models with many scalar fields can produce isocurvature fluctuations in addition to the adiabatic ones. The imprints on the CMB angular power spectrum of these fluctuations are very different from the adiabatic ones and they show how isocurvatures alone cannot explain the structure formation. However, a detection of the presence of isocuvature perturbations could be crucial in order to discriminate between different models of inflation. In fact, instead of considering only adiabatic or isocurvature

fluctuations, we can study a mixture of the two and how they correlate, together with and the effects of the correlations.

This thesis is devoted to study these issues in the framework of scalar-tensor theories. These theories offer an alternative to the ΛCDM model in order to explain the nature of the dark energy. The gravitational sector is changed adding a scalar field non-minimally coupled to the Ricci scalar which leads the acceleration of the Universe that we observe today through a non-zero potential. We consider in this thesis the simplest scalar-tensor model, called Induced Gravity, in which the coupling to the Ricci scalar is in the form $F(\varphi) = \gamma\varphi^2$, but our results are not specific of this model and can be extended to more general models.

The work is structured as follows:

1. In chapter 1 we briefly review some of the basic concepts of the cosmic concordance model and inflation. We then discuss the model of a time-varying dark energy called quintessence.

2. In chapter 2 we review the relativistic theory of cosmological perturbations and CMB anisotropies which we will use in the following chapters in order to find the solutions of the perturbed equations for IG which we will use as initial conditions for the cosmological perturbations.

3. In chapter 3 we give a detailed review on isocurvature perturbations in Einstein GR in order to compare the well known results in the literature, with our results in the framework of the IG theory. In particular we examine how correlated adiabatic and isocurvature perturbations in quintessence model can solve the issue of the lack of power in the low multipoles region in the CMB angular power spectrum. Finally, we show how isocurvature perturbations are produced in multi-field inflation models.

4. In chapter 4 we present the scalar-tensor model of IG and show how it can explain the acceleration of the Universe. We give the background

evolution of the scalar field and the perturbed equations in the synchronous gauge.

5. In chapter 5 we discuss our results. We first give the initial conditions for the cosmological perturbations in IG and see how the scalar field leads to a new original and regular isocurvature mode. We then compute the CMB angular power spectrum and show how the correlation between the new mode, or the generalization of the well known CDM isocurvature to IG, and the adiabatic mode lead to an interesting explanation of the lack of power in the low multipoles of the CMB angular power spectrum. In the last section, we show how a simple model of double inflation with two scalar field can produce isocurvature perturbations.

6. In the Appendix we give the generalization of these initial conditions to the Non-Minimally Coupled model where the coupling is $F(\varphi) = N_{\rm pl}^2 + \xi\varphi^2$ and the relative differences between the CMB power spectrum computed in chapter 5 and the original ones of the ΛCDM model.

Throughout this work, we consider natural units in which $\hbar = c = k_B = 1$ and we assume the metric signature $(-, +, +, +)$. When we consider tensors, we use Greek letters for space-time indices ($\mu = 0, \ldots, 3$), whereas we use Latin letters for spatial indices ($i = 1, \ldots, 3$).

Chapter 1

The Standard Big-Bang Cosmological Model

The aim of modern cosmology is to understand the origin and the evolution of our Universe. The formulation of the theory of general relativity at the begining of the last century, in 1916, enabled scientists to come up with a testable and mathematically rigorous theory of gravitation which led to a mathematical description of the Universe. In fact just a few years later Friedmann [1], in 1922, and independently Lemaitre [2], in 1927, derived the solution for the GR equations assuming isotropy and homogeneity, finding the Friedmann-Lemaitre-Robertson-Walker (FLRW) metric which describes the spacetime structure of the Universe; remarkably, nowadays we are still using their results. In 1930 Hubble [3] discovered that galaxies are receeding from us with a velocity proportional to the distance from the observer. That was the first evidence that the Universe is expanding. Much later, in 1998, it was understood that the Universe expansion is accelerating, thanks to the observations of distant type Ia supernovae [4]. What causes this accelerated expansion is still unknown and one possbility is that the acceleration is driven by an additional component of the Universe called dark energy.

Since the pioneering works of Friedmann and Lemaitre a huge effort has been done in the field of cosmology. What is called the standard Big-Bang

model is based on three assumptions:

- the laws of GR in describing the expansion of the Universe;
- the cosmological principle, i.e. the Universe is homogeneous and isotropic;
- the content of the Universe is modelled as a perfect fluid.

The standard Big-Bang cosmological model successfully explains the expansion of the Universe, the abundance of light elements from the primordial nucleosynthesis and the thermal nature of the relic blackbody radiation permeating the Universe, the cosmic microwave background (CMB), though it does not explain by itself the Universe acceleration, data on galaxy rotation suggesting the existence of a kind of matter that interacts only via gravitational attraction, for this reason it is usually called dark matter. The model which considers the existence of cold dark matter and dark energy in the form of a cosmological constant driving the acceleration of the Universe is called ΛCDM model and it is today the cosmic concordance model. However, in order to resolve some problems that we will see in this chapter, this model needs to be supplemented with an early stage of acceleratad expansion, called inflation.

1.1 General Relativity

Since its dawn, general relativity has became the best theory to describe gravitational interactions. The idea behind general relativity is very simple: the total matter* content of the Universe determines its geometry and, viceversa, the geometry determines the dynamic of the matter. In this framework, in contrast with the Newtonian concept of gravity as an external force acting on particles, we think of them moving freely in the curved spacetime.

An event is just a point of the 4-dimensional spacetime manifold and, once chosen a coordinate system, it can be described by its coordinates $x^\mu =$

*By *matter*, here, we mean any possible energy source in the Universe.

$(x^0, x^1x^2, x^3) = (t, x, y, z)$. In this framework all the information of interest are encoded in the 2-rank symmetric tensor $g_{\mu\nu}(x)$ called the metric tensor, that can be used to define distances and lengths of vectors on the manifold. If we consider two events x^μ and $x^\mu + dx^\mu$, with dx^μ being infinitesimal, then the spacetime interval

$$ds^2 = g_{\mu\nu}(x)dx^\mu dx^\nu \tag{1.1}$$

gives the squared distance between the two events.

As already mentioned, the effect of gravity are all described by the metric and test particles in general relativity move freely. In a flat spacetime a test particle, without forces acting on it, moves on a straight line, namely on the geodesics of the flat spacetime. Geodesics are the trajectories extremizing the particle's action using the variational principle; what we have to do is then just vary the action of the particle in curved spacetime and find the paths that make this variation vanish. This lead to the geodesic equations [5] for the path $x^\mu(\lambda)$

$$\frac{d^2x^\mu}{d\lambda^2} + \Gamma^\mu_{\rho\sigma}\frac{dx^\rho}{d\lambda}\frac{dx^\sigma}{d\lambda} = 0, \tag{1.2}$$

where we have introduced the Christoffel symbols:

$$\Gamma^\sigma_{\mu\nu} = \frac{1}{2}g^{\sigma\rho}\left(\frac{\partial g_{\nu\rho}}{\partial x^\mu} + \frac{\partial g_{\mu\rho}}{\partial x^\nu} - \frac{\partial g_{\mu\nu}}{\partial x^\rho}\right) \tag{1.3}$$

and λ is a monotonically increasing parameter to describe the particle's path. We can put this equation in an useful form introducing the energy-momentum vector:

$$P^\mu = (E, \vec{P}), \tag{1.4}$$

the advantage of this choice is that we can implicitly define the parameter λ as

$$P^\mu = \frac{dx^\mu}{d\lambda} \tag{1.5}$$

and the geodesic equation (1.2) then becomes

$$\frac{dP^\mu}{d\lambda} + \Gamma^\mu_{\rho\sigma}P^\mu P^\nu = 0. \tag{1.6}$$

The relationship between the metric and the matter content of the Universe is described by the Einstein field equations

$$G_{\mu\nu} \equiv R_{\mu\nu} - \frac{1}{2} g_{\mu\nu} R = 8\pi G T_{\mu\nu}. \tag{1.7}$$

This set of equations relate the total energy-momentum tensor describing the constituents of the Universe, on the right hand side, to the geometry of the Universe on the left hand side; the latter is encoded in the Ricci tensor and in its contraction, the Ricci scalar. They can conveniently be expressed in terms of the Christoffel symbols as

$$R_{\mu\nu} \equiv R^{\alpha}_{\mu\alpha\nu} = \Gamma^{\alpha}_{\mu\nu,\alpha} - \Gamma^{\alpha}_{\mu\alpha,\nu} + \Gamma^{\alpha}_{\beta\alpha}\Gamma^{\beta}_{\mu\nu} - \Gamma^{\alpha}_{\beta\nu}\Gamma^{\beta}_{\mu\alpha}. \tag{1.8}$$

An important consequence of the form of $R_{\mu\nu}$ is that the Einstein tensor $G_{\mu\nu}$ satisfies a set of equations called contracted Bianchi identities

$$\nabla_{\nu} G^{\mu\nu} = 0, \tag{1.9}$$

where the covariant derivative has been introduced. Applying Eq.(1.9) to the Einstein equations (1.7) leads to the conservation law of the total energy-momentum tensor

$$\nabla_{\nu} T^{\mu\nu} = 0. \tag{1.10}$$

1.1.1 The Principle of Minimal Gravitational Coupling and the Einstein Lagrangian

We shall now describe in details the principle of minimal gravitational coupling [6] or, sometimes, comma to semicolon rule [7]. The importance of this principle relies on its simplicity: if we know how a system is described in special relativity with equations written in tensorial form, all we have to do is just make the replacements

$$\eta_{\mu\nu} \to g_{\mu\nu} \tag{1.11}$$

$$\partial_{\mu} \to \nabla_{\mu} \tag{1.12}$$

and the equations obtained characterize the same system with the presence of a gravitational field. Therefore, if matter in Minkowski space has an action

$$S = \int d^4x \, \mathcal{L}_{\text{matter}}, \tag{1.13}$$

then, in curved spacetime, it just becomes:

$$S = \int d^4x \sqrt{-g} \, [\frac{R}{16\pi G} + \mathcal{L}_{\text{matter}}], \tag{1.14}$$

in which the first term on the right hand side is the Einstein gravity lagrangian and matter is minimally coupled to gravity, that is the coupling to gravity is all containend in the invariant volume element $d^4x\sqrt{-g}$, where $g = det[g_{\mu\nu}]$. As we will see the situation is completely different in scalar-tensor theories of gravitation, in which the matter has different couplings to gravity which will lead to a different form of the field equations.

1.2 The Friedmann-Robertson-Walker Metric

In principle, in order to determine the metric of the Universe, we must solve Eq.(1.7). However if we assume particular symmetries of the system they can strongly constrain the form of the metric and we can get much information without referring to the general Einstein equation.

1.2.1 Maximally Symmetric Spaces

A metric is said to be form-invariant if its functional form does not change after a transformation $x \to \tilde{x}$, that is

$$\tilde{g}_{\mu\nu}(x) = g_{\mu\nu}(x) \quad \text{for all } x. \tag{1.15}$$

Any transformation $x \to \tilde{x}$ that satisfies this equation is called an isometry and, if we restrict to the special case of an infinitesimal one

$$x'^{\mu} = x^{\mu} + \epsilon\xi^{\mu} \quad \text{with } \epsilon \ll 1, \tag{1.16}$$

we get the Killing equation

$$\xi_{\mu;\nu} + \xi_{\nu;\mu} = 0. \tag{1.17}$$

Any 4-vector satisfying Eq.(1.17) is called a Killing vector of the metric $g_{\mu\nu}(x)$. An N-dimensional space can have at most $N(N+1)/2$ Killing vectors. In particular if it has exactly $N(N+1)/2$ of them it said to be a maximally symmetric space. A maximally symmetric space in 3 or more dimensions has the important feature that its Ricci tensor is constant. It is then useful to introduce the curvature constant K as:

$$R = -N(N-1)K, \tag{1.18}$$

because in this way the space is uniquely determined by K and by the number of positive or negative eigenvalues of the metric [5]. It remains just to give two more definitions that are essential to derive the metric of the Universe: the defintion of isotropy and homogeneity.

A space is said to be homogeneus if there exist infinitesimal isometries that carry any given point X into any other point near it and it is said to be isotropic about a given point X if there exist infinitesimal isometries that leave X fixed. It can be proved that an isotropic space about every point is homogeneus and also maximally symmetric.

1.2.2 The Metric of the Universe

The cosmological principle mentioned at the beginning of this chapter assumes isotropy and homogeneity for our Universe. This assumption means that the Universe is spatially isotropic and homogeneus, so it can be described as a spacetime in which the hypersurfaces of constant time are maximally symmetric. The Universe can be described as a 4-dimensional spacetime with a maximally symmetric 3-dimensional subspace, then its metric can be written with the general form [5, 8, 9, 10]:

$$ds^2 = -dt^2 + a^2(t)\gamma_{ij}dx^i dx^j \tag{1.19}$$

where the spatial metric γ_{ij} given by

$$\gamma_{ij} = \delta_{ij} + k\frac{x_i x_j}{1 - k(x_k x^k)}, \tag{1.20}$$

and $k = -1, 0, +1$ for an hyperbolic, flat or spherical Universe respectively. Hereafter we will consider only the case $k = 0$ to simplify the calculation, but this restriction is also justified by the present day measurements of CMB [11] that are compatible with a nearly flat geomtery.

The metric (1.19) is the famous Friedmann-lemaitre-Robertson-Walker (FLRW) metric and we write it in spherical coordinates:

$$ds^2 = -dt^2 + a^2(t)(dr^2 + r^2 d\Omega^2). \tag{1.21}$$

This metric has a rescaling symmetry that can be used to put the scale factor $a(t)$ in units such that it is equal to unity today, i.e. $a(t_0) \equiv a_0 = 1$. The differential dr is the infinitesimal comoving distance, but to get the physical one we must multiply it to the scale factor $a(t)$, that describes the expansion of the Universe.

We can write the FLRW metric in one more way introducing the conformal time $d\tau = dt/a(t)$ so that (1.21) becomes

$$ds^2 = a^2(t)(-d\tau^2 + dr^2 + r^2 d\Omega^2). \tag{1.22}$$

1.2.3 Energy-Momentum Tensor

The fact that the Universe can be described by a 4-dimensional spacetime whose metric is form-invariant under spatial isometries helps us to find the form of its energy-momentum tensor $T^{\mu\nu}$ (that is required to be form-invariant too for the cosmological principle).Since these isometries are purely spatial, they transform T^{00} as a 3-scalar, T^{0i} as a 3-vector and T^{ij} as a 3-tensor. Isotropy and homogeneity imply that T^{0i} has to vanish and T^{ij} has to be proportional to the 3-metric g_{ij}. These results mean that the form of $T^{\mu\nu}$ has to be necessarily the same as a perfect fluid, in order to satisfy the cosmological principle:

$$T^{\mu\nu} = Pg^{\mu\nu} + (\rho + P)U^\mu U^\nu, \tag{1.23}$$

where $U^\mu = dx^\mu/\sqrt{-ds^2}$ is the 4-velocity vector, P is the total pressure and ρ the total density of the fluid.

1.3 Redshift and Hubble Law

The wavelength of light emitted from an object receeding from us is stretched out so that we observe a larger wavelength that the one emitted. This effect is quantified by the redshift z defined as

$$1 + z \equiv \frac{\lambda_{\rm obs}}{\lambda_{\rm emit}} = \frac{a(t_0)}{a(t)}. \tag{1.24}$$

For nearby sources, we can expand $a(t)$ in power series around t_0 to get

$$a(t) = a(t_0)[1 + (t - t_0)H_0 + \dots], \tag{1.25}$$

where we have introduced the Hubble constant

$$H_0 \equiv \left(\frac{\dot{a}(t)}{a(t)}\right)_{t=t_0} = 100h\,\text{km s}^{-1}\text{Mpc}^{-1}, \tag{1.26}$$

where the up to date value of h from Planck is $h = 0.67 \pm 0.01$ [11]. For close objects $t_0 - t$ is just the physical distance d and then the redshift increases linearly with distance $z \simeq H_0 d$.

The Hubble constant was historically first introduced by Hubble [3] to explain the redshift of the spectrum of galaxies with the famous Hubble law

$$v_{\rm gal} = Hd \tag{1.27}$$

that was actually the observational proof that the Universe is expanding. Contrary to the far ones, nearby galaxies show a blueshift instead of a redshift, because their motion is dominated by their peculiar velocit with respect to the comoving grid which is determined by local graviy.

1.4 Distances in the Universe

In a FLRW Universe the concept of distances can take different meanings and one has to be careful in defining distances. For example one can

redefine the radial coordinate $d\chi \equiv dr/\sqrt{1-kr^2}$. In order to investigate the propagation of light we note that photons follow null geodesics for which

$$ds^2 = 0. \tag{1.28}$$

For radial trajectory $\theta, \varphi = 0$ are geodesic, using the metric (1.22) we find that radial null geodesics are entirely determined by the condition

$$d\tau^2 - dr^2 = 0, \tag{1.29}$$

hence they are described by

$$\chi(\tau) = \pm\tau + \text{const} \tag{1.30}$$

that is, straight lines at $\pm 45°$ in the $\tau - \chi$ plane. We can now define the comoving distance $\chi(t)$ as:

$$\chi(t) = \int_t^{t_0} \frac{dt}{a(t)} = \int_0^r dr' = \int_0^z \frac{dz'}{H(z')}, \tag{1.31}$$

where in the second equality we considered a flat Universe with $k = 0$. However this distance is not observable. To get the physical distance one must just multiply for the scale factor

$$d_{\text{phys}}(t) = a(t)\chi(t). \tag{1.32}$$

Other important distances are the luminosity distance d_L and the angular diameter distance d_A. The first one relates the observed flux F of a source with luminosity L at comoving distance χ and redshift z

$$F = \frac{L}{4\pi\chi^2(1+z)} \equiv \frac{L}{4\pi d_L^2} \tag{1.33}$$

so we have

$$d_L = \chi(1+z) \tag{1.34}$$

Instead, the angular diameter distance measures the distance between us and the object when light was emitted and it is measured knowing the object physical size D and its angular size $\delta\theta$ as

$$d_A = \frac{D}{\delta\theta}. \tag{1.35}$$

We eventually find that

$$d_A = \frac{\chi}{1+z} \tag{1.36}$$

and then we get the relation between angular diameter and luminosity distance

$$d_A = \frac{d_L}{(1+z)^2} \tag{1.37}$$

1.4.1 Horizons in the FLRW Metric

If the Universe has a finite age, then light travels only a finite distance in that time and then we can receive information at a given moment only by a finite volume of the whole Universe. We call this volume's boundary the particle horizon and according to (1.30) its comoving size is given by[†]

$$\chi_{\rm ph}(\tau) = \tau - \tau_i = \int_{\tau_i}^{\tau} d\tau = \int_{\ln a_i}^{\ln a} (aH)^{-1} d\,\ln\, a \tag{1.38}$$

that can easily be converted into a physical size as usual.[‡]

In literature usually the particle horizon is used interchangeably for the Hubble radius H^{-1}. This is because when the dominating component of the Universe satisfies the strong energy condition $\rho+3P>0$ they are of the same magnitude. Nevertheless there are situations, as is the case of inflation, in which the two are different, so it is important to keep in mind their different meaning: the particle horizon is the maximum distance a photon can travel since the Big-Bang, instead the Hubble radius is the distance over which photon can travel in Hubble time H^{-1}[§]. In fact we can see from the expression (1.38) of the particle horizon that it is related to the comoving Hubble radius $(aH)^{-1}$, that thus affects the causal spacetime structure.

[†]Here τ_i means the initial Big-Bang singularity (see the next subsection).

[‡]To be meticulous the total information we can receive is encoded in the optical horizon defined with the substitution $\tau_i \to \tau_{\rm rec}$, in fact before recombination the Universe was opaque to radiation and therefore no electromagnetic messenger information can come before that time. However particle and optical horizon are numerically quite equals.

[§]Note that $c=1$ in our conventions: the Hubble radius and Hubble time have the same expression.

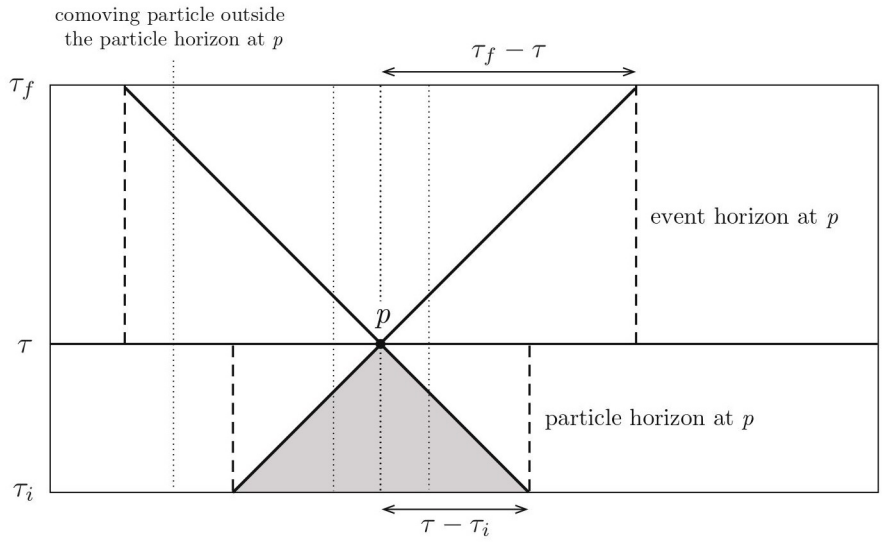

Figure 1.1: 2-dimensional spacetime diagram of constant θ, φ illustrating the concept of horizon. Dotted lines are worldlines of comoving objects. Figure taken from [10].

For completeness there is also another kind of horizon, but we will never run into it in the future. It is called the event horizon and it is the complement of the particle horizon

$$\chi_e(\tau) = \int_{\tau}^{\tau_f} d\tau = \tau_f - \tau \tag{1.39}$$

in which τ_f is the final moment of life of the Universe, if it expands forever then $\tau_f = +\infty$. The meaning of χ_e is that an observer will never receive in the future signals sent at a given moment τ from points with $\chi > \chi_e$ as can be seen in Fig.1.1.

1.5 Friedmann Equations

Once we have specified the form of the FLRW metric, we just need to determine the scale factor. This can be done by solving Einstein equations. Using the FLRW metric (1.19) and assuming the energy-momentum tensor

as in Eq.(1.23), the $0-0$ and the $i-i$ components of the Einstein equations (1.7) lead to the Friedmann equations

$$H^2 = \frac{8\pi G}{3}\rho - \frac{k}{a^2} \tag{1.40}$$

$$\dot{H} = -4\pi G(\rho + P) + \frac{k}{a^2} \tag{1.41}$$

that, combined together, give an equation for the second derivative of the scale factor

$$\ddot{a} = -\frac{4\pi G}{3}a(\rho + 3P). \tag{1.42}$$

We see from (1.42) that for a fluid with a pressure $p \equiv w\rho$ that satisfies the strong energy condition $w > -\frac{1}{3}$, we have $\ddot{a} < 0$ which means that the Universe is decelerating. Since ordinary matter pressure is always positive and then we need something else to explain the recent acceleration of our Universe. Because of Universe expansion we have $H > 0$, so the scale factor is a concave function of time, therefore there will exist a time in which $a(t) = 0$. This is the known Big-Bang singularity [12]. At that time the particle horizon vanishes and pressure and density are predicted to be infinite by classical physics.

It is useful to define the density parameter Ω_i for each component as

$$\Omega_i \equiv \frac{\rho_i}{\rho_{\text{crit}}} = \frac{8\pi G}{H^2}\rho_i \tag{1.43}$$

where ρ_{crit} is the density value corresponding to a flat Universe, as can be seen substituting $\rho = \rho_{\text{crit}}$ in the first of Eqs.(1.40). If the sum of the density parameters of each component $\Omega_{\text{tot}} = \sum_i \Omega_i$ is $>$, $<$ or $= 1$ we respectively have a closed, open or flat Universe.

In the following we will often use τ instead of the cosmic time t so we rewrite here the Friedmann equation (1.40) in conformal time

$$\mathcal{H}^2 = \frac{8\pi G}{3}a^2\rho - k \tag{1.44}$$

$$\mathcal{H}' = -\frac{4\pi G}{3}a^2(\rho + 3P) \tag{1.45}$$

where we have introduced the Hubble parameter in conformal time

$$\mathcal{H} \equiv \frac{a'}{a}, \tag{1.46}$$

where a prime $'$ denotes the derivative with respect to the conformal time.

To close the system of equations describing the Universe and its content we have the conservation equations for the energy-momentum tensor (1.10); if weconsider the 0-component of Eqs.(1.10), we find the continuity equation in conformal time:

$$\rho' = -3\mathcal{H}(\rho + P). \tag{1.47}$$

This equation can also be derived in a naive way from the first law of thermodynamics

$$dE = -pdV \tag{1.48}$$

just noting that $E = \rho V$ and $V \propto a^3$ in an expanding Universe.

If the different components of the Universe follow an hydrodynamic equation of state[¶] with w_i independent on time

$$P_i = w_i \rho_i \tag{1.49}$$

then Eq.(1.47) can be integrated to obtain the evolution of density with respect to the scale factor

$$\rho_i(t) = \rho_{0i} \left(\frac{a(t)}{a_0} \right)^{-3(1+w_i)}. \tag{1.50}$$

Looking at this expression for ρ we see that $\rho_m \propto a^{-3}$ whereas $\rho_r \propto a^{-4}$ therefore going back in time, as a decreases, radiation becomes dominant over matter. We can define the epoch at whichtheir densities were equal, that is called equivalence, which happened at $z_{\rm eq} \approx 4 \times 10^3$.

[¶]We have that $w = 0$ for matter, $w = 1/3$ for radiation and $w = -1$ for the cosmological constant.

1.5.1 Hot Big-Bang model and success of its predictions

We have just seen that in the standard Big-Bang model we can identify three epochs: a radiation dominated epoch at early stages, a matter dominated after equivalence at $z \approx 4 \cdot 10^3$ and a very recent epoch in which a dark energy component has began to dominate the Universe since $z \approx 0.3$. The radiation era itself can be divided into different stages

- *Quark era* $T > T_{\rm QH} \simeq 200 - 300$ MeV: at very high temperatures the matter in the Universe exists in the form of quark-gluon plasma. At $T = T_{\rm QH}$ the Universe undergoes a phase transitions and pairs of quarks and antiquarks join togheter to form hadrons, including pions and nucleons.

- *Hadron era* $T_{\rm QH} > T > T_\pi \simeq 130$ MeV: pion-pion interactions are very important and the perfect fluid approximation cannot be applied until pions and antipions annihilate at $T = T_\pi$.

- *Lepton era* $T_\pi > T > T_e \simeq 0.5$ MeV: leptons dominate Universe until positrons and electrons annihilate at $T = T_e$. Is in this era that the nucleosynthesis occurs.

- *Plasma era* $T_e > T > T_{\rm eq} \simeq 1$ eV: the content of the Universe is now photons, matter (protons, electrons and helium nuclei) and neutrinos, which have already decoupled from the background fluid of tightly coupled photons and baryons since the Lepton era.

After matter-radiation equivalence the baryons-photons fluid is still tightly coupled because of Thompson scattering between photons and electrons and can be considered as a single fluid in statistical equilibrium. As T decreases in the so called recombination after which the ionization fraction is very small electrons start to recombine in nuclei. Then Thompson scattering becomes more inefficient as the Universe expand and we have the decoupling of the

photons from the fluid. However, decoupling and recombination are not instantaneous processes, but are characterized by a small, but finite duration.

The model so far introduced has achieved three successful predictions:

- the prediction of light-element abundances during nucleosynthesis agree with observations [13];
- it accounts naturally for the expansion of the Universe;
- it explain the presence of the CMB as a relic of the hot thermal phase.

1.6 Problems of the Standard Big-Bang Model and Inflation

Despite the success in explaining nucleosynthesis and the presence of the CMB, the standard Big-Bang model does not explain why we do observe no magnetic monopoles in the universe, why the initial conditions on the curvature of the Universe have to be fine tuned and why the CMB is so isotropic on large scales. We refer to these problems as the monopole problem, the flatness problem and the horizon problem. We sketch them in the following:

- the monopole problem is related to the phase transitions in the early stage of the life of the Universe. In fact Great Unified Theories that try to explain the fundamental physics governing the behaviour of particles at such high energies, predict the production of topological defects like magnetic monopoles, cosmic strings or domain walls. The predicted density of these defects at present days is much higher than that of the matter [8], but no magnetic monopoles has yet been seen.
- The flatness problem can be formulated in term of the density parameter Ω. The Friedmann equation (1.40) becomes:

$$\Omega(t) - 1 = \frac{k}{(aH)^2} = -\Omega_k \tag{1.51}$$

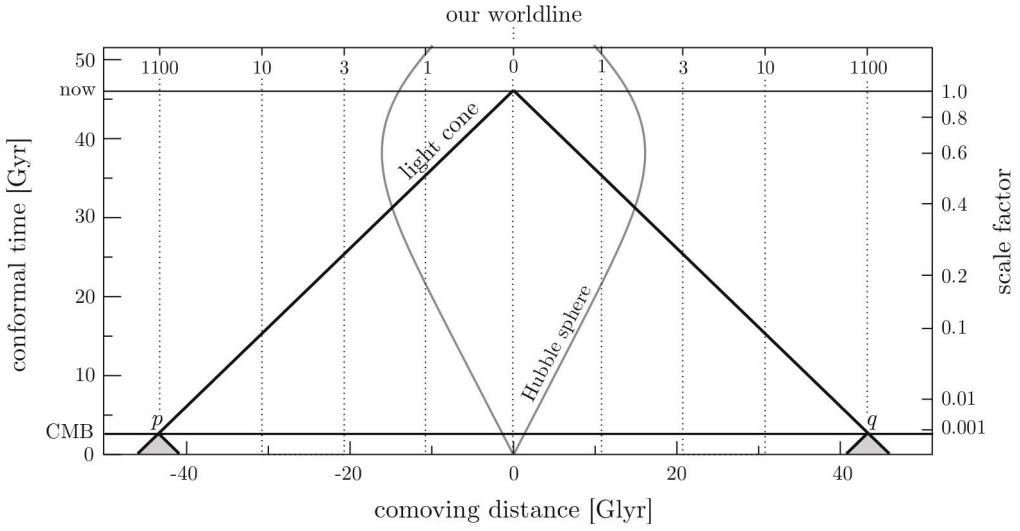

Figure 1.2: Representation of the horizon problem in the standard Big-Bang model. Figure taken from [10].

thus, to obtain a curvature k compatible with observations, the initial density parameter has to be very close to 1 [8]:

$$\Omega_i - 1 = (\Omega_0 - 1)\frac{(H_0 a_0)^2}{(H_i a_i)^2} = (\Omega_0 - 1)\left(\frac{\dot{a_0}}{\dot{a_i}}\right)^2 \leq 10^{-56}. \qquad (1.52)$$

We infer from this equation that the Universe has to be very close to being initially flat, leading to a fine tuning problem.

- The finiteness of the conformal time elapsed between the initial Big-Bang singula regions we observe in the sky were never in causal contact. As can be seen from Fig.1.6, if two different CMB photon were emitted close to t_i and were separated by a sufficient comoving distance their past light cones do not overlap. Therefore, eventhough we observe an almost isotropic temperature in the sky, a straightforward calculation (see for example [14]) can show that the angle subtended by the comoving horizon at recombination is $\theta_{\rm hor} = 1.16°$, so regions separated by an angle $\theta > 2\theta_{\rm hor}$ should not have come in causal contact.

The horizon problem comes from the fact that the Hubble radius for a Universe dominated by a fluid with $P = w\rho$ is given by

$$(aH)^{-1} = H_0^{-1} a^{\frac{1}{2}(1+3w)} \tag{1.53}$$

and then for ordinary matter satisfying the strong energy condition it grows with the expansion of the Universe, therefore the integral in Eq.(1.38) is dominated by the upper limits.

The solution to the horizon problem, and to all the other problems related to it, is then at hand: if we postulate a period of decreasing Hubble radius in the early Universe then Eq.(1.38) is dominated by the lower limit and the particle horizon becomes much larger than the Hubble one. This solution is called inflation. In this case also large scales λ become smaller than the comoving particle horizon and they could have been in causal contact in the past. It is worth noting that if the Hubble radius decreases then the initial singularity is pushed to negative conformal times $\tau_i \to -\infty$.

1.6.1 Single-field inflation

How can we obtain inflation? From Eq.(1.53) we see that this can be achieved simply by considering a fluid with negative pressure. We now consider a toy model satisfying this condition in which inflation is driven by an homogeneous scalar field $\phi(t)$, the inflaton. Its only time dependence comes from the cosmological principle.

The action of such a scalar field in a curved spacetime is

$$S = \int d^4x \sqrt{-g} \left[-\frac{1}{2} g^{\mu\nu} \partial_\mu \phi \partial_\mu \phi - V(\phi) \right]. \tag{1.54}$$

The energy-momentum tensor can be derived from Noether's theorem [15]:

$$T^\phi_{\mu\nu} = \partial_\mu \phi \partial_\nu \phi - g_{\mu\nu} \left(\frac{1}{2} g^{\rho\sigma} \partial_\rho \phi \partial_\sigma \phi - V(\phi) \right) \tag{1.55}$$

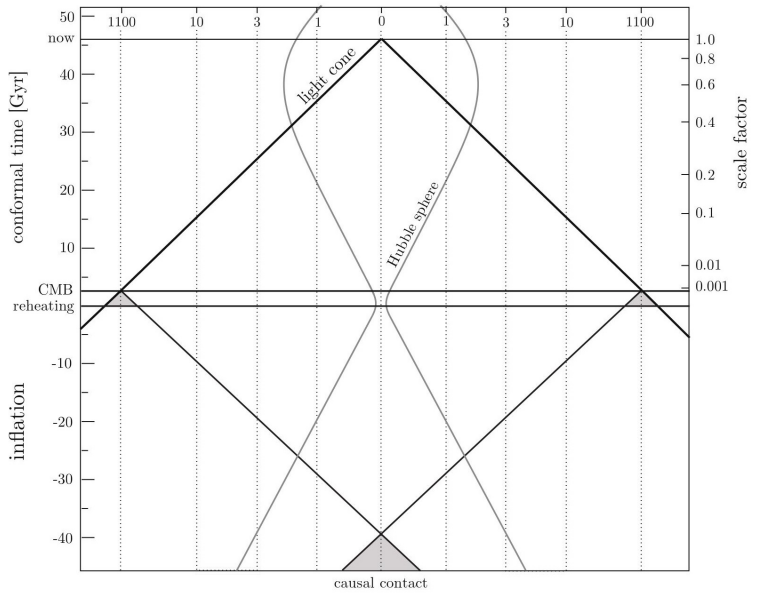

Figure 1.3: Representation of the horizon problem solution. Figure taken from [10].

and can be recasted in the form of a perfect fluid defining the scalar field density and pressure as

$$\rho_\phi = \frac{1}{2}\dot{\phi}^2 + V(\phi) \tag{1.56}$$

$$P_\phi = \frac{1}{2}\dot{\phi}^2 - V(\phi). \tag{1.57}$$

We then have that a field configuration in which the potential energy dominates over the kinetic one, leads to the violation of the strong energy condition, i.e. $P_\phi < -\frac{1}{3}\rho_\phi$, and then, to inflation.

Substituting ρ_ϕ and P_ϕ in Eqs.(1.40) gives the Friedmann equations

$$H^2 = \frac{1}{3M_{\rm pl}^2}\left[\frac{1}{2}\dot{\phi}^2 + V(\phi)\right] \tag{1.58}$$

$$\dot{H} = -\frac{1}{2}\frac{\dot{\phi}^2}{M_{\rm pl}^2}, \tag{1.59}$$

while the Euler-Lagrange equations of motion lead to the Klein-Gordon equa-

tion

$$\ddot{\phi} + 3H\dot{\phi} + \frac{\partial V}{\partial \phi} = 0. \tag{1.60}$$

The Klein-Gordon equation can be equally derived from the conservation of $T^{\mu\nu}_{\phi}$ and it is the equation describing a unit mass particle moving in a potential $V(\phi)$ with a frictional force $3H\dot{\phi}$.

It can be shown that the condition of a decreasing Hubble radius, in order to obtain inflation, is equal to the condition that the so called Hubble slow-roll parameters

$$\epsilon \equiv -\frac{\dot{H}}{H^2} \tag{1.61}$$

$$\eta \equiv \frac{\dot{\epsilon}}{H\epsilon} \tag{1.62}$$

$$\delta \equiv -\frac{\ddot{\phi}}{H\dot{\phi}} \tag{1.63}$$

are small, that is $\epsilon, |\delta| \ll 1$, that implies $|\eta| \ll 1$. As already said, inflation occurs when the kinetic energy is small with respect to the total energy density ρ_ϕ and this is why the parameter δ, measuring the acceleration of the scalar field, has to be small; this situation is called slow-roll inflation and corresponds to the inflaton slowly rolling toward the minimum of the potential. The condition $\epsilon \ll 1$ and $\delta \ll 1$ then legitimate us to neglect the kinetic energy and the acceleration of ϕ. Therefore we can rewrite the Friedmann and Klein-Gordon equations respectively as

$$H^2 \approx \frac{V}{M^2_{\rm pl}} \tag{1.64}$$

and

$$3H\dot{\phi} \approx -V_{,\phi}\,. \tag{1.65}$$

In this slow-roll approximation the Hubble slow-roll parameters ϵ and η become

$$\epsilon \approx \epsilon_V \equiv \frac{M^2_{\rm pl}}{2}\left(\frac{V_{,\phi}}{V}\right)^2 \tag{1.66}$$

$$|\eta| \approx |\eta_V| \equiv M^2_{\rm pl}\frac{V_{,\phi\phi}}{V}, \tag{1.67}$$

where ϵ_V and η_V are called potential slow-roll parameter and slow-roll inflation occurs for $\epsilon_V, \eta_V \ll 1$. These parameters are useful to determine if inflation can occur just considering the shape of the potential.

The existence of Universe as we observe it today implies that inflation needs to end. So the important questions are how much inflation do we need to explain the observed largest CMB scales? How does inflation end? These question are related to the shape of the potential. In particular we define the number of e-folds as

$$N \equiv \int_{a_I}^{a_E} d \ln a = \int_{t_I}^{t_E} dt\, H, \tag{1.68}$$

where t_I and t_E are the starting time and exit time from inflation, defined as $\epsilon(t_E) = 1$. The observed scales in CMB can be explained, in the simplest slow roll models, if inflation last more than $50 - 60$ e-folds, but in more complicated models this may vary.

But these features are not the only advantage of considering a period of inflation in the early stage of the Universe. In fact, although inflation was proposed to solve the Big-Bang problems, it also predict an adiabatic spectrum of small fluctuations on top of the homogeneus background. These small fluctuations can be explained as the quantum vacuum fluctuations of the inflaton field: their comoving scale get stretched during inflation and they cross the horizon and get freezed-out. When they cross the horizon they loose their quantum nature and they can be treated as a classical stochastic field. Eventually they re-enter the horizon after inflation and they become seeds for the large-scale structure we see today, like galaxies and clusters. These primordial fluctuations have been imprinted in the CMB anisotropies (see next Chapter): small temperature fluctuations of the order $\delta T/T \sim 10^{-5}$ around CMB average temperature $T_0 = 2.72548 \pm 0.00057\, K$ [16].

When inflation comes to an end there is a period called reheating in which the inflaton may start varying rapidly enough to produce the entropy of the Universe and then the field, or the entropy, may produce the baryons leaving the energy density ρ_ϕ small or zero.

1.7 ΛCDM Model

Observations show that the density parameters Ω_i of the different constituents of the Universe sum up to $\Omega_{\text{tot}} = 1$ with

$$\Omega_r \simeq 9.4 \times 10^{-5}, \;\; \Omega_m \simeq \Omega_c + \Omega_b \simeq 0.32, \;\; |\Omega_k| \lesssim 0.01, \;\; \Omega_\Lambda = 0.68.$$

We have split the matter density parameter into two contributions: $\Omega_b = 0.05$ from the ordinary matter (baryons and, of course, leptons, although the latter masses are negligibly compared to baryons) and $\Omega_c = 0.27$ from the cold dark matter (CDM). We do not know the particle nature of dark matter; there are candidates such as WIMPs and axions [17], but a direct detection is still missing. There is also the possibility that little amount of dark matter is in the form of hot relativistic dark matter (HDM). $|\Omega_k| \leq 0.01$ means that the curvature today is quite negligible and so it does in the past as it scales as a^{-2}. The presence of a small relativistic energy density $\Omega_r = 9.4 \times 10^{-5}$ is due to the CMB and the neutrinos background.

But the interesting thing is that today the budget of the Universe is dominated by a dark component called dark energy $\Omega_\Lambda = 0.68$ with an equation of state $w_\Lambda \approx -1$ that resembles that of a cosmological costant. This leads to the acceleration of the Universe we mentioned before.

The standard concordance model with the addition to a cosmological constant Λ, CDM and a period of inflation in the early stage of the life of Universe is called then ΛCDM model.

1.8 Dark Energy and the Accelerated Universe

The way to achieve accelerated expansion in the Universe, as we have seen before, is to have a negative pressure.

1.8.1 Cosmological Constant

Historically the first case of a negative pressure component was that of the cosmological constant Λ[‖] introduced by Einstein himself [18] in the Einstein equations (1.7), in order to satisfy the condition of a static Universw, that was a common model at the epoch

$$G_{\mu\nu} = 8\pi G T_{\mu\nu} + \Lambda g_{\mu\nu}. \tag{1.69}$$

This model, and the idea of a cosmological constant, were then later abandoned after Hubble discovery.

Nowadays we know that dark energy dominates the energy of the Universe, but we do not know its nature. A possibility, first proposed by Lemaitre [19, 20] and Eddington [21], is that the dark energy comes from the vacuum energy density of quantum physics. The idea was reconsidered widely by the community later on with the paper of Zel'dovich [22]. In laboratories, in fact, one computes energy differencies and the ground state energy of vacuum does not matter. However it enters in its own right in the Einstein equation. Despite the naturalness of this interpretation the value suggested by dimensional analysis is much larger than the one observed in the Universe. Those problems demand a search for a more fundamental understanding. The cosmological constant problem is sometimes considered as the most important problem in theoretical physics.

1.8.2 Quintessence

Another important point is that, although observations of an accelerated expansion are consistent with the existence of a constant vacuum energy, they cannot prove that this energy is really constant, therefore it is possible that the pressure-density ratio $w_{\rm DE} = P_{\rm DE}/\rho_{\rm DE}$ could be time-dependent.

A model that achieve such a scenario is called quintessence [23, 24, 25, 9, 26] and it assumes that the acceleration is driven by a scalar field, Q, as in

[‖] Λ has the dimension of length^{-2}

the model of inflation. There is, however, a big difference between the two models: while in inflation the inflaton evolution is set up to leave a zero ρ_ϕ, ending thus inflation, this obviously cannot be applied to dark energy, but one can imagine that the late time evolution of ρ_Q is slow. In particular if the evolution of ρ_Q is slower than ρ_m, it comes a time when ρ_Q comes to dominate and the Universe appears then to have a cosmological constant.

The scalar field theory is exactly the same we have seen in Sect.1.6.1 at page 21 making the substitution $\phi \to Q$. In particular, if the field is slowly rolling, we have the negative pressure leading the acceleration, as for inflation in the early Universe.

To avoid fine tuning problems we need that the behaviour of the field is independent from the initial conditions; this can be obtained with a potential with attractor properties. The simplest example of a potential with these features is [23, 27, 28, 29]

$$V(Q) = M^{4+\alpha} Q^{-\alpha} \tag{1.70}$$

where M is a constant with mass dimensions and $\alpha > 0$. For the moment we do not add a constant to (1.70) for it does not enter in the Klein-Gordon equation, but there is no special reason for excluding it. During radiation era we assume that $\rho_Q \ll \rho_r$, in order to avoid different helium abundance with respect to that observed, and then $H = 1/2t$. The Klein-Gordon equation (1.60) then becomes

$$\ddot{Q} + \frac{2}{(1+w)t}\dot{Q} - \alpha M^{4+\alpha} Q^{-\alpha-1} = 0, \tag{1.71}$$

where we left w generic for later convenience. A solution of this equation during the radiation era ($w = 1/3$) is

$$Q = \left(\frac{\alpha(2+\alpha)^2 M^{4+\alpha} t^2}{6+\alpha} \right)^{\frac{1}{2+\alpha}} \tag{1.72}$$

and therefore since $\rho_Q \propto t^{-2\alpha/(2+\alpha)}$ and $\rho_r \propto t^{-2}$ at very early times the former was smaller compared to the latter.

Perturbing Eq.(1.71) with a small perturbation δQ we have

$$\delta\ddot{Q} + \frac{3}{2t}\delta\dot{Q} + \frac{(6+\alpha)(1+\alpha)}{(2+\alpha)^2 t^2}\delta Q = 0, \tag{1.73}$$

with two independent solution

$$\delta Q \propto t^{\gamma}, \text{ with } \gamma = -\frac{1}{4} \pm \sqrt{\frac{1}{16} - \frac{(6+\alpha)(1+\alpha)}{(2+\alpha)^2}}. \tag{1.74}$$

Then, since both these solutions decay as t increase, while Q given by Eq.(1.72) increases, Eq.(1.72) is said to be a tracker solution or attractor, in the sense that any other solution that comes close to it will approach it.

The situation is exactly the same in the matter domination as can be seen from Eq.(1.71) with $w = 0$. Since both matter and radiation densities decrease with time as, respectively, t^{-2} and $t^{-8/3}$, of course faster than ρ_Q, they eventually will fall below ρ_Q.

Checking ρ_m and ρ_Q at the time t_c when this occurs we find

$$t_c \approx M^{-(4+\alpha)/2} G^{-(2+\alpha)/4} \tag{1.75}$$

and thus

$$Q(t_c) \approx G^{-1/2} = m_{\rm pl}^2, \tag{1.76}$$

where $m_{\rm pl}^2 = 1/G$ is the Planck mass**. After t_c the Klein-Gordon equation becomes

$$\ddot{Q} + \sqrt{24\pi G\rho_Q}\dot{Q} - \alpha M^{4+\alpha} Q^{-\alpha-1} = 0. \tag{1.77}$$

We can now guess that the inertial term $\ddot{Q}$ will become negligible with respect to the other to apply the slow-roll approximation and reduce the equation of motion to

$$\sqrt{24\pi G\rho_Q}\dot{Q} = \alpha M^{4+\alpha} Q^{-\alpha-1} \tag{1.78}$$

with solution

$$Q = M\left(\frac{\alpha(2+\alpha/2)t}{\sqrt{24\pi G}}\right)^{\frac{1}{2+\alpha/2}} \tag{1.79}$$

**The reduced Planck mass is, in our conventions, $M_{\rm pl}^2 = 1/(8\pi G)$.

and using this expression we can check our initial guess and find that the slow-roll approximation is actually justified. Numerical calculations show also that Eq.(1.79) is indeed the tracker solution as $t \to \infty$. We have that with this solution

$$\ln a \propto t^{\frac{2}{2+\alpha/2}} \tag{1.80}$$

that is the same dependence from the scale factor as that of a cosmological constant $\alpha = 0$, but otherwise less rapid. We stress that, since $\rho_Q \propto t^{-\alpha/(2+\alpha/2)}$, the derivation of Eq.(1.77) is indeed justified because the densities of all of the possible contents of the Universe have a faster rate of decrease.

As a final point we return on the issue of a possible additive constant in the expression (1.70) and we note that to agree with observations it is necessary arbitrarily to exclude it. Furthermore we need to adjust the constant M to give $t_c \approx t_0 \approx 1/H_0$ since we know that dark energy started very recently to dominate; this gives

$$M^{4+\alpha} \approx G^{-1-\alpha/2} H_0^2. \tag{1.81}$$

We will return on quintessence in the next chapters.

Chapter 2

Cosmological Perturbations Theory and CMB Anisotropies

We have summarized in the previous chapter the main assumptions of a FLRW cosmology based on the cosmological principle and then we trated the Universe as perfectly homogeneus and isotropic. However, we observe in the sky gravitational bound structures as galaxies, galaxy clusters and superclusters. These structures are generated by the gravitational instability of the primordial fluctuations generated during the inflation. By simply comparing the pressure force with gravity we can derive the Jeans length λ_J. If, at a given instant, there is a spherical inhomogeneity of radius λ and mass M, in a background fluid of density ρ, it will grow if the self-gravitational force per unit mass, $F_g \simeq GM/\lambda^2$ exceeds the opposing force per unit mass arising from pressure $F_P = P/(\rho\lambda^)$, that is when

$$\lambda > \lambda_J \equiv c_s^2 (G\rho)^{-1/2}, \tag{2.1}$$

viceversa the inhomogeneity propagates in the Universe as an oscillating wave. The concept of the Jeans length was developed in a Newtonian perturbation theory, that is an adequate description of what happens inside the Hubble radius. However, when the scale of the perturbation exceeds the Hubble radius such a Newtonian analysis fails and we have to consider General Relativity.

The perturbations treatment in general relativity has a gauge freedom: therefore it is important to take care to distinguish which are real perturbations and which are simply fictious perturbations induced by a change of coordinates.

A few words about conventions. We will follow in this chapter the conventions of [30]. In particular, the perturbations are considered at linear order and we treat density perturbations as a random Gaussian field so their Fourier modes are decoupled. Our notation for the Fourier transform is:

$$A(\mathbf{x},\tau) = \int \frac{d\mathbf{k}}{(2\pi)^3} A(\mathbf{k},\tau)\, e^{i\mathbf{k}\cdot\mathbf{x}}. \tag{2.2}$$

With these conventions, the power spectrum of the function A is then defined as

$$\langle A(k)A(k')\rangle = (2\pi)^3 \mathcal{P}(k)\delta^{(3)}(k-k'), \tag{2.3}$$

where $\delta^{(3)}(k-k')$ is the Dirac delta distribution function.

Throughout almost all of this chapter we will consider the flat FLRW metric (1.22) in conformal time.

2.1 Perturbations to the Metric

The idea is to consider small perturbations $\delta g_{\mu\nu}$ around the FLRW metric $\bar{g}_{\mu\nu}$, so that we can write the perturbed metric as

$$ds^2 = a^2(\tau)[-(1+2A)d\tau^2 + 2B_i dx^i d\tau + (\delta_{ij} + h_{ij})dx^i dx^j]. \tag{2.4}$$

From now on, we will raise and lower spatial indices just with the Kronecker delta δ_{ij}. The metric perturbations can be usefully divided into scalar, vector and tensor on the basis of their transformation properties under the group of 3-rotations and 3-translations. For instance δg_{00} is a scalar perturbation, whereas δg_{0i} can be composed as

$$B_i = \partial_i B + \hat{B}_i, \tag{2.5}$$

where $\hat{B}_i$ is the vector traceless ($\partial_i \hat{B}^i = 0$) part of B_i and B its scalar one. The situation is pretty different for δg_{ij} because it has also a tensorial component and moreover its scalar part can be further decomposed in a traceless part and another proportional to δ_{ij} as follows

$$h_{ij} = 2C\delta_{ij} + 2\partial_{\langle i}\partial_{j\rangle}E + 2\partial_{(i}\hat{E}_{j)} + 2\hat{E}_{ij}, \tag{2.6}$$

where we denote quantities with a hat as divergenceless and the first two terms on the right hand side are the scalar part of h_{ij}, the third is the vector one and the fourth the tensor part; the latter is not just divergenceless, but also tracefree. Furthermore

$$\partial_{\langle i}\partial_{j\rangle}E \equiv \left(\partial_i\partial_j + \frac{1}{3}\nabla^2\right)E, \tag{2.7}$$

$$\partial_{(i}\hat{E}_{j)} \equiv \frac{1}{2}(\partial_i\hat{E}_j + \partial_j\hat{E}_i). \tag{2.8}$$

We then have 10 degrees of freedom, 4 of which are scalar perturbations. A useful theorem called decomposition theorem [31] states that each type of perturbations evolves independently. Scalar perturbations are induced by energy density inhomogeneities. They exhibit gravitational instability and may lead to the formation of structure in the universe. Vector pertubations are related to the rotational motion of the fluid and decay very quickly. Tensor perturbations are a peculiar feature of general relativity and they describe gravitational waves.

For the rest of this and the next chapters we will consider only scalar perturbations since the effects of vector and tensor perturbations are subleading.

2.1.1 Gauge Transformations

Let us consider the infinitesimal coordinate transformation

$$x^\mu \to \tilde{x}^\mu = x^\mu + d^\mu(x^\nu) \tag{2.9}$$

where

$$d^0 = \alpha(x^\nu), \tag{2.10}$$

$$d^i = \partial^i \beta(x^\nu) + \epsilon^i(x^\nu); \tag{2.11}$$

$\partial^i\beta$ is longitudinal, i.e. irrotational ($\varepsilon_{ijk}\partial^j\partial^k\beta = 0$), and ϵ_i is transverse, i.e. divergenceless. We call this coordinate transformation a gauge transformation.

Under the transformation (2.9) the metric transforms as

$$\tilde{g}_{\alpha\beta}(\tilde{x}^\rho) = \frac{\partial x^\gamma}{\partial \tilde{x}^\alpha}\frac{\partial x^\delta}{\partial \tilde{x}^\beta} g_{\gamma\delta}(x^\rho). \tag{2.12}$$

Considering the translation parameter d^μ at the same order of the metric perturbations, we can linearize Eq.(2.12) and write $\tilde{g}_{\alpha\beta}$ as

$$\tilde{g}_{\alpha\beta}(\tilde{x}^\rho) = \bar{g}_{\alpha\beta}(\tilde{x}^\rho) + \delta\tilde{g}_{\alpha\beta} \tag{2.13}$$

to find the important relation between the new and the old metric induced by the gauge transformation

$$\delta g_{\alpha\beta} \to \delta\tilde{g}_{\alpha\beta} = \delta g_{\alpha\beta} - \bar{g}_{\alpha\beta,\gamma} d^\gamma - \bar{g}_{\beta\delta} d^\delta{}_{,\alpha} - \bar{g}_{\alpha\delta} d^\delta{}_{,\beta}\,, \tag{2.14}$$

in which the right and the left hand side are to be considered at same point $\tilde{x}^\rho$.

With the transformations (2.14) we find how the scalar degrees of freedom of the metric tranform:

$$A \to \quad A - \alpha' - \mathcal{H}\alpha \tag{2.15}$$

$$B \to \quad B + \alpha - \beta' \tag{2.16}$$

$$C \to C - \mathcal{H}T - \tfrac{1}{3}\nabla^2\beta \tag{2.17}$$

$$E \to \quad E - \beta. \tag{2.18}$$

Note that under the same transformationa 4-scalar $q(x^\rho) = \bar{q}(x^\rho) + \delta q$ transforms as:

$$\delta q \to \delta\tilde{q} = \delta q - \bar{q}_{,\alpha}\, d^\alpha. \tag{2.19}$$

On way to avoid the gauge problems is to define gauge invariant variables that do not change under the gauge transformation (2.9). The simplest gauge invariant quantities are the Bardeen variables [32]

$$\Psi_B \equiv A + \mathcal{H}(B - E') + (B - E')', \tag{2.20}$$

$$\Phi_B \equiv \ -C - \mathcal{H}(B - E') + \tfrac{1}{3}\nabla^2 E. \tag{2.21}$$

An infinite number of gauge invariant variables can be constructed as a linear combination of Ψ_B and Φ_B. With these definitions it is easy to see whether a perturbation is physical or just fictious, since Ψ_B and Φ_B are gauge invariant, if they vanish in a coordinate system, then they must vanish everywhere. So if both Ψ_B and Φ_B are zero the metric perturbations are fictious and can be removed with just a gauge transformation.

2.1.2 Gauge Fixing

Usually there are two ways to deal with the gauge freedom. The first one is to work with gauge invariant variables, the second is instead to use the gauge freedom to fix a particular coordinate system, tipically with properties useful to the treatment, that is, to fix the gauge by imposing two conditions on the scalar degrees of freedom of the metric. Once we have found a quantity in a particular gauge we can always make a gauge transformation to find its form and value in another gauge.

Among the several possible choices of gauge we will use the following [33]:

- *Newtonian (or longitudinal) gauge.* It is defined by the conditions

  $$B_l = E_l = 0 \tag{2.22}$$

  and we rename the two metric perturbations A and C respectively as Ψ and Φ. The metric then becomes

  $$ds^2 = a^2(\tau)[-(1 + 2\Psi)d\tau^2 + (1 - 2\Phi)\delta_{ij}dx^i dx^j]. \tag{2.23}$$

  This choice is fixed uniquely, in fact any transformation with $\beta \neq 0$ destroys the condition on E_l and so any $\alpha \neq 0$ breaks the condition

$B_l = 0$. The function Ψ plays the role of the gravitational potential in the weak field limit of the Einstein equations and thus has a useful physical meanings. The reason for we denote this way the two scalar perturbations is straightforward if we note that they are equal to Bardeen potentials (2.20) in modulus:

$$\Psi = \Psi_B \quad \text{and} \quad \Phi = -\Phi_B. \tag{2.24}$$

- *Synchronous gauge.* It is defined by

$$A_s = B_s = 0, \tag{2.25}$$

the metric becomes

$$ds^2 = a^2(\tau)[-d\tau^2 + (\delta_{ij} + h_{ij})dx^i dx^j]. \tag{2.26}$$

To get the connection with Ref.[30] we define $2C \equiv h/3$ and $2E \equiv \mu$. Moreover it is useful to write h_{ij} as a Fourier integral

$$h_{ij}(\mathbf{x},\tau) = \int \frac{d\mathbf{k}}{(2\pi)^3}\, e^{i\mathbf{k}\cdot\mathbf{x}} \left[\hat{k}_i\hat{k}_j h(\mathbf{k},\tau) + \left(\hat{k}_i\hat{k}_j - \frac{1}{3}\delta_i j\right) 6\eta(\mathbf{k},\tau)\right],\ \mathbf{k} = \hat{k}k. \tag{2.27}$$

Then the gauge is specified by the two functions h and μ in real space and by h and η in Fourier space. The disadvantage of such a gauge is that it is not fixed uniquely, since the choice of the initial hypersurface and its coordinate assignments are arbitrary. We expect that this fact will manifest itself in fictious gauge modes in the solutions to the Einstein equations. Usually this gauge freedom is fixed by setting the CDM velocity to zero $\theta_c = 0$, i.e. to consider the frame in wich CDM is at rest. The synchronous gauge is particular useful because of the numerical stability of the Einstein-Boltzmann codes in this gauge.

Other possible gauge choiches are the so called *spatially flat* and *comoving* gauge, that are useful in calculations in inflationary problems.

2.2 Einstein Equations at Linear Level

We now write the linearized Einstein equations in Fourier space. For it, note that all we have to do is just to make the replacement $\partial_i \to ik_i$.

If we split the Einstein and the energy-momentum tensors into a background and a perturbed part, then the perturbed Einsten equations are:

$$\delta G^{\mu}_{\nu} = 8\pi G \delta T^{\mu}_{\nu}. \tag{2.28}$$

Note that neither the right nor the left hand side is gauge invariant. One can find the gauge invariant quantities for δG^{μ}_{ν} and δT^{μ}_{ν} to write the perturbed Einstein equations in a gauge invariant manner, but we carry on with this notation since we eventually want to switch from one gauge to another.

First of all we need to derive the perturbations to the energy-momentum tensor (1.23) of a perfect fluid. If we write the density and pressure perturbations as $\delta\rho$ and δP and the coordinate velocities (which is considered a perturbations at the same order of $\delta\rho$ and δP) as $v^i \equiv dx^i/d\tau$, then the perturbed energy-momentum tensor becomes

$$T^0_0 = -(\bar{\rho} + \delta\rho), \tag{2.29}$$

$$T^0_i = (\bar{\rho} + \bar{P})v_i = -T^i_0, \tag{2.30}$$

$$T^i_j = (\bar{P} + \delta P)\delta^i_j + \Sigma^i_j, \tag{2.31}$$

where $\Sigma^i_j \equiv T^i_j - \delta^i_j T^k_k/3$ is the anisotropic shear perturbation to T^i_j and it is manifestly traceless. It is also useful to define the new variables θ and σ as

$$\theta \equiv ik^j v_j, \tag{2.32}$$

$$(\bar{\rho} + \bar{P})\sigma \equiv -(\hat{k}_i\hat{k}_j - \frac{1}{3}\delta_{ij})\Sigma^i_j \tag{2.33}$$

$$\delta \equiv \delta\rho/\rho. \tag{2.34}$$

For later convenience it might be useful to find the relations between the quantities in the synchronous and in the Newtonian gauge under the gauge

transformation (2.9). They are given by [30]

$$\delta^{(S)} = \delta^{(N)} - \alpha\frac{\bar{\rho}'}{\bar{\rho}}, \tag{2.35}$$

$$\theta^{(S)} = \theta^{(N)} - \alpha k^2, \tag{2.36}$$

$$\delta P^{(S)} = \delta P^{(N)} - \alpha\bar{P}', \tag{2.37}$$

$$\sigma^{(S)} = \sigma^{(N)}, \tag{2.38}$$

where, as usual, both the right and the left hand side are considered at the same space-time coordinate values. Moreover, the gravitational potentials in the Newtonian gauge are related to the synchronous metric perturbations as:

$$\Psi = \frac{1}{2k^2}\left[h'' + 6\eta'' + \mathcal{H}(h' + 6\eta')\right], \tag{2.39}$$

$$\Phi = \eta - \frac{1}{2k^2}\mathcal{H}(h' + 6\eta'). \tag{2.40}$$

With the perturbed energy-momentum tensor (2.29) we can finally write the Einstein equation [30, 34, 35] in the *synchronous gauge*

$$k^2\eta - \frac{1}{2}\mathcal{H}h' = -8\pi G a^2 \sum_i \frac{\delta\rho_i^{(S)}}{2}, \tag{2.41}$$

$$k^2\eta' = 8\pi G a^2 \sum_i (\bar{\rho}_i + \bar{P}_i)\frac{\theta_i^{(S)}}{2}, \tag{2.42}$$

$$h'' + 2\mathcal{H}h' - 2k^2\eta = -24\pi G a^2 \sum_i \delta P_i^{(S)}, \tag{2.43}$$

$$(h + 6\eta)'' + 2\mathcal{H}(h + 6\eta)' - 2k^2\eta = -24\pi G a^2 \sum_i (\bar{\rho}_i + \bar{P}_i)\sigma_i^{(S)}, \tag{2.44}$$

while in the *Newtonian gauge* they take the form

$$k^2\Phi + 3\mathcal{H}(\Phi' + \mathcal{H}\Psi) = -8\pi G a^2 \sum_i \frac{\delta\rho_i^{(N)}}{2}, \tag{2.45}$$

$$k^2(\Phi' + \mathcal{H}\Psi) = 8\pi G a^2 \sum_i (\bar{\rho}_i + \bar{P}_i)\frac{\theta_i^{(N)}}{2}, \tag{2.46}$$

$$\Phi'' + \mathcal{H}(\Psi + 2\Phi)' + \left(2\frac{a''}{a} - \mathcal{H}^2\right) + \frac{k^2}{3}(\Phi - \Psi) = 4\pi G a^2 \sum_i \delta P_i^{(N)}, \tag{2.47}$$

$$k^2(\Phi - \Psi) = 12\pi G a^2 \sum_i (\bar{\rho}_i + \bar{P}_i)\sigma_i^{(N)}, \tag{2.48}$$

where the index i runs over all the species contributing to the content of the Universe.

It remains to derive the conservation equation for the perturbed energy-momentum tensor at first order. Previous Eq.(1.10) is just valid for a single uncoupled fluid (which may be the total fluid), but they change once we take into account the interactions among fluids. We will analize them in the next section.

2.3 Boltzmann Equations for Matter and Radiation

The systematic way to deal with the interactions between the different components of the Universe is to write down and solve the Boltzmann equations for each species. In fact all the matter perturbations are coupled to gravity and so the metric interacts with each species that in turn interact among theirself by scattering processes.

We work in the phase space described by three positions x^i and their conjugate momenta P_i. Since we are considering perturbations to the metric, different conventions can be found in the literature so, as usual, we follow [30]. In particular we will consider in the following the Boltzmann equations in the synchronous gauge: this approach is not manifestly covariant, so when we do the calculations we need to switch from the gauge-dependent variables to the gauge-invariant ones.

The conjugate momentum is just the spatial part of the energy-momentum 4-vector (1.4) with lower indices. i.e. P_i. In synchronous gauge it is just

$$P_i = a(\delta_{ij} + \frac{1}{2}h_{ij})p^j, \tag{2.49}$$

where $p^j = \delta^{ji}p_i$ is the proper momentum measured by an observer at fixed spatial coordinates. The phase space infinitesimal volume is $dV = dx^1dx^2dx^3dP_1dP_2dP_3$ and, from Eq.(2.49), we see that its zeroth-order is proportional to a^3. For later convenience, since at the zeroth-order p_i scales

as a^{-1} for the background geodesic equation (1.6), it is useful to define [36] the quantity $q_j = ap_j$ and its magnitude q and direction n_j as $q_j = qn_j$, with $n^i n_i = 1$. We can also define $\epsilon = (q^2 + a^2m^2)^{1/2} = a(p^2 + m^2)^{1/2}$, where $(p^2+m^2)^{1/2}$ is the proper energy measured by a comoving observer and we can relate it to the zeroth component of the energy-momentum 4-vector $P_0 = -\epsilon$.

Having set up all this conventions we can now derive the Boltzmann equations for all the species we are interested in. The simplest form of the Boltzmann equation can be written as

$$\frac{df_j}{d\tau} = C[f_j], \tag{2.50}$$

where f_j is the phase space distribution for the j-th species * that gives the number of particles in dV

$$f(x^i, P_j, \tau)dV = dN \tag{2.51}$$

while $C[f_i]$ is the collision term describing all the scattering effects. We drop the subscript i for the moment. The zeroth-order phase space distribution is just the Fermi-Dirac (for fermions, $-$ sign) or the Bose-Einstein (for bosons, $+$ sign) distribution function and depends just on ϵ (or q)

$$f_0 = f_0(\epsilon) = g_s \left[e^{\epsilon/aT} \pm 1\right]^{-1} \tag{2.52}$$

where the factor g_s is the number of spin degrees of freedom.

We express then the perturbed phase-space distribution as an expansion around its zeroth-order

$$f(x^i, P_j, \tau) = f_0(q)(1 + \Upsilon(x^i, q, n_j, \tau)), \tag{2.53}$$

so that we can express in terms of the perturbation Υ the components of the energy-momentum tensor written in its general form

$$T_{\mu\nu} = \int \sqrt{-g} dP_1 dP_2 dP_3 \frac{P_\mu P_\nu}{P^0} f(x^i, P_j, \tau), \tag{2.54}$$

* $j = \nu, \gamma, b, c$ where respectively they stand for neutrinos, photons, baryons and cold dark matter.

we find that

$$T_0^0 = -\int q^2 dq d\Omega \, \frac{\sqrt{q^2 + m^2 a^2}}{a^4} f_0 (1 + \Upsilon), \tag{2.55}$$

$$T_i^0 = -\int q^3 dq d\Omega \, \frac{n_i f_0 \Upsilon}{a^4}, \tag{2.56}$$

$$T_j^i = -\int q^4 dq d\Omega \, \frac{n^i n_j}{a^4 \sqrt{q^2 + m^2 a^2}} f_0 (1 + \Upsilon), \tag{2.57}$$

where $d\Omega$ is the solid angle associated with n^i.

Now we can turn the total derivative with respect to τ in Eq.(2.50) into partial derivatives

$$\frac{df}{d\tau} = \frac{\partial f}{\partial \tau} + \frac{dx^i}{d\tau}\frac{\partial f}{\partial x^i} + \frac{dq}{d\tau}\frac{\partial f}{\partial q} + \frac{dn_i}{d\tau}\frac{\partial f}{\partial n_i} \tag{2.58}$$

and use the geodesic equation (1.6) to find the appropriate expression for $dq/d\tau$. Then the unintegrated Boltzmann equation in Fourier space in the synchronous gauge becomes

$$\frac{\partial \Upsilon}{\partial \tau} + i\frac{q}{\epsilon}(\mathbf{k}\cdot\hat{n})\Upsilon + \frac{d\ln f_0}{d\ln q}\left(\eta' - \frac{h' + 6\eta'}{2}\mu^2\right) = \frac{1}{f_0}C[f], \tag{2.59}$$

where $\mu \equiv \hat{k}\cdot\hat{n}$. Now it only remains to consider separately each different component, specify for each the appropriate collision factor and integrate the Boltzmann equation (2.59).

2.3.1 Neutrinos

We only consider massless neutrinos for which $\epsilon = q$. Their energy density, pressure and anistropic stress are given by Eq.(2.55). The procedure is to integrate out the q-dependence from Eq.(2.59), taking its moments, and to expand the angular dependence of the perturbation Υ in Legendre polynomials $P_l(\mu)$:

$$F_\nu(\mathbf{k}, \hat{n}, \tau) \equiv \frac{\int q^3 dq \, f_0 \Upsilon}{\int q^3 dq \, f_0} \equiv \sum_{l=0}^{\infty} (-i)^l (2l+1) F_{\nu l}(\mathbf{k}, \tau) P_l(\mu). \tag{2.60}$$

We note that

$$\delta_\nu = \frac{1}{4\pi}\int d\Omega\, P_0(\mu)F_\nu = F_{\nu 0}, \tag{2.61}$$

$$\theta_\nu = \frac{3i}{16\pi}\int d\Omega\, P_1(\mu)F_\nu = \frac{3}{4}kF_{\nu 1}, \tag{2.62}$$

$$\sigma_\nu = -\frac{1}{8\pi}\int d\Omega\, P_0(\mu)F_\nu = \frac{1}{2}F_{\nu 2}, \tag{2.63}$$

so that, to find the equations respectively for the neutrino density, velocity and stress, we just have to multiply the unintegrated Boltzmann equation (2.59) without collision terms, since they are weakly interacting with other particles, for the Legendre polynomials and then integrate over $d\mathbf{q}$. We then find a infinite hierarcy of equations and the usual way to deal with them is to truncate this hierarcy at some $l_{\max}$. For neutrinos the multiple $F_{\nu l}$ becomes negligible for $l \geq 3$ so it is safe to truncate the hierarcy to $l = 3$; we then obtain the equations

$$\delta'_\nu = -\frac{4}{3}\theta_\nu - \frac{2}{3}h', \tag{2.64}$$

$$\theta'_\nu = k^2\left(\frac{1}{4}\delta_\nu - \sigma_\nu\right), \tag{2.65}$$

$$2\sigma'_\nu = \frac{8}{15}\theta_\nu - \frac{3}{5}kF_{\nu 3} + \frac{4}{15}(h' + 6\eta'), \tag{2.66}$$

$$F'_{\nu l} = \frac{k}{2l+1}[lF_{\nu(l-1)} - (l+1)F_{\nu(l+1)}], \quad l \geq 3. \tag{2.67}$$

2.3.2 Photons

The evolution of the photon distribution can be treated similarly as the one of massless neutrinos. The main difference is that we cannot neglect the collision term. In fact photons before recombination are tightly coupled to baryons because of Thomson scattering; also after recombination, during the freestreaming, there remains a residual energy and momentum transfer with the matter. In both cases we need to consider the contribution of the Thomson scattering to the collision term.

Photons are polarized in a plane orthogonal to their propagation direction $\hat{n}$ due to scattering of electron density perturbation with wavevector $\mathbf{k}$. We

denote by $F_\gamma(\mathbf{k}, \hat{\mathbf{n}}, \tau)$, defined as in Eq.(2.60), the total intensity, i.e. the sum of the phase space densities in the two polarization states for $\mathbf{k}$ and $\hat{n}$, and by G_γ their difference, i.e. the Stokes parameter. Their explicit expressions can be found in Ref.[30, 37].

The Boltzmann equations take the form [30, 34]:

$$\delta'_\gamma = -\frac{4}{3}\theta_\gamma - \frac{2}{3}h', \tag{2.68}$$

$$\theta'_\gamma = k^2\left(\frac{1}{4}\delta_\gamma - \sigma_\gamma\right) + an_e\sigma_T(\theta_b - \theta_\gamma), \tag{2.69}$$

$$\sigma'_\gamma = \frac{4}{15}\theta_\gamma - \frac{3k}{10}F_{\gamma 3} + \frac{2}{15}(h' + 6\eta') - \frac{an_e}{20}\sigma_T(18\sigma_\gamma - G_{\gamma 0} - G_{\gamma 2}), \tag{2.70}$$

$$F'_{\gamma l} = \frac{k}{2l+1}[lF_{\gamma(l-1)} - (l+1)F_{\gamma(l+1)}] - an_e\sigma_T F_{\gamma l}, \;\; l \geq 3, \tag{2.71}$$

where we denote by n_e the proper mean density of the electrons and by $\sigma_T = 0.6652 \times 10^{-24}\text{cm}^{-2}$ the Thomson cross section and we truncated the hierarcy at $l = 2$ neglecting multipoles for $l \leq 3$.

2.3.3 Cold Dark Matter

The simplest case is that of cold dark matter, that can be treated as a pressureless perfect fluid since it interacts with other particles only through gravity. As stated before CDM can be used to define the synchronous coordinates setting $\theta_c = \sigma_c = w = w' = 0$. Therefore we have only the equation:

$$\delta'_c = -\frac{1}{2}h', \tag{2.72}$$

that could have been derived also from perturbing the continuity equation (1.47) with $P = 0$.

2.3.4 Baryons

Before recombination, baryons are tightly coupled to photons and this causes an energy-momentum transer represented by the term $an_e\sigma_T(\theta_b - \theta_\gamma)$

of Eq.(2.69). The Boltzmann equations for baryons then become [30, 34]:

$$\delta_b' = -\theta_b - \frac{1}{2}h', \tag{2.73}$$

$$\theta_b' = -\mathcal{H}\theta_b + c_s^2 k^2 \delta_b - \frac{4\rho_{\gamma 0}}{3\rho_{b0}} a n_e \sigma_T (\theta_b - \theta_\gamma). \tag{2.74}$$

Tight-Coupling Approximation

At early times the Hubble time $t_H \approx a\tau$ is big compared to the characteristic baryon-photons interaction time scale $t_{b\gamma} \approx 1/(n_e \sigma_T)$. Subtracting the Eqs.(2.69) and (2.74) for θ_γ and θ_b and regarding $\mathcal{H}\theta_b + \frac{1}{3}k^2\delta_\gamma$ as a forcing term, in the limit $\sigma_T \to \infty$, we obtain that $\theta_\gamma = \theta_b$. We therefore set $\theta_\gamma = \theta_b$ at early times and we obtain its evolution equation combining Eqs.(2.69) and (2.74) so that the scattering terms cancel [38]:

$$\left(\frac{4}{3}\Omega_\gamma + \Omega_b\right)\theta_\gamma' = -\Omega_b \mathcal{H}\theta_\gamma + \frac{1}{3}\Omega_\gamma k^2 \delta_\gamma. \tag{2.75}$$

For the reasons mentioned above, we will neglect the scattering terms also in the equations for the photons and baryons density contrasts and we will then use the following equations:

$$\delta_b' = -\theta_\gamma - \frac{1}{2}h', \tag{2.76}$$

$$\delta_\gamma' = -\frac{4}{3}\theta_\gamma - \frac{2}{3}h'. \tag{2.77}$$

2.4 CMB Anisotropies

As the Universe expanded it cooled down and the atoms started to recombine leading to the decoupling of radiation and matter. In this picture, at the time the primordial plasma recombined at redshift $z_{\rm rec} \approx 1100$, the mean free path for Thomson scattering grew to the horizon size and photons started to propagate freely. These photons represent the cosmic microwave background (CMB). A small fraction of photons underwent further scattering once the universe reionized, due to the ionizing radiation from the first stars, which will leave an imprint in CMB polarization.

The CMB has an almost perfect blackbody thermal spectrum, with a temperature $T_{\rm CMB} = 2.72548 \pm 0.00057\,\mathrm{K}$ isotropic in all directions in the sky [39, 16]. However, on top of this blackbody distribution we observe small temperature variations, called anisotropies, of the order $\delta T/T \equiv \Theta \sim 10^{-5}$.

The reason CMB is so important is that the CMB anisotropies are the imprints of primordial fluctuations generated by inflation.

We can divide the anisotropies in the CMB in primary anisotropies, that were originated at the time of decoupling, and secondary anisotropies, [40] generated during the photons journey from the last scattering surface to today.

Primary anisotropies are the result of different effects depending on the scale of interest. At large angular scales the dominant effect is the Sachs-Wolfe effect [41], that consists in an energy drop of the CMB photons climbing out of the gravitational potential wells or an energy gain for which roll down potential hills due to dark matter perturbations. This causes a fractional variation of the temperature to $\Theta = \frac{2}{3}\Phi$ and, since on large scales $2\Phi = -\delta$ in the case of adiabatic perturbations, hot spots in the CMB correspond to underdense regions, whereas overdense regions correspond to cold spots.

At intermediate scales we observe the acoustic oscillations due to the density and velocity fluctuations of the photon-baryons coupled fluid. The fluid oscillates on all scales within the horizon. For adiabatic perturbations (we will introduce the distinction between adiabatic and isocurvature perturbations in the next section), these oscillations behave like cosine oscillations and, since the CMB is quadratic in the perturbations, we find peaks in the angular power spectrum corresponding to the scales that were in the extrema of their oscillations at the time of recombination. We refer to this as to the baryon acoustic oscillations: their imprint in the matter power spectrum [42] is an important probe for the cosmological paradigm and it is complementary to the CMB.

At small scales we have a damping effect, the Silk damping, due to the fact that the baryons-photons perfect fluid is just an approximation valid

only if the scattering rate of photons off electrons is infinite. This condition is not met, because in reality photons travel a finite distance in between scatters. After a Hubble time a photon, with a mean free path $\lambda_{\rm mfp}$, has moved a distance of order λ_D. Any perturbation on scales smaller than λ_D is expected to be washed out.

Secondary anisotropies, instead, may provide information on structure formation and they consist of an ensemble of different effects:

- Gravitational lensing: we observe photons coming from a slightly different directions from the original since they are deflected by the gravitational potentials due to the large-scale distribution of matter.

- Sunayev-Zel'dovich effect: passing through the cluster of galaxies, photons may interact with free electrons of the hot inter-cluster medium by Inverse Compton scattering generating a spectral distortion.

- Integrated Sachs-Wolfe effect (ISW): the gravitational potential varies in time, so the photons passing in that potential suffer a shift in the energy. This effect can be divided into Early ISW, often considered as part of the primary anisotropies, that happens right after decoupling when radiation density still has non-negligible effect, and Late ISW due to the late time effect of dark energy on the potential. The latter is crucial in order to investigate the nature of dark energy with future large scale sctructure (LSS) data.

.

2.4.1 Angular Power Spectrum

The basic observables of the CMB are its temperature and polarization as a function of the direction on the sky $\hat{n}$ expressed in the two coordinates (θ, φ). We can expand the anisotropy $\Theta(\theta, \phi) \equiv \frac{\delta T(\theta,\phi)}{T}$ of the CMB in terms

of its multipole moments [43]:

$$\Theta(\theta,\phi) = \sum_{l=1}^{\infty}\sum_{m=-l}^{l} a_{lm}Y_{lm}(\theta\phi), \tag{2.78}$$

where Y_{lm} are the spherical harmonic functions [44] and the index l is related to the angular scale, $\theta \sim \frac{2\pi}{l}$ for large multipoles. If the distribution of δT is Gaussian, the multipole moments a_{lm} are fully characterized by their angular power spectrum:

$$\langle a^*_{l'm'}a_{lm}\rangle = \delta_{ll'}\delta_{mm'}C_l, \tag{2.79}$$

where the average is performed over an ensemble of different angular power realizations. In practice, a real observer is limited to one Universe and so the spectra are computed averaging over the different $2l+1$ independent modes:

$$C_l = \frac{1}{2l+1}\sum_{m=-l}^{m=l}|a_{lm}|^2. \tag{2.80}$$

The fundamental limitation to how accurately the CMB angular power spectrum can be known is set by the cosmic variance, i.e. the fact that there are only $2l+1$ independent modes for each l. The error on each C_l is then:

$$\Delta C_l = \sqrt{\frac{2}{2l+1}}C_l. \tag{2.81}$$

In Figure 2.1 is shown the angular power spectrum multiplied by $\mathcal{D}_l \equiv l(l+1)/(2\pi)$ and the best-fit obtained by Planck 2015 [11]. On large angular scales the shape is given by the Sachs-Wolfe effect that leads to a plateau for small l in the plane $l(l+1)C_l/(2\pi)$ vs l and this is one of the reasons why the angular power spectra are often plotted in bandpowers $\mathcal{D}_l$. The dominance of dark energy at recent times enhances the spectrum through the late ISW effects on very small multipoles ($l < 10$). Going toward smaller scales we observe the characteristic peaks of the acoustic oscillations. The first peak, located at $l \approx 220$, corresponds to the angular scale of the horizon at recombination ($\theta \sim 1^\circ$) and it can give us an estimation for the total density parameter. After that, we observe a sequence of acoustic peaks that is damped when the

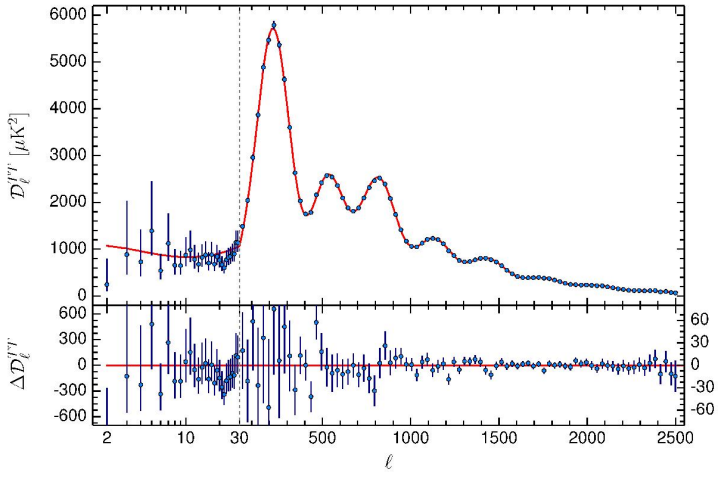

Figure 2.1: Temperature anisotropies power spectrum and best fit measured by Planck. Here the quantity $\mathcal{D}_l = l(l+1)C_l$ has been plotted. Figure taken from [11].

Silk damping starts acting for $l > 1000$ leading to a suppression of the tail on small angular scales.

2.4.2 CMB Anisotropies in Polarization

CMB anisotropies are also polarized [31, 45, 46]. In fact the Thomson scattering on an anisotropic photon distribution before decoupling induces a polarization. We expect the polarization anisotropies to be much weaker than the ones in the temperature field. In fact they are about 10% of the total temperature fluctuations for small angular scales and just 1% for large angular scales. Contrary to the usual treatment in terms of the Stoke parameters Q and U ($V = 0$ for the CMB), for the CMB analysis are used combinations of the Stokes parameters which are invariant under the rotation of the observation frame. In fact, the polarization field is decomposed in the E and the B modes. The formers are scalar functions describing the even parity part of the polarization, they correlate with temperature fluctuations, which are also even, whereas the B modes describe its odd part and they do not correlate with Θ. The E modes are related to the density perturbations

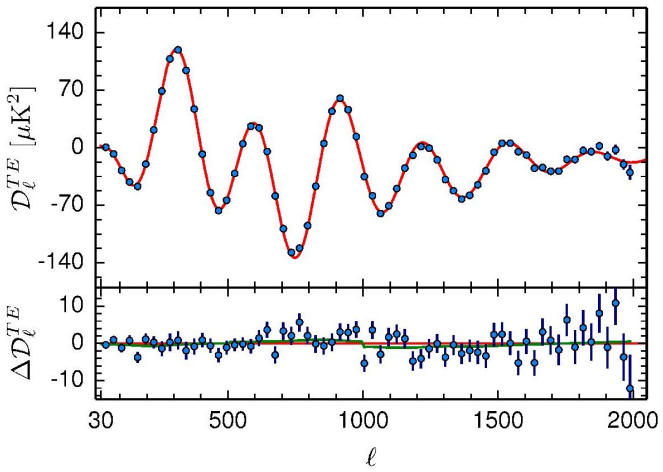

Figure 2.2: Temperature and E-mode polarization cross-correlation power spectrum measured by Planck and best-fit. The quantity $\mathcal{D}_l^{TE} = l(l+1)C_l^{TE}$ has been plotted. Figure taken from [11].

while the B modes are a unique signature of primordial gravitational waves generated during inflation or exotic models with vector modes. Expanding the E and the B modes in spherical harmonics it is possible to define the C_ls for these quantities as:

$$C_l^{EE} \equiv \langle E_{lm}^* E_{lm} \rangle, \tag{2.82}$$

$$C_l^{TE} \equiv \langle T_{lm}^* E_{lm} \rangle, \tag{2.83}$$

$$C_l^{BB} \equiv \langle B_{lm}^* B_{lm} \rangle. \tag{2.84}$$

In Fig.2.2 and 2.3 we show the EE and TE spectrum and best fit from temperature data noly measured by Planck in 2015 [11]. It can be seen that the peaks in the EE spectrum are π out of phase with respect to those for temperature, since polarization results from scattering, so its effect is maximum when the fluid velocity is maximal. Like temperature anisotropies, also polarization is affected by gravitational lensing which lenses E modes into B modes generating a peculiar B mode signal on small angular scales, which represents one of the main noise source in primordial B modes detection.

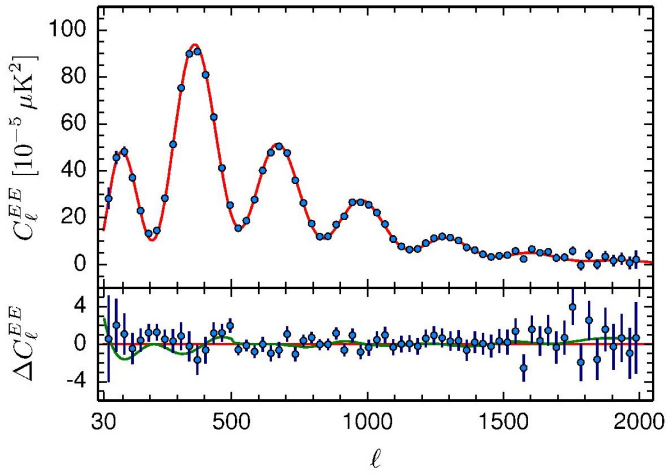

Figure 2.3: E-mode polarization power spectrum measured by Planck and best-fit. Figure taken from [11].

2.5 Initial Conditions for Cosmological Perturbations

To compute the CMB angular spectrum we need to define the initial conditions for the perturbations, that is a sort of '*Cauchy problem*' for the set of coupled differential equations used to compute the C_ls. To this purpose we recall that a given mode is said to be inside the Hubble horizon if its physical frequency is larger than the Hubble horizon, i.e. $k\tau > 1$, since for a universe filled with radiation $a \sim \tau$ and $\mathcal{H} \sim \frac{1}{\tau}$, viceversa it is said to be a super-horizon mode when $k\tau < 1$. The mode is crossing the horizon for $k\tau \approx 1$.

It is costumary to define the initial conditions for cosmological perturbations deep in the radiation era after neutrino decoupling. When we set the initial conditions we find the large scale solutions for the perturbations in the Einstein-Boltzmann system, because only modes with wavelength larger than the horizon at that time will be relevant for the CMB anisotropies observed today.

2.5.1 Adiabatic and Isocurvature Perturbations

It is important for the purposes of this Section to distinguish between adiabatic and isocurvature initial conditions. We consider, for instance, a matter and radiation plasma before the equivalence: the entropy per matter particle is given by $\Gamma = T^3/n_m$, where n_m is the number density of matter particles. Then, if we define the entropy perturbation $\mathcal{S}$ as $\mathcal{S} = \delta\Gamma/\Gamma$, it is given by:

$$\mathcal{S} = 3\frac{\delta T}{T} - \delta_m = \frac{3}{4}\delta_r - \delta_m, \tag{2.85}$$

since $\rho_r \propto T^4$. We thus obtain the following condition for having a vanishing entropy perturbation:

$$\delta_\gamma \simeq \delta_\nu \simeq \frac{4}{3}\delta_c \simeq \frac{4}{3}\delta_b. \tag{2.86}$$

A more general and manifestly gauge invariant way, that we will use in the following chapters, to define the entropy perturbation is given by:

$$\mathcal{S} = H\left(\frac{\delta P}{\dot{p}} - \frac{\delta\rho}{\dot{\rho}}\right). \tag{2.87}$$

For two barotropic fluids with constant $w_i = P_i/\rho_i$ the relative entropy perturbation is given by [47]:

$$\mathcal{S}_{ij} = \frac{\delta_i}{1+w_i} - \frac{\delta_j}{1+w_j}. \tag{2.88}$$

Perturbations that satisfy Eq.(2.86) are said to be adiabatic perturbations or curvature perturbations. In fact, they are associated, through the Einstein equations, to a perturbation to the local geometry of the Universe since there is a global perturbation of the matter content. They are also called isentropic perturbations since the relative entropy perturbations (2.88) vanish for density perturbations satisfying Eq.(2.86). But it is possible to perturb the matter components without perturbing the geometry: this is the case of isocurvature perturbations, that give a non-vanishing entropy perturbations.

Adiabatic and isocurvature perturbations have very different imprints on the CMB power spectrum. As we mentioned before, an adiabatic initial condition generates a cosine oscillatory mode in the photons-baryons fluid with a

first peak located around $l \simeq 220$. An isocurvature mode, instead, generates a sine oscillatory mode with a first acoustic peak located around $l \simeq 330$. This leads to the conclusion that isocurvature modes cannot dominate over the adiabatic one. This has also been confirmed by the Planck mission [11] and is enforced by the predictions of the nearly Gaussian adiabatic spectrum predicted by the simplest models of inflation [48]. However, this does not exclude the presence of a subdominant isocurvature perturbation, possibly correlated with the adiabatic one. Finally, we note that we refer to an isocurvature mode with the meaning that this mode was an isocurvature mode deep in the radiation era, indeed this primordial isocurvature mode can have an adiabatic component at late time (today), because the decomposition between isocurvature and adiabatic is not time invariant.

For all of this reasons, in addition to the adiabatic mode (in the synchronous gauge) [30]:

$$h = Ck^2\tau^2, \tag{2.89}$$

$$\eta = 2C - C\frac{5+4R_\nu}{6(15+4R_\nu)}k^2\tau^2, \tag{2.90}$$

$$\delta_c = \delta_b = \frac{3}{4}\delta_\gamma = \frac{3}{4}\delta_\nu = -\frac{C}{2}k^2\tau^2, \tag{2.91}$$

$$\theta_c = 0, \tag{2.92}$$

$$\theta_b = \theta_\gamma \equiv \theta_{\gamma b} = -\frac{C}{18}k^4\tau^3, \tag{2.93}$$

$$\theta_\nu = -\frac{C}{18}\frac{23+4R_\nu}{15+4R_\nu}k^4\tau^3, \tag{2.94}$$

$$\sigma_\nu = \frac{4C}{3(12+R_\nu)}k^2\tau^2, \tag{2.95}$$

$$\tag{2.96}$$

where C is an overall normalization constant and R_ν is the neutrinos fraction $\rho_{\nu 0}/(\rho_{\nu 0} + \rho_{\gamma 0})$, we have also four isocurvature modes to take into account for the initial conditions [38]. They are the baryon isocurvature mode, the CDM isocurvature mode, the neutrino density isocurvature mode and the neutrino velocity isocurvature mode.The neutrino velocity mode is divergent in the Newtonian gauge, so we will use the synchronous gauge in which all

the modes are finite.

2.5.2 The Curvature Perturbation

When isocurvature modes and more than one species are present the relation $c_i^2 = w_i$ between the speed of sound and the equation of state ceases to be valid. It is then useful to connect the total pressure perturbation to the density fluctiation as:

$$\delta P = c_s^2 \delta\rho + \delta P_{\rm nad}, \tag{2.97}$$

where

$$c_s^2 = \left(\frac{\delta P}{\delta\rho}\right)_\Gamma \tag{2.98}$$

is the adiabatic speed of sound, while

$$\delta P_{\rm nad} = \left(\frac{\delta P}{\delta\Gamma}\right)_\rho \delta\Gamma \tag{2.99}$$

is the non-adiabatic contribution to the total pressure. Of course, for the adiabatic mode $\delta P_{\rm nad}$ vanishes.

The importance of the non-adiabatic pressure relies in its keyrole in the evolution equation for the quantity $\mathcal{R}$, called comoving curvature perturbation, defined as [49]:

$$\mathcal{R} = \Phi + \mathcal{H}\frac{\theta}{k^2} \tag{2.100}$$

in the Newtonian gauge. Using the background and the perturbed Einstein equation, we obtain another useful expression for $\mathcal{R}$ [50]:

$$\mathcal{R} = \Phi + \frac{\mathcal{H}}{\mathcal{H}^2 - \mathcal{H}'}(\Phi' + \mathcal{H}\Phi) = \Phi + \frac{2\mathcal{H}}{a^2(\rho + P)}(\Phi' + \mathcal{H}\Phi). \tag{2.101}$$

Finally, combining the perturbed Einstein equations (2.45), we can find the useful equation

$$\Phi'' + \mathcal{H}[\Psi' + (2+3c_s^2)\Phi'] + [\mathcal{H}^2(1+2c_s^2) + 2\mathcal{H}']\Psi + k^2 c_s^2 \Psi - \frac{1}{3}(\Psi - \Phi) = 4\pi G a^2 \delta P_{\rm nad}. \tag{2.102}$$

Taking the derivative of Eq.(2.100) with respect to the conformal time and using Eq.(2.102), we then find the evolution of the comoving curvature perturbation:

$$\mathcal{R}' = \frac{\mathcal{H}}{P+\rho}\delta P_{\rm nad} + k^2 \frac{\mathcal{H}}{4\pi G a^2(\rho+P)}\left[\left(c_s^2 - \frac{1}{3}\right)\Psi + \frac{1}{3}\Phi\right]. \qquad (2.103)$$

We thus see that for adiabatic perturbations and large scale, so that we can neglect terms proportional to k, the comoving curvature perturbation remains constant outside the horizon. This is the reason for which adiabatic perturbations are often called curvature perturbations, indeed adiabatic perturbations can be characterized by the comoving curvature perturbation $\mathcal{R}$. Since the entropy perturbation is related to the non-adiabatic pressure by $\mathcal{S} = H\delta P_{\rm nad}/\dot{P}$, if isocurvature are present we must consider the effects of a non-vanishing $\delta P_{\rm nad}$ and the situation is completely different [51].

Chapter 3

Isocurvature Perturbations in General Relativity

The simplest models of inflation predict an approximately scale invariant spectrum of adiabatic and Gaussian fluctuations [48]. As mentioned in the last chapter, the curvature perturbatin remains constant on super horizon scale and therefore allow cosmologists to probe directly the physics of inflation from current CMB and large scale structure observations. However, as we will see in this chapter, multi-field inflationary models [52], in which inflation is driven by many scalar fields, predict that there might also be isocurvature perturbations together with the adiabatic one. In what follows, we start with an overview of the dynamics of these isocurvature modes in general relativity considering their imprints on the CMB power spectra. Then we consider a possible statistical correlation between adiabatic and isocurvature modes and introduce the formalism to deal with it. We next we analize how dark energy in the form of a quintessence field may lead to isocurvature modes. Finally we give a brief review of the generation of isocurvature modes during inflation.

3.1 Isocurvature Initial Conditions

In addition to the adiabatic mode (2.89), solving the coupled set of Einstein and Boltzmann equations deep in the radiation era before recombination, but well after neutrino decoupling, for a Universe filled with baryons, neutrinos, photons and CDM particles, should give other possible solutions that can be used as initial conditions for the CMB. A review of these modes has been carried out by Bucher et al. in Ref.[38], where they found that four new regular isocurvature modes arise. In fact, each fluid component is described by its density and velocity, so adding a fluid means adding two differential equations to the set and thus two more solutions can be found, one of which is a gauge mode. Since we are not interested in distinguishing neutrino flavours (we are only interested in how the perturbations in the neutrino fluid affect cosmological observations of the density and CMB today) we have four different fluid components and thus in principle we have more than just the five, 1 adiabatic plus 4 isocurvature, modes mentioned. However it is important to identify how many of these modes are physical and not gauge modes. This can be done in the synchronous gauge, in which the two gauge modes for scalar perturbations are easily identified. For this reason, and for the numerical stability of this gauge, unless otherwise stated, we will use the synchronous gauge in this section. In addition to the gauge modes, we are also not interested in the decaying modes, i.e. in modes which show a singular behaviour for $\tau \to 0$; indeed these modes decay with time and become negligible, moreover for these modes the perfect fluid approximation breaks up at early times [53]. Thus, if we consider only regular modes (regular up to gauge modes), we obtain just four isocurvature solutions for the set of differential equations. In this way, any quadratic observable, like the matter or the CMB power spectra, is completely determined by a 5×5 real, symmetric power spectral matrix function of k in which off-diagonal elements estabilish correlations between modes. We now describe in detail these four regular isocurvature modes.

Baryon and CDM Isocurvature Modes

Since the imprints of the baryon and the CDM isocurvature modes on the CMB power spetrum are just related by a simple rescaling factor and thus qualitatively similar [54], we derive only the expression for the CDM isocurvature mode (see Ref.[38] for the baryon solution). For these solutions all the relative entropy perturbations (2.88) vanish with the exception of $\mathcal{S}_{CDM} \equiv \mathcal{S}_{\gamma c} \neq 0$ for the CDM mode ($\mathcal{S}_b \equiv \mathcal{S}_{\gamma b} \neq 0$ for the baryon mode) and the density perturbation of the CDM (baryons) compensate the photon one to give an overall vanishing photon-CDM (baryon) density perturbation. This mode is given by:

$$h = 4\Omega_{c0}\tau - 6\Omega_{c0}\tau^2, \tag{3.1}$$

$$\eta = -\frac{2}{3}\Omega_{c0}\tau + \Omega_{c0}\tau^2, \tag{3.2}$$

$$\delta_c = 1 - 2\Omega_{c0}\tau + 3\Omega_{c0}\tau^2, \tag{3.3}$$

$$\delta_b = -2\Omega_{c0}\tau + 3\Omega_{c0}\tau^2, \tag{3.4}$$

$$\delta_\gamma = -\frac{8}{3}\Omega_{c0}\tau + 4\Omega_{c0}\tau^2, \tag{3.5}$$

$$\delta_\nu = -\frac{8}{3}\Omega_{c0}\tau + 4\Omega_{c0}\tau^2, \tag{3.6}$$

$$\theta_c = 0, \tag{3.7}$$

$$\theta_{\gamma b} = -\frac{1}{3}\Omega_{c0}k^2\tau^2, \tag{3.8}$$

$$\theta_\nu = -\frac{1}{3}\Omega_{c0}k^2\tau^2, \tag{3.9}$$

$$\sigma_\nu = -\frac{2\Omega_{c0}}{3(2R_\nu + 15)}k^2\tau^3, \tag{3.10}$$

where $\Omega_{c0} = \rho_{c0}/4(\rho_{\nu 0} + \rho_{\gamma 0})$ and $R_\nu = \rho_{\nu 0}/(\rho_{\nu 0} + \rho_{\gamma 0})$. And using Eq.(2.39), the gravitational potentials at leading order are:

$$\Psi = \frac{(4R_\nu - 15)\Omega_{c0}}{2(15 + 2R_\nu)}\tau, \tag{3.11}$$

$$\Phi = -\frac{(4R_\nu - 15)\Omega_{c0}}{6(15 + 2R_\nu)}\tau. \tag{3.12}$$

A model, called primeval isocurvature model (PBI), in which the sole baryon isocurvature mode was considered the source of cosmological per-

turbations was introduced by Peebles [55, 56], but its predictions were in disagreement with the observations, being characterized by a lower small-scale relative peculiar velocities, greater large-scale flow velocities, earlier reionization and earlier galaxy and star formation [57]. The CDM isocurvature mode have been considered by Bond and Efstathiou in Ref.[58, 59] where they assumed this isocurvature mode as the dominant over the adiabatic, motivated by an axion model in which quantum fluctuations in the amplitude of the axion field during inflation may produce isocurvature fluctuations. The spectrum of density fluctuations has the same power law as for adiabatic perturbations with a scale-free spectrum $\mathcal{P}(k) \sim k$ on large scales, but compared to adiabatic scale-free fluctuations, the turnover to $\mathcal{P}(k) \sim k^{-3}$ behaviour on small scales occurs on a larger scale for the isocurvature case and this is the reason for which it was abandoned [38].

Neutrino Density Mode

In the neutrino density isocurvature (NDI) mode the only relative entropy perturbation that differs from zero is the one between photons and neutrinos $\mathcal{S}_\nu \equiv \mathcal{S}_{\gamma\nu} \neq 0$ and the neutrino density perturbation compensates the photon one. To obtain this solution (and the neutrino velocity mode), since one of the Einstein equations is redundant, we use the a combination of the first and the third of the Einstein equations in order to cancel out the perturbations in the radiation sector from these equations. The equation that we use is obtained multiplying Eq.(2.41) by a factor 2 and subtracting Eq.(2.43), in order to obtain the following equation:

$$h'' + 3\mathcal{H}h' - 5k^2\eta = -6\pi G a^2(\delta\rho_c + \delta\rho_b). \tag{3.13}$$

Using this equation instead of Eq.(2.43), the neutrino density mode is given by:

$$h = \frac{\Omega_{b0} R_\nu}{10 R_\gamma} k^2 \tau^3, \tag{3.14}$$

$$\eta = -\frac{R_\nu}{6(15 + 4R_\nu)} k^2 \tau^2, \tag{3.15}$$

$$\delta_c = -\frac{\Omega_{b0} R_\nu}{20 R_\gamma} k^2 \tau^3, \tag{3.16}$$

$$\delta_b = \frac{R_\nu}{8 R_\gamma} k^2 \tau^2, \tag{3.17}$$

$$\delta_\gamma = -\frac{R_\nu}{R_\gamma} + \frac{1}{6}\frac{R_\nu}{R_\gamma} k^2 \tau^2, \tag{3.18}$$

$$\delta_\nu = 1 - \frac{1}{6} k^2 \tau^2, \tag{3.19}$$

$$\theta_c = 0, \tag{3.20}$$

$$\theta_{\gamma b} = -\frac{1}{4}\frac{R_\nu}{R_\gamma} k^2 \tau + \frac{3\Omega_{b0} R_\nu}{4 R_\gamma^2} k^2 \tau^2, \tag{3.21}$$

$$\theta_\nu = \frac{1}{4} k^2 \tau, \tag{3.22}$$

$$\sigma_\nu = \frac{1}{2(4R_\nu + 15)} k^2 \tau^2, \tag{3.23}$$

where $\Omega_{b0} = \rho_{b0}/4(\rho_{\nu 0} + \rho_{\gamma 0})$ and $R_\gamma = \rho_{\gamma 0}/(\rho_{\nu 0} + \rho_{\gamma 0})$. The gravitational potentials are constant at leading order:

$$\Psi = -\frac{2R_\nu}{(15 + 4R_\nu)}, \tag{3.24}$$

$$\Phi = \frac{R_\nu}{(15 + 4R_\nu)}. \tag{3.25}$$

As can be seen from Eqs.(3.14), one starts with the sum of the neutrino and photon densities unperturbed and when a mode enters the horizon ($k\tau > 1$), the photons behave as a perfect fluid because of Thomson scattering, whereas the neutrinos freestream creating non-uniformity in the energy density, pressure and momentum and so generating the metric perturbations h and η.

Neutrino Velocity Mode

The neutrino velocity isocurvature (NVI) mode refers to fluctuations in the neutrino velocity relative to the average bulk velocity of the cosmic fluid and we can arrange the photon-baryon and neutrino fluids to have equal and opposite momentum density. This mode is given by:

$$h = \frac{3}{2}\frac{\Omega_{b0}R_\nu}{R_\gamma}k\tau^2, \tag{3.26}$$

$$\eta = -\frac{4R_\nu}{3(5+4R_\nu)}k\tau + \left(\frac{20R_\nu}{(5+4R_\nu)(15+4R_\nu)} - \frac{\Omega_{b0}R_\nu}{4R_\gamma}\right)k\tau^2, \tag{3.27}$$

$$\delta_c = -\frac{3\Omega_{b0}R_\nu}{4R_\gamma}k\tau^2, \tag{3.28}$$

$$\delta_b = \frac{R_\nu}{R_\gamma}k\tau - \frac{3\Omega_{b0}R_\nu(R_\gamma+2)}{4R_\gamma^2}k\tau^2, \tag{3.29}$$

$$\delta_\gamma = \frac{4R_\nu}{3R_\gamma}k\tau - \frac{\Omega_{b0}R_\nu(R_\gamma+2)}{R_\gamma^2}k\tau^2, \tag{3.30}$$

$$\delta_\nu = -\frac{4R_\nu}{3R_\gamma}k\tau - \frac{\Omega_{b0}R_\nu}{R_\gamma^2}k\tau^2, \tag{3.31}$$

$$\theta_c = 0, \tag{3.32}$$

$$\theta_{\gamma b} = -\frac{R_\nu}{R_\gamma}k + \frac{3\Omega_{b0}R_\nu}{R_\gamma^2}k\tau + \frac{R_\nu 3\Omega_{b0}}{R_\gamma^2}\left(1 - \frac{3\Omega_{b0}}{R_\gamma}\right)k\tau^2 + \frac{R_\nu}{6R_\gamma}k^3\tau^3, \tag{3.33}$$

$$\theta_\nu = k - \frac{(9+4R_\nu)}{6(5+4R_\nu)}k^3\tau^2, \tag{3.34}$$

$$\sigma_\nu = \frac{4}{3(5+4R_\nu)}k\tau + \frac{16R_\nu}{(5+4R_\nu)(4R_\nu+15)}k\tau^2, \tag{3.35}$$

$$F_{\nu 3} = \frac{4}{7(5+4R_\nu)}k^2\tau^2. \tag{3.36}$$

We observe that the gravitational potentials are singular:

$$\Psi = -\frac{4R_\nu}{(15+4R_\nu)}k^{-1}\tau^{-1}, \tag{3.37}$$

$$\Phi = \frac{4R_\nu}{(15+4R_\nu)}k^{-1}\tau^{-1}, \tag{3.38}$$

however this singularity must be regarded as a coordinate singularity, since the description in the synchronous gauge is regular. The initial perturbation

in the total momentum density vanishes, in this way the metric perturbations are regular. If they were not perfectly matched, the latter would diverge for $\tau \to 0$. We point out that at present a mechanism for exciting this mode is lacking [60, 61].

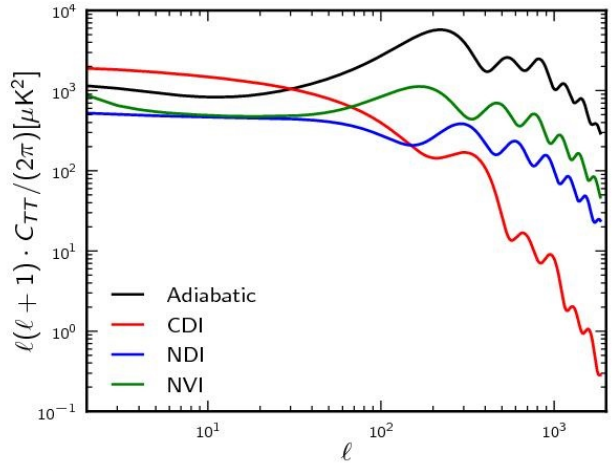

Figure 3.1: C^{TT} anisotropy shapes for the three isocurvature modes and for the adiabatic one. All the modes have the same amplitude parameters. Figure taken from [60].

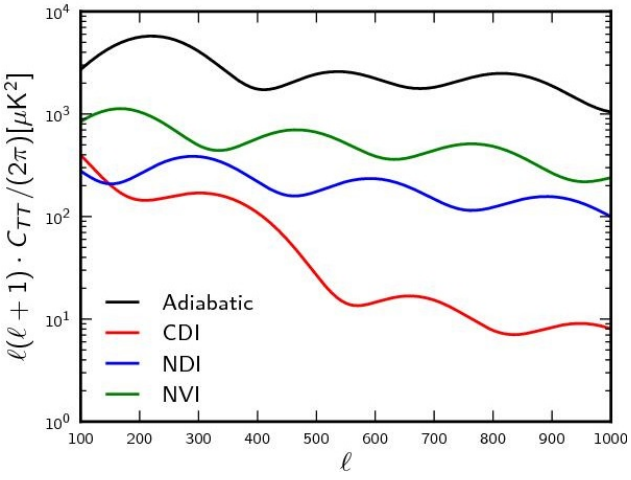

Figure 3.2: Zoom on a narrower l range to show the positions of the acoustic peaks in the different modes. Figure taken from [60].

3.2 Imprints of Pure Isocurvature Perturbations on the CMB

As already mentioned, the baryon and CDM isocurvature modes yield identical angular spectra, with a slightly different amplitude, because the deficit of one is balanced by an excess of the other. Therefore, following [54], we define the effective cold dark matter isocurvature mode (CDI) by $\mathcal{S}_{CDI} \equiv \mathcal{S}_{CDM} + (\Omega_{b0}/\Omega_{c0})\mathcal{S}_b$. This effective mode encodes both CDM and baryon isocurvature fluctuations.

We show the imprints on the CMB temperature spectrum of the three different modes together with the adiabatic mode in figure 3.1.

As can be seen they lead to different shape of the power spectrum, in particular the acoustic peak structure for the isocurvature modes is totally different from the adiabatic one, as can be seen from figure 3.2. Since the adiabatic CMB power spectrum fits the data very well, the possibility of considering isocurvature modes as the sole source of perturbations has been ruled out [62].

3.3 Correlated Adiabatic and Isocurvature Perturbations

So far, we have considered adiabatic and isocurvature pertubations and their distinct behaviour for what concerns their imprints on the CMB and on the comoving curvature perturbation. However, as we will see in the next section, there are situations in which isocurvature perturbations can source adiabatic perturbations on large scales. Also, isocurvature and adiabatic perturbations may be correlated [63, 64, 65]. We can parameterize the transformation of the curvature (adiabatic) perturbation $\mathcal{R}$ and the entropy (isocurvature) perturbation $\mathcal{S}$ from the time to horizon exit during inflation

to the beginning of radiation dominated era by:

$$\begin{pmatrix}\mathcal{R}_{\rm rad}\\ \mathcal{S}_{\rm rad}\end{pmatrix}=\begin{pmatrix}1\ T_{\mathcal{RS}}\\ 0\ T_{\mathcal{SS}}\end{pmatrix}\begin{pmatrix}\mathcal{R}_{*}\\ \mathcal{S}_{*}\end{pmatrix}, \tag{3.39}$$

where the subscript $*$ means that the perturbations on the right hand side must be evaluated at horizon crossing $k=\mathcal{H}$. We have assumed $T_{\mathcal{SR}}=0$ and $T_{\mathcal{RR}}=1$ since physically an adiabatic perturbation cannot source isocurvature perturbations on large scales [66] and for purely adiabatic perturbations the curvature perturbation is conserved. Since large scale fluctuations are produced during inflation, the slow evolution of light fields after horizon crossing translates into a weak scale dependence of both the perturbations at horizon crossing and the matrix coefficients $T_{\mathcal{RS}}$ and $T_{\mathcal{SS}}$. Therefore the scale dependence of $\mathcal{R}_{\rm rad}$ and $\mathcal{S}_{\rm rad}$ comes from the initial scale dependence of $\mathcal{R}_{*}$ and $\mathcal{S}_{*}$, which can be expressed in term of classical random Gaussian fields, respectively $\hat{a}_r$ and $\hat{a}_s$, with unit variance $\langle\hat{a}_r\hat{a}_s\rangle=(2\pi)^3\delta_{rs}$. Thus we can write the perturbations in the radiation era as:

$$\mathcal{R}_{\rm rad}=A_r k^{n_1}\hat{a}_r+A_s k^{n_3}\hat{a}_s, \tag{3.40}$$

$$\mathcal{S}_{\rm rad}=B k^{n_2}\hat{a}_s, \tag{3.41}$$

where the initial amplitudes at horizon crossing and the matrix elements of (3.39) have been absorbed into the amplitudes A_s, A_r and B.

If we consider the simplest case when $n_1=n_2\neq n_3$, the power spectra and the cross-correlation spectrum are:

$$\mathcal{P}_{\mathcal{R}}(k)=(A_r^2+A_s^2)k^{2n_1}\equiv A^2k^{n_{\rm ad}-1}, \tag{3.42}$$

$$\mathcal{P}_{\mathcal{S}}(k)=B^2k^{2n_2}\equiv A^2f_{\rm iso}^2k^{n_{\rm iso}-1}, \tag{3.43}$$

$$\mathcal{P}_{\mathcal{RS}}(k)=A_sBk^{n_2+n_3}\equiv A^2f_{\rm iso}\cos\theta\,k^{(n_{\rm ad}+n_{\rm iso})/2-1}, \tag{3.44}$$

where $A=\sqrt{A_s^2+A_r^2}$, $f_{\rm iso}\equiv B/A$ is the relative $\mathcal{S}$ to $\mathcal{R}$ amplitude, $n_{\rm ad}\equiv 2n_1+1$, $n_{\rm iso}\equiv 2n_2+1$ and we parameterize the correlation between $\mathcal{S}$ and $\mathcal{R}$ with the angle θ given by

$$\cos\theta=\frac{\langle\mathcal{R}_r\mathcal{S}_r\rangle}{\sqrt{\langle\mathcal{R}_r^2\rangle}\sqrt{\langle\mathcal{S}_r^2\rangle}}=\frac{{\rm sign}(B)A_sk^{n_3}}{\sqrt{A_r^2k^{2n_1}+A_s^2k^{2n_3}}}={\rm sign}(B)\frac{A_s}{A}. \tag{3.45}$$

We note that in the case considered $\cos\theta$ is scale independent, but, in general, it is a function of k. The two modes are said to be fully correlated if $\cos\theta = 1$ and fully anti-correlated if $\cos\theta = -1$. It is also important to point out that with these definitions we are implicitly defining the quantities $f_{\rm iso}, n_{\rm ad}$ and $n_{\rm iso}$ at some pivot scale k_0.

3.3.1 Contribution to the CMB Power Spectrum

The different amount of correlation between isocurvature and adiabatic modes can give different imprints in the CMB angular power spectrum, which can be obtained from the radiation transfer function $\Theta_l^{\rm ad}(k)$ and $\Theta_l^{\rm iso}(k)$ for the pure adiabatic and isocurvature initial conditions. Apart from a possible normalization factor, the transfer function for a generic source $S(k,\tau)$ for the temperature anisotropy, is given by [31]:

$$\Theta_l^{\rm S}(k) = \int_0^{\tau_0} d\tau\, S(k,\tau) j_l[k(\tau-\tau_0)], \tag{3.46}$$

where j_l is the spherical Bessel function. We can thus write the temperature anisotropies as follows:

$$C_l^{\rm ad} = \int \frac{dk}{k} \left(\frac{k}{k_0}\right)^{n_{\rm ad}-1} [\Theta_l^{\rm ad}(k)]^2, \tag{3.47}$$

$$C_l^{\rm iso} = \int \frac{dk}{k} \left(\frac{k}{k_0}\right)^{n_{\rm iso}-1} [\Theta_l^{\rm iso}(k)]^2, \tag{3.48}$$

$$C_l^{\rm corr} = \int \frac{dk}{k} \left(\frac{k}{k_0}\right)^{(n_{\rm ad}+n_{\rm iso})/2-1} \Theta_l^{\rm ad}(k)\Theta_l^{\rm iso}(k) \tag{3.49}$$

and the total angular power spectrum becomes

$$C_l^{\rm tot} = A^2 C_l^{\rm ad} + B^2 C_l^{\rm iso} + 2AB\cos\theta C_l^{\rm corr}, \tag{3.50}$$

or simply

$$C_l^{\rm tot} = A^2[C_l^{\rm ad} + f_{\rm iso}^2 C_l^{\rm iso} + 2 f_{\rm iso}\cos\theta C_l^{\rm corr}]. \tag{3.51}$$

Another possible notation can be employed (see for example [67, 61]), identifying $\alpha \equiv B^2/(A^2+B^2)$ and $\beta \equiv \cos\theta$ in order to characterize the

C_ls with the isocurvature fraction α that runs from purely adiabatic $\alpha = 0$ to purely isocurvature $\alpha = 1$. The two parameterizations are related by $\alpha = f_{\rm iso}^2/(1 + f_{\rm iso}^2)$ and the angular power spectrum is now given by:

$$C_l^{\rm tot} = (A^2 + B^2)[(1-\alpha)C_l^{\rm ad} + \alpha C_l^{\rm iso} + 2\beta\sqrt{\alpha(1-\alpha)}C_l^{\rm corr}]. \qquad (3.52)$$

To compute the CMB power spectrum for the partial correlation case, it is sufficient to compute the two pure adiabatic and isocurvature spectrum $C_l^{\rm ad}$ and $C_l^{\rm iso}$ and the total spectrum $C_l^{\rm tot}$ for the fully correlated case. Then one just computes $C_l^{\rm corr}$ using Eq.(3.50) and uses this value to compute $C_l^{\rm tot}$ for partial correlation case. If $\cos\theta = 0$ the correlation vanishes and therefore $C_l^{\rm tot} = C_l^{\rm ad} + C_l^{\rm iso}$.

3.4 Isocurvature Perturbations in Quintessence Models

It is crucial to review the main results, well known in the literature, of the quintessence perturbations, in order to compare these with our results in scalar tensor dark energy models.

Since its weakly coupled nature, the quintessence field is an unthermalized component in the Universe and thus it is possible that its perturbations are not exactly adiabatic. We parameterize the scalar quintessence field Q with the equation of state parameter w_Q and with the adiabatic sound speed $c_Q^2 = \dot{p}_Q/\dot{\rho}_Q$. In figure 3.3 we show a typical scenario [68, 69] for the background evolution of the scalar field. During the radiation era the quintessence field starts out subdominat in the so called kinetic phase in which $w_Q = 1$, then the kinetic energy eventually decays leading to the potential phase in which the density of the scalar field is dominated by the potential $V(Q)$ and $w_Q = -1$. When $\Omega_Q \equiv \rho_Q/\rho_{\rm tot}$ becomes of order unity, the scalar field undergoes a transition and it enters the tracking regime in which it follows the equation of state of the background. As mentioned in Sec.1.8.2, in the tracking regime the quintessence kinetic and potential

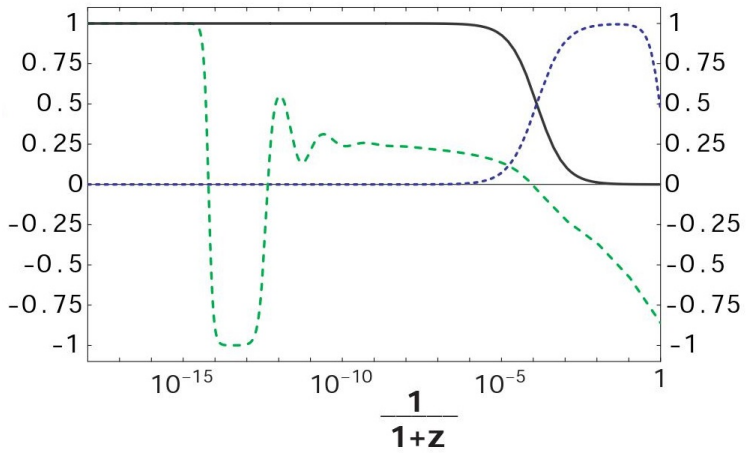

Figure 3.3: Densities of radiation (solid line) and matter (dotted line), and the equation of state for the scalar field (dashed line), as a function of redshift for a model with potential $V(Q) = M^4 e^{f/Q}$. In this plot $M^4 = 10^{-70} M_{\rm pl}^4$ and $f = M_{\rm pl}$. Figure taken from [68].

energy have a fixed ratio and the relation $\dot{Q}^2 \propto V(Q)$ holds. It can be shown that, if this condition holds, the energy density of the quintessence field takes the simple power law form a^{-n}, with n constant. On the other side the density of the dominant component evolves as $\rho_D \propto a^{-m}$. Whether $n = m$ or $n \neq m$ it depends only on the model considered. For example, the AS model considered in [70] has $n = m$ and thus ρ_Q can be a sizable fraction of the total energy density at early epoch. In the Ratra-Peebles model [23] $n < m$ and ρ_Q decreases more slowly than ρ_D and thus cannot be a significant fraction of the energy density in the early universe and it is negligible until recent times. At late times, finally, the quintessence field starts to dominate leading to the acceleration of the Universe we observe today.

We can measure how closely the quintessence field tracks the background with the help of the quantity $\gamma \equiv V_{,QQ}\, V/(V_{,Q}^2)$. When the equation of state parameter w_Q is constant, the sound speed c_Q^2 is constant in the same way; if this is the case, also γ is constant and it can be approximated to [68]:

$$\gamma \simeq 1 + \frac{w_F - w_Q}{2(1 + w_Q)}, \tag{3.53}$$

where $F = r, m$ stands for radiation for $t \ll t_{\rm eq}$ and for matter for $t \gg t_{\rm eq}$.

3.4.1 Evolution of Quintessence Perturbations

To analize the fluctuations of the quintessence field we decompose it into the sum of an unperturbed space-independent part and a perturbation as follow:

$$Q(t, \mathbf{x}) = \bar{Q}(t) + \delta Q(t, \mathbf{x}), \tag{3.54}$$

where δQ follows the perturbed Klein-Gordon equation in the Newtonian gauge [71]

$$\ddot{\delta Q} + 3H\dot{\delta Q} + \frac{k^2}{a^2}\delta Q + V_{,QQ}\,\delta Q = (\dot{\Psi} + 3\dot{\Phi})\dot{Q} - 2V_{,Q}\,\Psi. \tag{3.55}$$

In the long wavelength limit, the equation for the density contrast of the dominant component is [30]:

$$\dot{\delta}_F = 3(1 + w_F)\dot{\Psi} \tag{3.56}$$

for which we have the simple solution

$$\delta_F - 3(1 + w_F)\Phi = \text{const.} \tag{3.57}$$

We can solve the homogeneus equation associated to Eq.(3.55) neglecting the gravitational potentials and switching to the conformal time. To do this we define $\delta\tilde{Q} \equiv a^{1/2*}$ and consider the radiation dominated era in which $a \propto \tau$ and $\mathcal{H} = 1/\tau$, Eq.(3.55) becomes:

$$\delta\tilde{Q}'' + \frac{1}{\tau}\delta\tilde{Q}' + \left[k^2 + a^2 V_{,QQ} - \frac{1}{\tau^2}\right]\delta\tilde{Q} = 0. \tag{3.58}$$

The solution of this equation in the tracking regime where $V_{,QQ} = \text{const} \equiv \alpha H^2$ is:

$$\delta Q \sim \tau^{-1/2} \times \begin{cases} J_{|\nu|}(k\tau) \\ J_{-|\nu|}(k\tau), \end{cases} \tag{3.59}$$

*If we had considered the matter dominated era the right substitution would have been $\delta\tilde{Q} \equiv a^{3/4}$. Nevertheless the results would have been the same.

where

$$\nu^2 = \frac{1}{4} - \alpha. \tag{3.60}$$

These solutions decay in time, unless $\alpha \to 0$; if this is the case, the first solution in Eq.(3.59) is constant. If we include the gravitational potentials in the equation and neglect anisotropic stresses, thus assuming $\Psi = \Phi$, then we have a constant particular solution to the inhomogeneus differential equation Eq.(3.55):

$$\Phi(t) = \Phi^c, \tag{3.61}$$

$$\delta Q(t) = \delta Q^c \simeq -2\frac{V_{,Q}}{V_{QQ}}\Phi_c, \tag{3.62}$$

since in the tracking regime $V_{,Q}\,/V_{,QQ}$ is approximately constant. This solution holds for any potential $V(Q)$ as long as the latter quantity is constant, i.e. as long as there is tracking.

The energy densities of quintessence and of the dominant fluid can be related to this constant solution through the 0-0 component of the Einstein equations (2.45) neglecting the energy densities of subdominant fluids. Thus, in the tracking regime, the following relationship among the quintessence and dominant fluid densities and the gravitational potential (3.61) holds:

$$\delta_Q^c \simeq \delta_F^c \simeq -2\Phi^c, \tag{3.63}$$

thus the two fluids are indistinguishable and we expect isocurvature perturbations to be suppressed during the tracking regime. This means that tracking is a gravitational mechanism that plays the role of thermal equilibrium and tends to reduce isocurvature perturbations between the two fluids. Although it ceases to be time independent, the solution (3.61) is a good approximation even during the quintessence domination, in fact when tracking ends, despite the attractor disappearing, most modes have already settled down to the same value and then experience the same evolution.

To study the evolution of isocurvature perturbations it is important to compute the non-adiabatic pressure (2.99). In the tracking regime, when

radiation dominates, it is given by [68]:

$$\delta P_{\rm nad} \simeq \frac{\dot{Q}^2}{\rho_{\rm tot}} + P_{\rm tot}(w_r - c_Q^2)(\rho_r \delta_r - 2\Phi\rho_Q) + \mathcal{O}[(\gamma - 1)\rho_Q \Phi] \tag{3.64}$$

and it vanishes for exact tracking ($\gamma = 1$). Indeed the entropy perturbation between radiation and quintessence vanishes in this case, i.e. $\mathcal{S}_{rQ} = 0$. If the tracking is not exact, since in general $\delta P_{\rm nad} \propto \rho_Q$, it is small when the energy contribution of quintessence is very subdominant, but it does not vanish. However, a possibility that allows for significant isocurvature fluctuations from quintessence, which can leave imprints on the CMB power spectrum, is that the quintessence fields enters the tracking regime at later times so that the fluctuations may not damp so much.

Finally, we define the following quantity to parameterize the size of the quintessence isocurvature contribution [71]:

$$r_Q = \frac{\delta Q}{M_{\rm pl}\Psi_{\rm rad}}, \tag{3.65}$$

where $\Psi_{\rm rad}$ is Ψ from the adiabatic mode contribution from the inflaton fluctuations in the deep radiation dominated epoch, that is given by [72]:

$$\Psi_{\rm rad} = \frac{4}{9}\left(\frac{H_{\rm inf}V_{\rm inf}}{2\pi M_{\rm pl}^2 V'_{\rm inf}}\right), \tag{3.66}$$

where $V_{\rm inf}$ is the inflaton potential, $H_{\rm inf}$ is the Hubble parameter during inflation and here a prime $'$ denotes the derivative with respect to the inflaton field.

3.4.2 Imprints of Quintessence Perturbations on the CMB

The imprints on the CMB power spectrum of the quintessence fluctuations have been studied by several authors [73, 71, 74, 75, 76]. Since the small scales fluctuations of the quintessence fields damp when they cross the horizon [68], they affect the CMB spectrum only on large angular scales and

thus their effects are especially important for low multipoles. This region is characterized by some anomalies observed by Planck and WMAP which may benefit from particular quintessence contributions [77].

In particular in [71, 75] it has been investigated the possibility to alleviate the low quadrupole issue by including quintessence perturbations and isocurvatures.

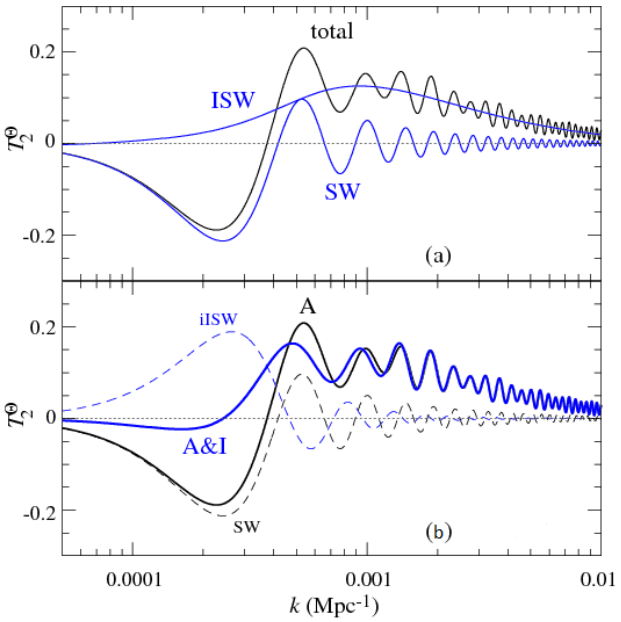

Figure 3.4: Panel (a): temperature quadrupole transfer function in the fiducial adiabatic model. Panel (b) ISW and SW contribution from the isocurvature fluctuation and transfer function for the correlated adiabatic and isocurvature mode (A& I). Dark energy equation of state $w_Q = -1$, nonrelativistic matter density $\Omega_m h^2 = 0.14$, baryon density $\Omega_b h^2 = 0.024$, dark energy density relative to critical $\Omega_Q = 0.73$ and optical depth to reionization $\tau = 0.17$. In our notations $T_2^\Theta = \Theta_2^T$. Figure taken from [75].

A modification of the ISW or SW may have an impact on the quadrupole: as pointed out in Ref.[74] isocurvature quintessence fluctuations produced by the model considered in the last section can lower the low multipoles behavior of the CMB power spectrum if $r_Q > 0$, that is for positive correlation with

the metric perturbation $\Psi_{\rm rad}$. Instead, when there is a situation of anti-correlation where $r_Q <= 0$ then we have an enhancement of C_ls at low multipoles. Therefore a positive correlation with the metric perturbation $\Psi_{\rm rad}$ is required in order to obtain the suppression of the C_ls at low multipoles.

If this is the case, as can be seen from the lower panel of figure 3.4, the effect of the isocurvaure ISW (labelled iISW in the figure) cancels the SW effect for the temperature quadrupole, but it leaves the shape of the transfer function at lower scales unaffected. As a result, the correlated adiabatic and isocurvature transfer function has the same shape of pure the adiabatic mode (labelled A in the figure) for high k, whereas the SW effect in the quadrupole in the pure adiabatic mode has been cancelled. This is reflected in a suppression of the C_ls at low multipoles without affecting their shape at high multipoles.

3.5 Generation of Isocurvature Perturbations during Inflation

Finally, we consider in this section the issue of how isocurvature perturbations can be generated. Since the adiabatic perturbations are generated during inflation, leading to a superhorizon constant curvature perturbation, that seeds the inhomogeneities at its horizon re-entry, we examine how inflation can produce a spectrum of isocurvature perturbations in addition to the adiabatic ones.

Adiabatic modes are always present, indeed there is a theorem [49] that states that the field equations for cosmological perturbations in the Newtonian gauge always have two adiabatic solutions: a growing solution for which $\mathcal{R}$ is constant in all eras in the limit of large wavelength and a decaying solution for which $\mathcal{R} = 0$ for large wavelength. If there are no anisotropic stresses, we have $\Psi = \Phi$ and the adiabatic solutions for the metric perturbation Φ and for the perturbation of any four-scalar $s(\mathbf{x}, t) = \bar{s}(t) + \delta s(\mathbf{x}, t)$

are given by [78, 79, 9]:

$$\Phi = C_1 \left(1 - \frac{H}{a}\int_T^t dt'\, a(t')\right) + C_2 \frac{H}{a}, \tag{3.67}$$

$$\frac{\delta s}{\dot{\bar{s}}} = \frac{1}{a}\left(C_1 \int_T^t dt'\, a(t') - C_2\right), \tag{3.68}$$

where T is an arbitrary integration time and C_1, C_2 are the time independent coefficients for the growing and decaying adiabatic modes, for which $\mathcal{R} = C_1$ and $\mathcal{R} = 0$ respectively. However, this theorem does not guarantee the existence of isocurvature perturbations, that therefore must be analized for each different model.

In the simplest case of a single field inflation with an action (1.54), isocurvature modes cannot be produced. On the contrary, in multiple field inflation models [52], where the inflation is driven by many scalar fields, say N, their N indipendent branches of non-decaying quantum fluctuations generated during the inflationary stage produce $N-1$ isocurvature solutions in addition to the adiabatic mode [80, 81, 79]. The isocurvature perturbations so produced can then survive up to the present only if at least one of the inflaton scalar fields remains unthermalized and uncoupled to the usual matter during the whole evolution of the Universe from the end of the inflationary era up to the present time, as in the case in which quintessence partecipate to inflation as one of the inflaton fields [82].

The general action of multiple field inflation models is given by[†] [9]:

$$S = \int d^4x\, \frac{\sqrt{-g}}{2}\left[\frac{R}{8\pi G} - g^{\mu\nu}\gamma_{nm}(\phi)\frac{\partial\phi_n}{\partial x^\mu}\frac{\partial\phi_m}{\partial x^\nu} - V(\phi)\right], \tag{3.69}$$

where $n, m = 1, \ldots, N$, $V(\phi)$ is an arbitrary potential and the arbitrary real positive-definite matrix $\gamma_{nm}(\phi)$ is called the field metric. For simplicity we will consider the simplest model in which $\gamma_{nm} = \delta_{nm}$ (for multifield inflation with non-canonical kinetic terms see, for example, [83, 84, 85, 9]) and the scalar fields interact mutually only through gravity, i.e. $V(\phi) = \sum_{n=1}^{N} V_n(\phi_n)$.

[†]The summation over the field indices is understood.

In this simple case, the equation of motion can be derived applying the action principle to the action (3.69) at zero order are the Einstein equations:

$$H^2 = \frac{8\pi G}{3}\sum_{j=1}^{N}\left[\frac{\dot{\bar{\phi}}_j^2}{2} + V_j(\bar{\phi}_j)\right], \tag{3.70}$$

$$\dot{H} = -4\pi G\sum_{j=1}^{N}\dot{\bar{\phi}}_j^2 \tag{3.71}$$

and the usual Klein-Gordon equations for each of the N fields

$$\ddot{\bar{\phi}}_j + 3H\dot{\bar{\phi}}_j + V_j'(\bar{\phi}_j), \quad j = 1, \ldots, N, \tag{3.72}$$

where, here a prime $'$ denotes a derivative with respect to the j-th scalar field for notation convenience. We can see from Eq.(3.71) that in these models H always decreases with time.

The equations for the perturbations in the Newtonian gauge are [79, 86]:

$$\dot{\Phi} + H\Phi = 4\pi G\sum_{j=1}^{N}\dot{\bar{\phi}}_j\delta\phi_j, \tag{3.73}$$

$$\delta\ddot{\phi}_j + 3H\delta\dot{\phi}_j + \left(\frac{k^2}{a^2} + V_j''\right)\delta\phi_j = 4\dot{\bar{\phi}}_j\dot{\Phi} - 2V_j'\Phi, \tag{3.74}$$

for $j = 1, \ldots, N$. The theorem mentioned above ensures that the adiabatic solution to this system of differential equations has the form of Eqs.(3.67) and (3.68). So far no mention on inflation has been made. However, since we are interested in finding the perturbations set up during inflation, we now use the slow-roll approximation for the N scalar fields:

$$|\ddot{\phi}_j| \ll 3H|\dot{\phi}_j|, \;\; \dot{\phi}_l^2 \ll 2V(\phi), \;\; |\dot{H}| \ll H^2, \;\; j = 1, \ldots, N, \tag{3.75}$$

so that we can neglect the fields kinetic energies in Eq.(3.70) and their accelerations in Eq.(3.72). In addition, since the solutions for non-decreasing isocurvature and growing adiabatic modes depend weakly on time [78, 81], we can neglect terms proportional to $\delta\ddot{\phi}_j$ and $\dot{\Phi}$ in the perturbed equations (3.73). With these assumptions, the general non-decaying solution of the

perturbed equations is:

$$\Phi = -C_1 \frac{\dot{H}}{H^2} - H \frac{d}{dt}\left(\frac{\sum_j V_j d_j}{\sum_j V_j}\right), \tag{3.76}$$

$$\frac{\delta\phi_j}{\dot{\phi}_j} = \frac{C_1}{H} - 2H\left(\frac{\sum_k V_k d_k}{\sum_k V_k} - d_j\right), \quad j,k = 1,\ldots,N, \tag{3.77}$$

where only $N-1$ out of the N integrations constants d_j are linearly independent. Comparing these solutions to Eqs.(3.67) and (3.68), since during inflation $\frac{\dot{H}}{H^2} \simeq -\left(-1 + \frac{H}{a}\int_T^t dt'\, a(t')\right)$ [83], we see that the mode with the coefficient C_1 is the growing adiabatic mode, while the remaining $N-1$ are the isocurvature modes. A similair procedure may be followed to find the decaying adiabatic and isocurvature modes [81], but we are not interested in them.

The next step is to match the coefficients C_1 and d_j to the amplitudes of quantum fluctuations of scalar fields generated during inflation. To do this, we need to invert Eqs.(3.76) and (3.77), obtaining:

$$C_1 = 8\pi G \sum_j \frac{V_j}{V_j'}\delta\phi_j, \tag{3.78}$$

$$d_j = \frac{\delta\phi_j}{2H\dot{\phi}_j} - \frac{C_1}{2H^2} + \frac{\sum_k d_k V_k}{\sum_k V_k}, \quad j,k = 1,\ldots,N, \tag{3.79}$$

where the use of the zero order Klein-Gordon equation has been made to find Eq.(3.78). We can use the linear dependence of the N coefficients d_j to add a constant term to them, in order to cancel out the last two term of Eq.(3.79), in this way both C_1 and d_j dependes only on the perturbed scalar fields $\delta\phi_j$ and it becomes simple to match them to the quantum fluctuations. All the scalar fields in the slow-roll regime behave as massless fields, i.e. $|m^2_{\text{eff}}| \equiv |V_j''| \ll H^2$, so the standard quantization rules for the long-wavelength perturbations $\delta\phi_j$ give the well known results [87, 33, 8]:

$$\delta\phi_j(\mathbf{k}) = \frac{H_k}{\sqrt{2k^3}} e_j(\mathbf{k}), \tag{3.80}$$

where H_k is the Hubble parameter evaluated at the time t_k of the first horizon crossing $k \simeq aH$ of the comoving scale $\mathbf{k}$ and $e_j(\mathbf{k})$ are a set of classical

random Gaussian variables with $\langle e_j(\mathbf{k})\rangle = 0$ and $\langle e_j(\mathbf{k})e^*_{j'}(\mathbf{k}')\rangle = \delta_{jj'}\delta(\mathbf{k}-\mathbf{k}')$. Substituting these results into Eqs. (3.76) and (3.77), we obtain the following results for the integration constants C_1 and d_j:

$$C_1(k) = -\frac{8\pi GH}{\sqrt{2k^3}}\sum_j \frac{V_j}{V'_j}e_j, \tag{3.81}$$

$$d_j(k) = -\frac{3H}{2\sqrt{2k^3V'_j}}e_j, \quad j = 1,\ldots,N. \tag{3.82}$$

It is now simple to compute the power spectrum of these quantities:

$$\mathcal{P}_{C_1}(k) = \frac{32\pi^2G^2H^2}{k^3}\sum_j \frac{V_j^2}{V'^2_j}, \tag{3.83}$$

$$\mathcal{P}_{d_j}(k) = \frac{9H^2}{8k^3V'^2_j}, \quad j = 1,\ldots,N. \tag{3.84}$$

Since for isocurvature perturbations we do not have general expressions like Eqs.(3.67) and (3.68), their behaviour after inflation depends strongly on the model considered. As we mentioned previously in this chapter, the most natural way in which they may still be present nowadays, is to assume that one of the inflaton fields remains uncoupled from usual matter since the end of inflation up to present and that its particles, or products of their decay, constitute now a part of the CDM. In this case it is possible to match the primordial isocurvature perturbations set up during inflation with the perturbations in the radiation dominated era [79, 63].

3.5.1 Adiabatic and Entropy Fields

A formalism, which introduces no new physics, but is very useful for working with the adiabatic and isocurvature perturbations produced in multi-field inflation has been introduced by Gordon et al. [86]. The idea at its basis is to split the trajectory in the space of the N fields into a component tangent to the background classical trajectory, which represents the adiabatic perturbations, and $N-1$ components orthogonal to the trajectory, that represent the isocurvature perturbations, as shown in figure 3.5. We explicitly

show the example of double inflation with $N = 2$ inflaton fields, but it is straightforward to extend these results to a multi-field inflation with a generic number N of inflatons.

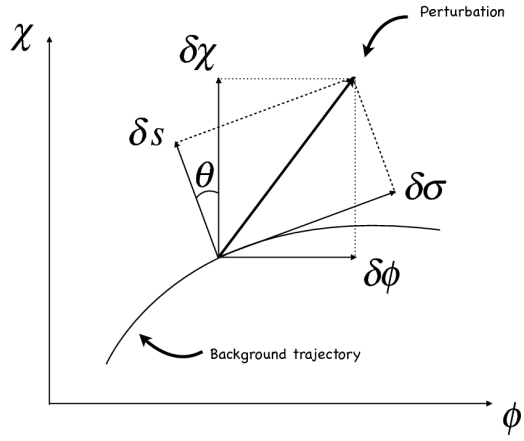

Figure 3.5: Illustration of the decomposition of the two-field perturbation into an adiabatic ($\delta\sigma$) and an entropy field (δs). θ is the angle between $\delta\sigma$ and $\delta\phi$. Figure taken from [86].

For double inflation driven by two scalar fields χ and ϕ, we perform a rotation in the field space to define the adiabatic field σ as:

$$\dot{\sigma} = \frac{\dot{\phi}}{\sqrt{\dot{\phi}^2 + \dot{\chi}^2}}\dot{\phi} + \frac{\dot{\chi}}{\sqrt{\dot{\phi}^2 + \dot{\chi}^2}}\dot{\chi} \equiv (\cos\theta)\dot{\phi} + (\sin\theta)\dot{\chi}. \tag{3.85}$$

This field represent the path length along the classical trajectory in the field space defined by the background Klein-Gordon equations (3.72) for ϕ and χ, that can be recasted in the form:

$$\ddot{\sigma} + 3H\dot{\sigma} + V_{,\sigma} = 0, \tag{3.86}$$

where $V_{,\sigma} = (\cos\theta)V_{,\phi} + (\sin\theta)V_{,\chi}$. We define then the entropy (or isocurvture) perturbation field s, as the field whose fluctuations are orthogonal to the background classical trajectory, that is:

$$\delta s = (\cos\theta)\delta\chi - (\sin\theta)\delta\phi, \tag{3.87}$$

so that $s = \text{const}$ along the classical trajectory and $\delta\sigma$ describes adiabatic field perturbations in the case when $\delta s = 0$. We can compute the comoving curvature perturbation $\mathcal{R}$ from its general expression (2.100) in term of the total energy-momentum tensor of the two-field lagrangian, as straightforward calculation gives the results [86, 9]:

$$\mathcal{R} = \Phi + H\frac{\delta\sigma}{\dot{\sigma}} \tag{3.88}$$

and its time evolution can be obtained combining Eqs.(2.87) and (2.103), giving, on large scales, the following equation

$$\dot{\mathcal{R}} = -3H\frac{\dot{P}}{\dot{\rho}}\mathcal{S}. \tag{3.89}$$

In the case considered, P and ρ are the total pressure and density of the two-fields energy-momentum tensor and the entropy perturbation $\mathcal{S}$ is given by [86]:

$$\mathcal{S} = -\frac{V_{,\sigma}}{6\pi G\dot{\sigma}^2(3H\dot{\sigma} + 2V_{,\sigma})}\left(\frac{k^2}{a^2}\Phi\right) - \frac{2V_{,s}}{3\dot{\sigma}^2}\delta s, \tag{3.90}$$

where $V_{,s} = (\cos\theta)V_{,\chi} - (\sin\theta)V_{,\phi}$. Therefore the evolution of the comoving curvature perturbations can be expressed in terms of the new fields as:

$$\dot{\mathcal{R}} = \frac{H}{\dot{H}}\frac{k^2}{a^2}\Phi + \frac{2H}{\dot{\sigma}}\dot{\theta}\delta s, \tag{3.91}$$

where $\dot{\theta} = -\frac{V_{,s}}{\dot{\sigma}}$. The power of this formalism is now clear: from the Eq.(3.91) we can immediately see the connection between isocurvature generation and the variation of the curvature perturbation. In fact, if the background solution follows a curved trajectory in the field space (see figure 3.5), isocurvature perturbations can be significant and $\mathcal{R}$ can change appreciably with time.

In order to find the Klein-Gordon equations for the new fields, we define the gauge-invariant Mukhanov-Sasaki variable for the adiabatic field [88, 89] as:

$$Q_\sigma = \delta\sigma + \frac{\dot{\sigma}}{H}\Phi \tag{3.92}$$

and the second derivative of the potential with respect to the new fields

$$V_{,\sigma\sigma} = (\sin^2\theta)V_{,\chi\chi} + (\sin 2\theta)V_{,\phi\chi} + (\cos^2\theta)V_{,\phi\phi}\,, \tag{3.93}$$

$$V_{,ss} = (\sin^2\theta)V_{,\phi\phi} - (\sin 2\theta)V_{,\phi\chi} + (\cos^2\theta)V_{,\chi\chi}\,. \tag{3.94}$$

Using the Klein-Gordon equations (3.72) and the above definitions, we obtain the following equations for Q_σ and δs:

$$\ddot{Q}_\sigma + 3H\dot{Q}_\sigma + \left[\frac{k^2}{a^2} + V_{,\sigma\sigma} - \dot{\theta}^2 - \frac{8\pi G}{a^3}\left(\frac{a^3\dot{\sigma}^2}{H}\right)\right] Q_\sigma = 2\frac{d}{dt}(\dot{\theta}\delta s) - 2\left(\frac{V_{,\sigma}}{\dot{\sigma}} + \frac{\dot{H}}{H}\right)\dot{\theta}\delta s, \tag{3.95}$$

$$\ddot{\delta s} + 3H\dot{\delta s} + \left(\frac{k^2}{a^2} + V_{,ss} + 3\dot{\theta}^2\right)\delta s = \frac{\dot{\theta}}{\dot{\sigma}}\frac{k^2}{2\pi G^2}\Phi. \tag{3.96}$$

From Eq.(3.96) we observe that the isocurvature perturbations are essentially decoupled from the adiabatic field fluctuations in the large scale limits and so they remain zero if they were initially zero. Moreover, in order to have a production of large scale entropy perturbations from the small scale quantum fluctuations during inflation, the entropy field must be light and its effective mass must be small, i.e. $m_s^2 \equiv V_{,ss} + 3\dot{\theta}^2 \ll \frac{3}{2}H^2$. However, for what concerns adiabatic perturbations, even on large scales, we can see directly from Eq.(3.95) that the entropy fields fluctuations can source them, unless $\dot{\theta} = 0$, that is unless the trajectory in the field space is a straight line.

As we did in the last section, it would be now straightforward to match the entropy and adiabatic perturbations to the quantum fluctuations of the fields at horizon crossing. The main advantage of this formalism, however, is that it makes very easy to calculate the correlations between isocurvature and adiabatic modes as seen in section 3.3.

Chapter 4

Scalar-Tensor Theories of Gravity

In general relativity the gravitational force is mediated by the metric, namely a single 2-rank symmetric tensor. As we mentioned in Sec.1.1.1, in the GR picture, all the fields are coupled to the metric through the determinant of the metric $\sqrt{-g}$ in the so called minimal coupling scheme. Although this is the simplest way to achieve Einstein equivalence principle, the existence of additional fields that could contribute to the gravitational sector can be postulated.

In 1955 Jordan [90] and, independently, in 1960 Brans and Dicke [91], on the basis of the ideas of Eddington and Dirac of a time varying Newton constant G_N, developed a theory in which such a variation is due to the presence of a scalar field with a direct coupling to the Ricci scalar and a non-canonical kinetic term. The Jordan-Brans-Dicke model is the archetypl version of a more general class of theories called Scalar-Tensor (ST) theories of gravity in which a scalar field is non-minimally coupled to gravity. Scalar-tensor theories, in turn, are a special case of a broader class of general scalar-tensor theories with second-order field equations worked out by Horndeski [92, 93, 94].

The importance of studying ST theories, however, is not only of academic

interest, since these theories arise naturally as the dimensionally reduced effective theories of higher dimensional theories, such as Kaluza-Klein and string models. It has also been shown that scalar-tensor theories generically contain an attractor mechanism toward general relativity during the matter dominated era [95].

This chapter is intended to give a brief introduction to the ideas behind ST theories and to the cosmology that therive from them, in particular we will show how scalar tensor theories can lead to an accelerated expansion at late times.

4.1 Scalar Tensor Models

The most generic action for scalar tensor gravity is given by [96, 97]

$$S = \int d^4x \sqrt{-g} \left[F(\varphi)R - \epsilon Z(\varphi) g^{\mu\nu} \partial_\mu \varphi \partial_\nu \varphi - 2V(\varphi) + \mathcal{L}_m \right], \qquad (4.1)$$

where $F(\varphi)$ and $Z(\varphi)$* are two functions of the scalar field φ and $V(\varphi)$ its potential. The paramater ϵ can take the values -1 and 1, but from now on we consider $\epsilon = 1$ to avoid the possibility of ghosts. It is important to stress that the ordinary matter Lagrangian $\mathcal{L}_m$ is minimally coupled to gravity as in standard general relativity. This is necessary to ensure that the weak equivalence principle (WEP) applies. This principle states that any object under the influence only of the gravitational force falls locally with a common acceleraton, i.e. its motion follows geodesic trajectories. A more restrictive formulation of this principle is given by the strong equivalence principle (SEP): in a freely falling frame we recover the same special relativistic physics, independently from position or velocity. The SEP is reflected in the constant value of the Newton constant G_N in both space and time. Although the action (4.1) well satisfies the WEP, the presence of the scalar field influences the metric and spoils the validity of the SEP. This is indeed

*Hereafter we will drop the dependence from the scalar field and write just F instead of $F(\varphi)$.

reflected in the Newton constant dependence of the scalar field φ and thus, since $\varphi = \varphi(t)$ in cosmological settings, it varies with time [98].

Varying the action (4.1) with respect to the metric gives the generalization of the Einstein equations [97]:

$$G_{\mu\nu} = \frac{1}{F}\tilde{T}_{\mu\nu}, \tag{4.2}$$

where

$$\tilde{T}_{\mu\nu} = g_{\mu\alpha}g_{\nu\beta}\frac{2}{\sqrt{-g}}\frac{\delta\left[\sqrt{-g}(\mathcal{L}_m + \mathcal{L}_\varphi)\right]}{\delta g_{\alpha\beta}} \tag{4.3}$$

is the total effective energy-momentum tensor. We note from Eq.(4.2) that scalar-tensor theories are described by the usual Einstein equations with an effective time-varying Newton constant $G_N(\varphi) = (8\pi F)^{-1}$, however, as we will see in the following sections, it does not have the same physical meaning as in general relativity.

In the case of canonical kinetic terms, $Z = 1$, as we will see later the Eq.(4.2) becomes [96, 93]:

$$G_{\mu\nu} = \frac{1}{F}\left[T^m_{\mu\nu} + \partial_\mu\varphi\partial_\nu\varphi - \frac{1}{2}g_{\mu\nu}\partial_\rho\varphi\partial^\rho\varphi - g_{\mu\nu}V + (\nabla_\mu\nabla_\nu - g_{\mu\nu})F\right]. \tag{4.4}$$

We can see that the terms in the square brackets on the right hand side which contain the scalar field resemble the energy-momentum tensor of a scalar field in general relativity, however the term $(\nabla_\mu\nabla_\nu - g_{\mu\nu})F$ has no analogus in Einstein gravity and makes the perfect fluid approximation not valid for the energy-momentum tensor of φ. If we want to put the energy-momentum tensor (4.3) into the form of a perfect fluid, we must define the scalar field density and pressure as follows:

$$\rho_\varphi = \frac{\dot{\varphi}^2}{2} + V - 3H\dot{F}, \tag{4.5}$$

$$P_\varphi = \frac{\dot{\varphi}^2}{2} - V + \ddot{F} + H\dot{F}. \tag{4.6}$$

In fact, this is better understood if we derive the Friedmann equations from the Einstein equations (4.2):

$$3FH^2 = \rho_m + \frac{1}{2}\dot{\varphi}^2 - 3H\dot{F} + V, \tag{4.7}$$

$$-2F\dot{H} = (\rho_m + P_m) + \dot{\varphi} + \ddot{F} - H\dot{F}. \tag{4.8}$$

The variation of the action (4.1) with respect to the scalar field gives the Klein-Gordon equation

$$(\ddot{\varphi} + 3H\dot{\varphi}) = 3F_{,\varphi}\,(\dot{H} + 2H^2) - V_{,\varphi}\,. \tag{4.9}$$

The continuity equation Eq.(1.47) continues to hold for the ordinary matter contents separately thanks to the minimal coupling to gravity and we can still write

$$\dot{\rho}_i = -3H(\rho_i + P_i), \tag{4.10}$$

where the index i runs over the different matter (and radiation) species filling the universe.

4.1.1 Jordan-Brans-Dicke and Induced Gravity Theory

The simplest and most famous scalar-tensor theory is the Jordan-Brans-Dicke theory, described by the action (4.1) with $V(\phi) = 0$, $F(\phi) = \phi/(16\pi)$ and $Z(\phi) = \omega_{\rm BD}/(16\pi)$ [91, 90]:

$$S = \int d^4x\,\sqrt{-g}\left[\frac{\phi}{16\pi}R - \frac{\omega_{\rm BD}}{16\pi\phi}g^{\mu\nu}\partial_\mu\phi\partial_\nu\phi + \mathcal{L}_m\right]. \tag{4.11}$$

When the adimensional parameter of the theory tends to large values, i.e. $\omega_{\rm BD} \to \infty$ this model approaches general relativity. Solar System experiments can set high constraints on the value of the parameter $\omega_{\rm BD}$. The present limit on $\omega_{\rm BD}$ is very strong $\omega_{\rm BD} \geq 20000$ [99]. However,as we will see cosmological observations could test scalar tensor theories on larger scales, completely different from the solar system ones [100, 101, 102].

The equations of motions are easily obtained varying the action (4.11) with respect to the metric and to the Jordan-Brans-Dicke scalar field ϕ, giving:

$$R_{\mu\nu} - \frac{1}{2}g_{\mu\nu}R = 8\pi T^m_{\mu\nu} + \frac{\omega_{\rm BD}}{\phi^2}\left[\partial_\mu\phi\partial_\nu\phi - \frac{1}{2}g_{\mu\nu}(\partial\phi)^2\right] + \frac{1}{\phi}\left(\nabla_\mu\nabla_\nu\phi - g_{\mu\nu}\Box\phi\right), \tag{4.12}$$

$$\Box\phi = \frac{\phi R}{2\omega_{\rm BD}} - \frac{1}{2\phi}(\partial\phi)^2, \tag{4.13}$$

$$\nabla_\mu T^{\mu\nu}_m = 0, \tag{4.14}$$

where the last equation is the conservation law for the energy-momentum tensor of the usual matter content.

We note that the action (4.11) contains a non-canonical term. Redefining the coupling to the Ricci scalar and the scalar field as:

$$\omega_{\rm BD} \equiv \frac{1}{4\gamma}, \qquad \frac{\phi}{8\pi} \equiv \gamma\varphi^2, \tag{4.15}$$

we can cast the action (4.11) into the standard canonical form and we obtain the action describing the Induced Gravity (IG) theory [103]

$$S = \int d^4x\,\sqrt{-g}\left[\frac{\gamma\varphi^2}{2}R - \frac{1}{2}g^{\mu\nu}\partial_\mu\varphi\partial_\nu\varphi - V(\varphi) + \mathcal{L}_m\right]. \tag{4.16}$$

General relativity is recovered in this model for $\gamma \to 0$. The actual constraint γ is $\gamma \leq 0.0017$ [104]. The IG model is globally scale invariant [105, 106], in fact the parameter γ is adimensional, and it was introduced to implement the idea of Einstein gravity as arising from a dynamical symmetry breaking [107]. For a self-interacting potential $\lambda\varphi^4/4$ (note that, again, λ is adimensional), it was shown [108, 109, 110] that this simple IG model has an attractor to general relativity plus a cosmological constant on breaking scale invariance as we will see in the next section. The IG theory will be the main model of interest of the next chapter.

The Friedmann equations for the action (4.16) in conformal time are[†]:

$$\mathcal{H}^2 = a^2\frac{(\rho_m + V)}{3\gamma\varphi^2} + \frac{\varphi'^2}{6\gamma\varphi^2} - \frac{2\mathcal{H}\varphi'}{\varphi}, \tag{4.17}$$

$$\mathcal{H}' = -\frac{a^2}{\varphi^2}\left(\frac{\rho_m + P_m}{2\gamma} + \frac{\rho_m - 3P_m}{(1+6\gamma)}\right) + \frac{a^2}{(1+6\gamma)\varphi}\left(V_{,\varphi} - \frac{4V}{\varphi}\right) - \frac{\varphi'^2}{2\gamma\varphi^2} + \frac{4\mathcal{H}\varphi'}{\varphi}, \tag{4.18}$$

[†]Here the subscript m denotes the usual matter content of the universe. For example: $\rho_m = \rho_\gamma + \rho_\nu + \rho_c + \rho_b$.

where the second term on the right hand side of Eq.(4.18) vanishes for $V = \lambda\varphi^4/4$. Moreover, the Klein-Gordon equation for the scalar field φ is:

$$\varphi'' = -2\mathcal{H}\varphi' - \frac{\varphi'^2}{\varphi} + \frac{a^2}{(1+6\gamma)}\left[\frac{\rho_m - 3P_m}{\varphi} - \left(V_{,\varphi} - \frac{4V}{\varphi}\right)\right] \tag{4.19}$$

and, once again, the last term on the right hand side vanishes for the choice of the potential given above.

The density and pressure of the scalar field, Eqs.(4.5) and (4.6), take the form:

$$\rho_\varphi = \frac{\varphi'^2}{2a^2} + V - 6\gamma\frac{\mathcal{H}\varphi\varphi'}{a^2}, \tag{4.20}$$

$$P_\varphi = \frac{\varphi'^2}{2a^2} - V + 2\gamma\frac{\varphi\varphi'' + \varphi'^2 + \mathcal{H}\varphi\varphi'}{a^2}. \tag{4.21}$$

4.1.2 Non-Minimal Coupling

Another model of scalar-tensor theory that we will investigate in the appendix is the Non-Minimally Coupled model [111] where

$$F(\varphi) = N_{\rm pl}^2 + \xi\varphi^2. \tag{4.22}$$

This model reduces to Einstein gravity when $\xi = 0$ and $N_{\rm pl}^2 = M_{\rm pl}^2 = 2.44 \cdot 10^{18}$GeV, whereas it reduces to IG for $N_{\rm pl}^2 = 0$. Usually the first term in Eq.(4.22) is taken to be dominant over the second, as required from observations $\xi \leq 5 \cdot 10^{-3}(\sqrt{G_N}\varphi_0)^{-1}$ [111].

4.1.3 Effective Newtonian Constant

As we mentioned before, the original idea that led to the first JBD model was that of a time-varying gravitational constant. We saw in the previous sections, that scalar tensor-theories achieve naturally such a requirement, however the gravitational 'constant' that we defined as G_N is that only for the tensor part of the gravitational force. The presence of the scalar field creates an additional gravitational force on long range, scales $\leq H_0^{-1}$ [112],

and thus, the gravitational constant measured in any phisical situations includes the contribution from the scalar field as well. We call this measurable gravitational constant G_{eff}.

To find its expression for the IG model, we should derive the Newtonian limit of the field equations (4.17), (4.18) and (4.19) for the metric and scalar field. This is usually called the weak field limit [113] and consists in expanding the Einstein and Klein-Gordon equations at first order around the flat Minkowski metric and a constant value v for the scalar field φ with the dimension of a mass. The latter should be interpreted as a 'vacuum expectation value' in quantum field theory. Thus we should expand the scalar field and the metric as

$$\varphi(\mathbf{x}, \tau) = v + \delta\varphi(\mathbf{x}, \tau), \tag{4.23}$$

$$g_{\mu\nu} = \eta_{\mu\nu} + h_{\mu\nu}, \tag{4.24}$$

and write Eqs.(4.17), (4.18) and (4.19) at first order in $h_{\mu\nu}$ and $\delta\varphi$ and solve these equations for the latter variables. We do not show the calculations, since they are rather long and they can be found in standard textbooks (see for example [5, 96]). What interests us is that, once we have found the solution, we can compare the 0-0 component of the metric perturbation h_{00}, which can be interpreted as the Newtonian gravitational potential [7], with the 0-0 component of the weak field limit of the Schwartzschild solution [114, 115]. The result is that the effective G_{eff}, that regulates the attraction between two test masses, in the IG model, is given by [110]:

$$G_{\text{eff}}(\varphi) = G_N(\varphi)\frac{1+8\gamma}{1+6\gamma}. \tag{4.25}$$

Current experiments constrain the variation rate of the gravitational constant $\dot{G}_N/G_N$ to be $\leq 10^{-11}\,\text{yr}^{-1}$ [116].

4.2 Accelerated Universe from the IG Theory

The aim of this section is to show how a simple model of Induced Gravity can lead to the acceleration of the Universe. However, differently from the quintessence model, in which the minimally coupled scalar field is actually the dark energy component, in scalar-tensor theories things are more complicated. In fact, in these models, the acceleration is due to the non-trivial interaction of the scalar field with gravity and we must be careful to find a meaningful definition of the dark energy density and pressure [117]. Thus, in order to compare scalar-tensor theories with Einstein gravity quintessence models, following [97, 110], we define the dark energy density and pressure as

$$\rho_{\rm DE} = \frac{3\gamma\varphi_0^2\mathcal{H}^2}{a^2} - \rho_m, \tag{4.26}$$

$$\rho_{\rm DE} + P_{\rm DE} = -\frac{2\gamma\varphi_0^2\mathcal{H}'}{a^2} - (\rho_m + P_m) \tag{4.27}$$

and the relative densities for the fluids as

$$\Omega_m = \frac{a^2\rho_m}{3\mathcal{H}^2\gamma\varphi_0^2}, \tag{4.28}$$

$$\Omega_{\rm DE} = \frac{a^2\rho_{\rm DE}}{3\mathcal{H}^2\gamma\varphi_0^2}, \tag{4.29}$$

where $\Omega_m + \Omega_{\rm DE} = 1$. These definitions follow from the representation of the scalar-tensor field equations (4.2) in an Einstein gravity form with the Newtonian constant $G_0 \equiv G_N(\tau_0)$:

$$G_{\mu\nu} = 8\pi G_0(T^m_{\mu\nu} + T^{\rm DE}_{\mu\nu}). \tag{4.30}$$

With these definitions, the usual conservation law for the dark energy density applies:

$$\rho'_{\rm DE} = -3\mathcal{H}(\rho_{DE} + P_{DE}). \tag{4.31}$$

Thus we can define the equation of state parameter $w_{\rm DE} = P_{\rm DE}/\rho_{\rm DE}$ exactly

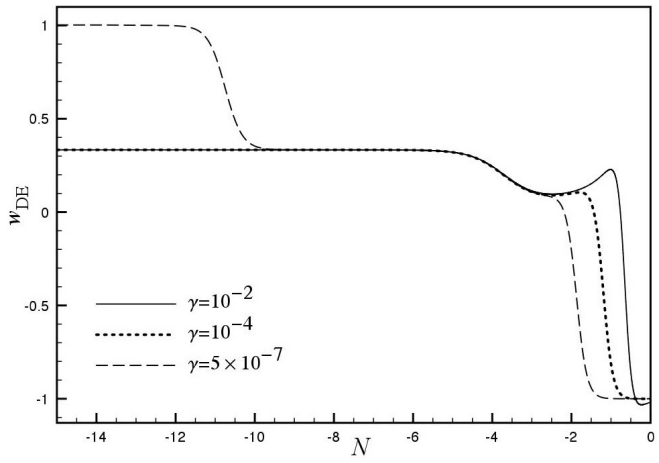

Figure 4.1: Evolution of the equation of state parameter $w_{\rm DE}$ for the IG model with $V = \lambda\varphi^4/4$ for three different values of γ. In this plot $N = \ln a$. Figure taken from [110].

as we did in Sec.3.4 for the quintessence model. From Eq.(4.31), the time evolution of the dark energy sector is given by [97]:

$$\frac{\rho_{\rm DE}(z)}{\rho_{\rm DE,0}} = \exp\left[3\int_0^z dz'\,\frac{1+w(z')}{1+z'}\right]. \tag{4.32}$$

A numerical calculation for the evolution of the equation of state parameter has been done in Ref.[110]; it is represented in Fig.4.1 for different values of the coupling γ. We can see from Fig.4.1 that in the IG model $w_{\rm DE}$ has a behaviour similair to that of the quintessence studied in Sec.1.8.2 and follows the dominant component: it has a value of $w_{\rm DE} \simeq \frac{1}{3}$ during the radiation dominated era and it tends to decrease toward zero during the matter domination. Finally at present epoch it becomes negative $w_{\rm DE} \simeq -1$ and thus, as we argued, the scalar-tensor theory mimics the presence of a dark energy component.

4.3 The Parameterized Post-Newtonian (PPN) Approximation

The Post-Newtonian approximation is a method to compare general relativity to generic theories in which the metric has the same physical interpretation as in general relativity. This method was first developed to study the deviations to the static and isotropic Schwartzschild solution due to the planet gravitational fields in the solar system, in fact this method is adapted to a system of slowly moving particles [118]. The idea is to create a construction that encompasses a wide range of gravitational theories and that contains parameters that can easily be constrained by observations, for example by solar system experiments, in a reasonably straightforward fashion [119]. In this way on one hand observations can constrain these parameters independently from any theory and, on the other, the theorists can test each theory by comparing its precitions to the derived bounds on these parameters. In the limit of slow motion and weak field most metrics have the same structure and can be expanded on top of the Minkowski flat metric $\eta_{\mu\nu}$ in a perturbative way. For this purpose we need to define the perturbative orders as follows

$$U \sim v^2 \sim \frac{P}{\mu} \sim \frac{\rho}{\mu} \sim \mathcal{O}(2), \tag{4.33}$$

$$\frac{|\partial/\partial t|}{|\partial/\partial x|} \sim \mathcal{O}(1), \tag{4.34}$$

where μ is the rest-mass densit of the fluid element, v its 3-velocity and U is the Newtonian potential. In the post-Newtonian limit for time-like particles, the metric components are required to be known at orders [93]:

$$g_{00} \sim \mathcal{O}(4), \tag{4.35}$$

$$g_{0i} \sim \mathcal{O}(3), \tag{4.36}$$

$$g_{ij} \sim \mathcal{O}(2). \tag{4.37}$$

The procedure is the following:

- one identifies the fields in the theory and expand them around their background values counting the perturbation orders with the help of Eqs. (4.33) and (4.34). The appropriate expansions for the metric and for the hypothetical scalar field are

$$g_{00} = -1 + h_{00}^{(2)} + h_{00}^{(4)} + \mathcal{O}(6), \tag{4.38}$$

$$g_{0i} = h_{0i}^{(3)} + \mathcal{O}(5), \tag{4.39}$$

$$g_{ij} = \delta_{ij} + h_{ij}^{(2)} + \mathcal{O}(4), \tag{4.40}$$

$$\phi = \phi_0 + \phi^{(2)} + \phi^{(4)} + \mathcal{O}(6). \tag{4.41}$$

- One substitutes the above expressions into the field equations and solve the leading order for $h_{00}^{(2)}$ and then for all the higher perturbations.

- One compares the results with the standard PPN test metric [119, 93]:

$$\begin{aligned} g_{00} = -1+2GU-2\beta G^2U^2-2\xi G^2\Phi_W+(2\gamma_{\rm PPN}+2+\alpha_3+\beta_1+2\xi)G\Phi_1+, \\ +2(1+3\gamma_{\rm PPN}-2\beta+\beta_2+\xi)G^2\Phi_2+2(1+\beta_3)G\Phi_3-(\beta_1-2\xi)G\mathcal{A}+ \\ +2(3\gamma_{\rm PPN}+3\beta_4-2\xi)G\Phi_4, \end{aligned} \tag{4.42}$$

$$g_{0i} = -\frac{1}{2}(3+4\gamma_{\rm PPN}+\alpha_1-\alpha_2+\beta_1-2\xi)GV_i - \frac{GW_i}{2}(1+\alpha_2-\beta_1+2\xi), \tag{4.43}$$

$$g_{ij} = (1+2\gamma_{\rm PPN}GU)\delta_{ij}. \tag{4.44}$$

  The parameters denoted with the greek letters β, ξ, $\gamma_{\rm PPN}$ and α are the PPN parameters, whereas the greek letters Φ and $\mathcal{A}$, V_i and W_i denote the post-Newtonian gravitational potentials.

For general relativity we have $\beta = \gamma_{\rm PPN} = 1$, all the others parameters being zero, whereas in the JBD theory the only that differs from general relativity is [120]:

$$\gamma_{\rm PPN} = \frac{1+\omega_{\rm BD}}{2+\omega_{\rm BD}} = \frac{1+4\gamma}{1+8\gamma}. \tag{4.45}$$

The tightest constraint on $\gamma_{\rm PPN}$ comes from the Doppler tracking of the Cassini spacecraft, that gives $\gamma_{\rm PPN} = 1 - (2.1 \pm 2.3) \cdot 10^{-5}$ [99].

4.4 Conformal Transformations

A conformal transformation transforms a metric $g_{\mu\nu}$ into another metric $g^*_{\mu\nu}$ according to the rule [121]:

$$g^*_{\mu\nu} = \Omega^2(x) g_{\mu\nu}, \tag{4.46}$$

where $\Omega(x)$ is an arbitrary function of space time coordinate x and we wrote the transformations using its square value in order to keep the sign of ds^2 unchanged. In fact, under the transformation (4.46), the line element transforms as:

$$ds^2_* = \Omega^2(x) ds^2, \tag{4.47}$$

and thus it changes the physical distances. However, since this is done without specifying any direction, the distances change isotropically. Since the distances we are considering are distances in space and time, this means that changes in spatial distance and in time interval should occur at the same rate. The limit in which the function $\Omega(x) = \text{const}$ is just a scale transformation, in this sense a conformal transformation may be view as a localized scale transformation. When we apply the transformation (4.46), we say that we are moving from one conformal frame to another. In doing so, the transformation on the metric lead to the following transformations for the quantities related to it [96]:

$$g^{\mu\nu} = \Omega^2 g^{\mu\nu}_*, \tag{4.48}$$

$$\sqrt{-g} = \Omega^{-4}\sqrt{-g_*}, \tag{4.49}$$

$$\Gamma^\mu_{\nu\lambda} = \Gamma^\mu_{*\nu\lambda} - (f_{,\nu}\,\delta^\mu_\lambda + f_{,\lambda}\,\delta^\mu_\nu - \tilde{g}^{\mu\sigma} f_{,\sigma}\, g_{*\nu\lambda}), \tag{4.50}$$

$$R = \Omega^2(R_* + 6\Box_* f - 6 g^{\mu\nu}_* f_{,\mu}\, f_{,\nu}\,), \tag{4.51}$$

where $f \equiv \ln\Omega$. The conformal frame in which the matter Lagrangian $\mathcal{L}_m$ does not contain the scalar field non-minimally coupled to gravity is called Jordan frame. Starting from the Jordan frame of scalar-tensor action with a generic coupling to gravity $F(\varphi)$, we can apply a conformal transformation

with $\Omega = F^{1/2}$ and redefine the new scalar field as

$$\varphi_* = \int d\varphi \left[\frac{3}{2}\left(\frac{1}{F}\frac{dF}{d\varphi}\right)^2 + \frac{Z}{F}\right]^{1/2}, \tag{4.52}$$

in order to recast the original action into a new action in which the new scalar field is minimally coupled to the new Ricci scalar

$$S_* = \int d^4x \sqrt{g_*}\left[\frac{1}{2}R_* - \frac{1}{2}g_*^{\mu\nu}\partial_\mu\varphi_*\partial_\nu\varphi_* + \mathcal{L}_m^*\right]. \tag{4.53}$$

In this frame, which is called the Einstein frame, the field equations has the simpler form of the usual Einstein equations and thus it is easier to solve them. However in this frame the matter Lagrangian is coupled to the scalar field and thus the weak equivalence principle is violated and test matter particles do not follow geodesic trajectories. The question of which between these two frames is the physical one is still open [122, 123]. In the next sections, we will consider the equations in the Jordan frame, since it is there that we can use the Boltzmann equations in the form given in Sec.2.3.

4.5 IG Background Evolution Deep in the Radiation Era

In the next chapter we will compute the initial conditions for the cosmological perturbations in the IG model, so it is important to study the background evolution on top of which these perturbations will be computed. As we noticed in Sec.2.5, the initial conditions must be computed deep in the radiation era and after neutrino decoupling. The Hubble parameter for general relativity is $\mathcal{H} \sim 1/\tau$ in that era, so we expand it in Laurent series starting from a simple pole in $\tau = 0$ to find its expression in the IG model. For the same reason we expand also the scale factor a and the scalar field φ in a Taylor series around $\tau = 0$. Inserting these expansions in the Friedmann equations (4.17) and (4.18) and in the Klein-Gordon equations (4.19), we

find the following expressions for the background quantities:

$$a(\tau) = \sqrt{\frac{\rho_{\rm rad0}}{3\gamma\varphi_i^2}}\left[\tau + \frac{\omega}{4}\tau^2 - \frac{5\omega^2\gamma}{16}\tau^3\right], \tag{4.54}$$

$$\mathcal{H}(\tau) = = \left[\frac{1}{\tau} + \frac{\omega}{4} - \frac{\omega^2(1+16\gamma+60\gamma^2)}{16(1+6\gamma)}\tau\right], \tag{4.55}$$

$$\varphi(\tau) = \varphi_i\left(1 + \frac{3\gamma\omega}{2}\tau - \frac{\gamma\omega^2(2+21\gamma+54\gamma^2)}{8(1+6\gamma)}\tau^2\right), \tag{4.56}$$

where

$$\omega \equiv \frac{\rho_{\rm mat0}}{\sqrt{3\gamma\rho_{\rm rad0}}(1+6\gamma)\varphi_i}, \tag{4.57}$$

$\rho_{\rm rad0}$ and $\rho_{\rm mat0}$ are the densities of radiation and matter at the present time and φ_i is the initial value of the scalar field.

4.6 Equations for Cosmological Perturbations in Scalar-Tensor Models

In this section we give the expressions for the perturbed field equations in both the Induced Gravity and the Non-Minimally Coupling models. For later convenience, we give them in the synchronous gauge (2.26) and conformal time, since in the next chapter we will use this gauge. However, the perturbed equations in the Newtonian gauge are given in Appendix A.

The cosmological perturbation theory in generalized Einstein gravity theory has been firstly considered in Ref.[124]. The procedure is the same that we saw in Secs.2.2 and 3.4. Since in the Jordan frame the energy-momentum tensor of all the species in the Universe are separately conserved, the density contrasts, the velocities and the anisotropic stresses of baryonic matter, CDM, radiation and neutrinos are the same as in general relativity and thus we will use for them the Boltzmann equations of Sec.2.3 and the tight-coupling approximation (2.75). For this reason we need only to find the perturbed field equations for the metric and for the scalar field φ and we thus split it into the sum of a background space-independent part and a

perturbation

$$\varphi(\mathbf{x},\tau) = \bar{\varphi}(\tau) + \delta\varphi(\mathbf{x},\tau). \tag{4.58}$$

Although this convention, in the following equations we will use just φ in place of $\bar{\varphi}$ to not weigh down the notation. The equations for the Induced Gravity model can be recasted in a simple way, similair to the Einstein equations in general relativity if we define the total density perturbation $\delta\tilde{\rho}$, the total pressure perturbation $\delta\tilde{P}$, the total velocity $\tilde{\theta}$ and the total anisotropic stress $\tilde{\sigma}$ as:

$$\delta\tilde{\rho} \equiv \frac{\delta\rho_m}{\gamma\varphi^2} + \frac{h'\varphi'}{a^2\varphi} - \frac{2}{a^2}\left\{\frac{\delta\varphi'}{\varphi}\left(\mathcal{H} - \frac{\varphi'}{2\gamma\varphi}\right) + \right.$$
$$\left. + \frac{\delta\varphi}{\varphi}\left[\frac{a^2\rho_m}{\gamma\varphi^2} + \frac{\varphi'^2}{2\gamma\varphi^2} + \frac{a^2}{\gamma\varphi}\left(\frac{V}{\varphi} - \frac{V_{,\varphi}}{2}\right) - \frac{3\mathcal{H}\varphi'}{\varphi} + k^2\right]\right\}, \tag{4.59}$$

$$(\tilde{\rho} + \tilde{P})\tilde{\theta} \equiv \frac{(\rho_m + P_m)\theta_m}{\gamma\varphi^2} + \frac{2k^2}{a^2}\left\{\frac{\delta\varphi}{\varphi}\left[\frac{\varphi'}{2\gamma\varphi}(1+2\gamma) - \mathcal{H}\right] + \frac{\delta\varphi'}{\varphi}\right\}, \tag{4.60}$$

$$\delta\tilde{P} \equiv \frac{1}{(1+6\gamma)\varphi^2}\left(2\delta\rho_m + \frac{\delta P_m}{\gamma}\right) - \frac{1}{3a^2}\left\{\frac{3\delta\varphi'}{\varphi}\left(2\mathcal{H} - \frac{\varphi'}{\gamma\varphi}\right) + \right.$$
$$+ \frac{\delta\varphi}{\varphi}\left[\frac{6a^2P_m}{\gamma\varphi^2} + \frac{12a^2(\rho_m - 3P_m)}{(1+6\gamma)\varphi^2} + \frac{3\varphi'}{\varphi}\left(\frac{\varphi'}{\gamma\varphi} - 2\mathcal{H}\right) + 2k^2 + \right.$$
$$\left.\left. + \frac{6a^2}{(1+6\gamma)}\left(V_{,\varphi\varphi} + \frac{V_{,\varphi}}{2\gamma\varphi}(1-4\gamma) - \frac{V}{\gamma\varphi^2}(1-2\gamma)\right)\right] + \frac{h'\varphi'}{\varphi}\right\}, \tag{4.61}$$

$$(\tilde{\rho} + \tilde{P})\tilde{\sigma} \equiv \frac{(\rho_m + P_m)\sigma_m}{\gamma\varphi^2} + \frac{1}{3a^2}\left[\frac{4k^2\delta\varphi}{\varphi} + 2(h' + 6\eta')\frac{\varphi'}{\varphi}\right]. \tag{4.62}$$

The perturbed Einstein equations then become:

$$k^2\eta - \frac{1}{2}\mathcal{H}h' = -\frac{a^2\delta\tilde{\rho}}{2}, \tag{4.63}$$

$$k^2\eta' = \frac{a^2(\tilde{\rho} + \tilde{P})\tilde{\theta}}{2}, \tag{4.64}$$

$$h'' + 2\mathcal{H}h' - 2k^2\eta = -3a^2\delta\tilde{P}, \tag{4.65}$$

$$(h'' + 6\eta'') + 2\mathcal{H}(h' + 6\eta') - 2k^2\eta = -3a^2(\tilde{\rho} + \tilde{P})\tilde{\sigma}. \tag{4.66}$$

The perturbed Klein-Gordon equation becomes:

$$\delta\varphi'' = -2\delta\varphi'\left(\mathcal{H}+\frac{\varphi'}{\varphi}\right) - \delta\varphi\left[k^2 - \frac{\varphi'^2}{\varphi^2} + \frac{a^2(\rho_m - 3P_m)}{(1+6\gamma)\varphi^2} + \right.$$
$$\left. + \frac{a^2}{(1+6\gamma)}\left(V_{,\varphi\varphi} + \frac{4V}{\varphi^2} - \frac{4V_{,\varphi}}{\varphi}\right) + \frac{a^2(\delta\rho_m - 3\delta P_m)}{(1+6\gamma)\varphi} - \frac{h'\varphi'}{2}\right]. \quad (4.67)$$

Chapter 5

Initial Conditions for Cosmological Perturbations in Induced Gravity

In this chapter we derive the initial conditions for cosmological perturbations for the IG theory studied in Sec.4.1.1 in which $F(\varphi) = \gamma\varphi^2$. These extend the well known initial conditions in Einstein GR [38] seen in Sec.3.1 to this gravity model. However, as we will show in Appendix B, these initial conditions are not specific to a particular model of scalar-tensor theories; rather they can be easily extended to the more general case of the Non-Minimally Coupled model of Sec.4.1.2. As we will see, the well known adiabatic and isocurvature modes still exist and are modified by the presence of the scalar field, but they still mantain the main properties that they have in Einstein GR and they reduce to the usual initial conditions in the limit $\gamma \to 0$. However, the presence to the scalar field lead to a new isocurvature mode that has no counterpart in general relativity, since the non-trivial coupling $F(\varphi)$ makes the limit $\gamma \to 0$ for this mode rather peculiar.

Next, we compute the CMB angular power spectrum of these pure isocurvature modes with the help of a modified version of the CLASS code [125] for the IG model [126, 127, 104] to study the differences with general relativ-

ity which arise from these initial conditions. In addition to the temperature power spectrum we give the E modes polarization and lensing power spectrum and the crosscorrelation between temperature and E modes.

Finally, using the formalism of Sec.3.3 we show how a correlation between the adiabatic and these IG isocurvature modes can be an alternative to the quintessence perturbations mentioned in Sec.3.4 in lowering the CMB temperature angular power spectrum at low multipoles l.

5.1 Adiabatic and Isocurvature Initial Conditions

We give here the results for the solutions of the coupled set of the synchronous gauge Einstein, Boltzmann and Klein-Gordon equations of Sec.2.3 and 4.6. Following [30, 38], we expand these equations in Laurent series for $\tau \to 0$ and match the orders in τ to find the leading orders in $k\tau$* of the Taylor series for the perturbations. The description of these modes is given in the synchronous gauge and conformal time as already mentioned. However, we give for each of these modes the results for the comoving curvature perturbation $\mathcal{R}$ (2.100), for the Newtonian potentials Φ and Ψ (2.39) and for the scalar field perturbation in the Newtonian gauge:

$$\delta\varphi_I = \delta\varphi + \frac{1}{2k^2}\varphi'(h' + 6\eta'), \tag{5.1}$$

where $\delta\varphi$ is simply the perturbation in the synchronous gauge, and the subscript I means that $\delta\varphi_I$ is gauge-invariant, as can be easily checked using the metric transformations (2.14).

In the following we fix the residual gauge freedom of the synchronous gauge to the CDM rest frame with $\theta_c = 0$ and we use the tight-coupling approximation (2.75) assuming $\theta_\gamma = \theta_b$.

*From here now we will write 'leading order' for the more complete expression 'leading orders in $k\tau$'.

As we will see all of these modes are independent on the choice of the potential $V(\varphi)$, provided that we consider only positive power law potentials. This means that the following analysis does not hold for tracking models of quintessence as Ratra-Peebles [23].

Adiabatic Mode

The adiabatic mode is given by:

$$\delta_\gamma = -\frac{2}{3}Ck^2\tau^2 + \frac{2}{15}Ck^2\tau^3\omega, \tag{5.2}$$

$$\theta_\gamma = -\frac{1}{36}Ck^4\tau^3 + \frac{C\omega(5(1+6\gamma)R_b - R_\nu + 1)}{240(1-R_\nu)}k^4\tau^4, \tag{5.3}$$

$$\delta_b = -\frac{1}{2}Ck^2\tau^2 + \frac{1}{10}Ck^2\tau^3\omega, \tag{5.4}$$

$$\delta_c = -\frac{1}{2}Ck^2\tau^2 + \frac{1}{10}Ck^2\tau^3\omega, \tag{5.5}$$

$$\delta_\nu = -\frac{2}{3}Ck^2\tau^2 + \frac{2}{15}Ck^2\tau^3\omega, \tag{5.6}$$

$$\theta_\nu = -\frac{C(4R_\nu+23)}{18(4R_\nu+15)}k^4\tau^3 + \frac{C\omega\left(8R_\nu^2 + 60\gamma(5-4R_\nu) + 50R_\nu + 275\right)}{120(2R_\nu+15)(4R_\nu+15)}k^4\tau^4, \tag{5.7}$$

$$\sigma_\nu = \frac{4C}{3(4R_\nu+15)}k^2\tau^2 + \frac{C(1+6\gamma)(4R_\nu-5)\omega}{3(4R_\nu+15)(2R_\nu+15)}k^2\tau^3, \tag{5.8}$$

$$F_3 = \frac{8C}{21(4R_\nu+15)}k^3\tau^3 + \frac{5C(1+6\gamma)(4R_\nu-5)\omega}{2(2R_\nu+15)(4R_\nu+15)}k^3\tau^4, \tag{5.9}$$

$$h = Ck^2\tau^2 - \frac{1}{5}C\omega k^2\tau^3, \tag{5.10}$$

$$\eta = 2C - \frac{C(4R_\nu+5)}{6(4R_\nu+15)}k^2\tau^2 + \frac{C\omega(-750\gamma + 8R_\nu(75\gamma+2R_\nu+35)+325)}{60(2R_\nu+15)(4R_\nu+15)}k^2\tau^3, \tag{5.11}$$

$$\delta\varphi = -\frac{1}{4}\gamma C\omega\varphi_i k^2\tau^3 + \frac{1}{40}(4+15\gamma)\gamma C\omega^2\varphi_i k^2\tau^4, \tag{5.12}$$

where ω is given by Eq.(4.57) and the constant C is an overall normalization constant, in analogy to that mentioned for the Einstein GR adiabatic mode (2.89). This constant multiply each Fourier mode and encodes the primordial power spectrum. The following results are given up to this time-independent

constant. Since the contribution of the scalar field is very subdominant with respect to the leading orders of the other perturbations, we expect this mode to behave similarly to its counterpart (2.89) in general relativity.

The background evolution of the homogeneus field φ reveals itself in the amplitude of the perturbations, which contains the initial value of the scalar field φ_i. Since this value is very low, we expect the scalar field to rise only slight differences with respect to the original adiabatic mode. The comoving curvature perturbation, the gravitational potentials and the gauge-invariant perturbation to the scalar field are given by:

$$\mathcal{R} = -2C + \frac{5C\omega}{2(4R_\nu + 15)}\tau, \tag{5.13}$$

$$\Psi = \frac{4C(2R_\nu + 5)}{4R_\nu + 15} - \frac{5C\omega(-90\gamma + 8(9\gamma + 2)R_\nu + 15)}{4(2R_\nu + 15)(4R_\nu + 15)}\tau, \tag{5.14}$$

$$\Phi = \frac{20C}{4R_\nu + 15} + \frac{5C\omega(8(27\gamma + 5)R_\nu - 15(18\gamma + 1))}{4(2R_\nu + 15)(4R_\nu + 15)}\tau, \tag{5.15}$$

$$\delta\varphi_I = -\frac{15\gamma C\omega\varphi_i}{4R_\nu + 15}\tau. \tag{5.16}$$

We see from these equations that at leading orders they are simply the results of [30].

Baryon Isocurvature Mode (BI)

In addition to the growing adiabatic mode, we have five isocurvature modes. We thus start giving the four modes which may be interpreted as an extension of the well-known isocurvature modes in Einstein general relativity [38] and we give an expression for the new one arising in scalar-tensor theories of dark energy.

The first one is the baryon isocurvature mode (BI):

$$\delta_\gamma = -\frac{2R_b}{3}\tau\omega + \frac{(15\gamma + 2)R_b}{8}\tau^2\omega^2 + \frac{k^2R_b}{108}\tau^3\omega\left(4 + \frac{(16k^2 - 9(324\gamma^2 + 82\gamma + 5)\omega^2}{5k^2}\right), \tag{5.17}$$

$$\theta_\gamma = -\frac{1}{12}k^2 R_b \tau^2 \omega + \frac{1}{96}k^2 R_b \tau^3 \omega \left((15\gamma + 2)\omega + \frac{6(6\gamma+1)R_b\omega}{R_\gamma} \right) + k^3\tau^4 \frac{R_b\omega(8k^2R_\gamma^2 - \omega^2(90(1+6\gamma)^2R_b^2 + 225\gamma(6\gamma+1)R_bR_\gamma + 2(324\gamma^2+82\gamma+5)R_\gamma^2))}{1920R_\gamma^2}, \tag{5.18}$$

$$\delta_c = -\frac{R_b}{2}\tau\omega + \frac{3}{32}(15\gamma+2)R_b\tau^2\omega^2 + \frac{R_b\omega}{720}\tau^3(16k^2 - 9(324\gamma^2+82\gamma+5)\omega^2), \tag{5.19}$$

$$\delta_b = 1 - \frac{R_b}{2}\tau\omega + \frac{3}{32}(15\gamma+2)R_b\tau^2\omega^2 + \frac{k^2R_b\omega}{80}\tau^3\left(4 - \frac{(324\gamma^2+82\gamma+5)\omega^2}{k^2}\right), \tag{5.20}$$

$$\delta_\nu = -\frac{2R_b}{3}\tau\omega + \frac{1}{8}(15\gamma+2)R_b\tau^2\omega^2 + \frac{R_b\omega}{60}\tau^3(4k^2 - (324\gamma^2+82\gamma+5)\omega^2), \tag{5.21}$$

$$\theta_\nu = -\frac{1}{12}k^2R_b\tau^2\omega + \frac{1}{96}(15\gamma+2)k^2R_b\tau^3\omega^2 + \frac{1}{240}k^4R_b\tau^4\omega\left(\frac{60\gamma+2R_\nu+25}{2R_\nu+15} - \frac{(324\gamma^2+82\gamma+5)\omega^2}{4k^2}\right), \tag{5.22}$$

$$\sigma_\nu = -\frac{(1+6\gamma)k^2R_b\tau^3\omega}{6(2R_\nu+15)} \tag{5.23}$$

$$F_3 = -\frac{(1+6\gamma)k^3R_b\tau^4\omega}{7(2R_\nu+15)}, \tag{5.24}$$

$$h = R_b\tau\omega - \frac{3R_b\omega^2}{16}(15\gamma+2)\tau^2 + \frac{R_b\omega}{360}\tau^3(9(324\gamma^2+82\gamma+5)\omega^2 - 16k^2), \tag{5.25}$$

$$\eta = -\frac{R_b\tau\omega}{6} + \frac{1}{32}(15\gamma+2)R_b\tau^2\omega^2 + \frac{R_b\tau^3\omega(-(324\gamma^2+82\gamma+5)\omega^2)}{240} + \frac{R_b\tau^3\omega(2k^2(-150\gamma+4R_\nu+5))}{240(2R_\nu+15)}, \tag{5.26}$$

$$\delta\varphi = \frac{3}{2}\gamma R_b\tau\omega\varphi_i - \frac{1}{8}\gamma(18\gamma+5)R_b\tau^2\omega^2\varphi_i + \frac{1}{48}\gamma R_b\tau^3\omega\varphi_i((27\gamma(9\gamma+4)+11)\omega^2-6k^2) - \frac{\gamma R_b\tau^4\omega^2\varphi_i(3(\gamma(1296\gamma(23\gamma+13)+3127)+184)\omega^2 - 8k^2(180\gamma+4R_b+47))}{7680}. \tag{5.27}$$

The leading order results for the other perturbations of interest are:

$$\mathcal{R} = \frac{1}{4}R_b\tau\omega, \tag{5.28}$$

$$\Psi = -\frac{R_b\tau\omega(-90\gamma+4R_\nu+15)}{8(2R_\nu+15)}, \tag{5.29}$$

$$\Phi = \frac{R_b\tau\omega(-270\gamma+4R_\nu-15)}{8(2R_\nu+15)}, \tag{5.30}$$

$$\delta\varphi_I = \frac{3}{2}\gamma R_b\tau\omega\varphi_i, \tag{5.31}$$

which have essentially the same behavior of the corresponding quantities found in [38] and reduce to them in the limit $\gamma \to 0$. However differently from the adiabatic mode, for this isocurvature mode the gravitational potentials Φ and Ψ have an explicit dependence on the coupling parameter γ right at the leading order, in addition to the implict dependence on it encoded in ω.

CDM Isocurvature Mode (CDI)

In general relativity the CDM isocurvature mode (CDI) is basically the same of the BI, with the substitution $R_b \to R_c$, with the only difference that now the only relative entropy perturbation that differs from zero is $\mathcal{S}_{\gamma c}$ and thus the perturbation δ_c to the CDM density has a leading constant term, while the leading term for δ_b goes as $\sim \tau$. As mentioned in chapter 3, this leads to the same imprints on the CMB angular power spectrum and, for this reason, usually the spectrum is computed for an effective mode given by the sum of the BI and CDI. However, since they are two independent modes we give here the perturbations for both the two modes. Furthermore, since the non-minimal coupling lead to non-trivial additional terms in the perturbed equations, it is interesting to investigate whether the extensions of these two

modes mantain the same structure, or acquire significant differences due to the presence of the scalar field.

The CDI mode for the IG model is given by:

$$\delta_\gamma = -\frac{2R_b}{3}\tau\omega+\frac{(15\gamma+2)R_b}{8}\tau^2\omega^2+\frac{k^2R_b}{108}\tau^3\omega\left(4+\frac{(16k^2-9(324\gamma^2+82\gamma+5)\omega^2}{5k^2}\right), \tag{5.32}$$

$$\theta_\gamma = -\frac{1}{12}k^2R_c\tau^2\omega+\frac{1}{96}k^2R_c\tau^3\omega\left((15\gamma+2)\omega+\frac{6(6\gamma+1)R_b\omega}{R_\gamma}\right) +k^3\tau^4\frac{R_c\omega(8k^2R_\gamma^2-\omega^2(90(1+6\gamma)^2R_b^2+225\gamma(6\gamma+1)R_bR_\gamma+2(324\gamma^2+82\gamma+5)R_\gamma^2))}{1920R_\gamma^2}, \tag{5.33}$$

$$\delta_c = 1-\frac{R_c}{2}\tau\omega+\frac{3}{32}(15\gamma+2)R_c\tau^2\omega^2+\frac{R_c\omega}{720}\tau^3(16k^2-9(324\gamma^2+82\gamma+5)\omega^2), \tag{5.34}$$

$$\delta_b = -\frac{R_c}{2}\tau\omega+\frac{3}{32}(15\gamma+2)R_c\tau^2\omega^2+\frac{k^2R_c\omega}{80}\tau^3\left(4-\frac{(324\gamma^2+82\gamma+5)\omega^2}{k^2}\right), \tag{5.35}$$

$$\delta_\nu = -\frac{2R_c}{3}\tau\omega+\frac{1}{8}(15\gamma+2)R_c\tau^2\omega^2+\frac{R_c\omega}{60}\tau^3(4k^2-(324\gamma^2+82\gamma+5)\omega^2), \tag{5.36}$$

$$\theta_\nu = -\frac{1}{12}k^2R_c\tau^2\omega+\frac{1}{96}(15\gamma+2)k^2R_c\tau^3\omega^2 +\frac{1}{240}k^4R_c\tau^4\omega\left(\frac{60\gamma+2R_\nu+25}{2R_\nu+15}-\frac{(324\gamma^2+82\gamma+5)\omega^2}{4k^2}\right), \tag{5.37}$$

$$\sigma_\nu = -\frac{(1+6\gamma)k^2R_c\tau^3\omega}{6(2R_\nu+15)} \tag{5.38}$$

$$F_3 = -\frac{(1+6\gamma)k^3R_c\tau^4\omega}{7(2R_\nu+15)}, \tag{5.39}$$

$$h = R_c\tau\omega - \frac{3R_c\omega^2}{16}(15\gamma+2)\tau^2 + \frac{R_c\omega}{360}\tau^3(9(324\gamma^2+82\gamma+5)\omega^2 - 16k^2), \quad (5.40)$$

$$\eta = -\frac{R_c\tau\omega}{6} + \frac{1}{32}(15\gamma+2)R_c\tau^2\omega^2 + \frac{R_c\tau^3\omega(-(324\gamma^2+82\gamma+5)\omega^2)}{240} + \frac{R_c\tau^3\omega(2k^2(-150\gamma+4R_\nu+5))}{240(2R_\nu+15)}, \quad (5.41)$$

$$\delta\varphi = \frac{3}{2}\gamma R_c\tau\omega\varphi_i - \frac{1}{8}\gamma(18\gamma+5)R_c\tau^2\omega^2\varphi_i + \frac{1}{48}\gamma R_c\tau^3\omega\varphi_i((27\gamma(9\gamma+4)+11)\omega^2 - 6k^2) - \frac{\gamma R_c\tau^4\omega^2\varphi_i(3(\gamma(1296\gamma(23\gamma+13)+3127)+184)\omega^2 - 8k^2(180\gamma+4R_b+47))}{7680}. \quad (5.42)$$

As we can see, apart from the substitution $R_b \to R_c$ that leads to greater amplitude for this mode, the structure of the perturbations is the same as in the BI mode previously seen. In appendix B, we will show that this is a more general feature shared also by Non-Minimal Coupled models.

As in the BI mode, the comoving curvature perturbation, the Newtonian potentials and the gauge-invariant perturbation to the scalar field have the following behaviour:

$$\mathcal{R} = \frac{1}{4}R_c\tau\omega, \quad (5.43)$$

$$\Psi = -\frac{R_c\tau\omega(-90\gamma+4R_\nu+15)}{8(2R_\nu+15)}, \quad (5.44)$$

$$\Phi = \frac{R_c\tau\omega(-270\gamma+4R_\nu-15)}{8(2R_\nu+15)}, \quad (5.45)$$

$$\delta\varphi_I = \frac{3}{2}\gamma R_c\tau\omega\varphi_i. \quad (5.46)$$

Neutrino Density Mode (NID)

The neutrino density mode (NID) is given by:

$$\delta_\gamma = -\frac{R_\nu}{R_\gamma} + \frac{k^2R_\nu\tau^2}{6R_\gamma} - \frac{k^2R_bR_\nu\tau^3\omega}{12R_\gamma}\left(\frac{1+6\gamma}{R_\gamma} + \frac{1}{5}\right), \quad (5.47)$$

$$\theta_\gamma = -\frac{k^2 R_\nu \tau}{4R_\gamma} + \frac{3(1+6\gamma)k^2 R_b R_\nu \tau^2 \omega}{16R_\gamma^2} + \frac{k^3 R_\nu \tau^3}{8R_\gamma}\left(\frac{k}{9} - \frac{3(1+6\gamma)R_b\omega^2(3(1+6\gamma)R_b - R_\gamma)}{8kR_\gamma^2}\right), \quad (5.48)$$

$$\delta_b = \frac{k^2 R_\nu \tau^2}{8R_\gamma} - \frac{k^2 R_b R_\nu \tau^3 \omega}{16R_\gamma}\left(\frac{1+6\gamma}{R_\gamma} + \frac{1}{5}\right), \quad (5.49)$$

$$\delta_c = -\frac{k^2 R_b R_\nu \tau^3 \omega}{80R_\gamma} + k^4\tau^4\frac{R_\nu}{72(4R_\nu+15)} + k^4\tau^4\left(\frac{R_b R_\nu \omega^2(2(1+6\gamma)R_b + (17\gamma+2)R_\gamma)}{512k^2R_\gamma^2}\right), \quad (5.50)$$

$$\delta_\nu = 1 - \frac{k^2\tau^2}{6} - \frac{k^2 R_b R_\nu \tau^3 \omega}{60R_\gamma}, \quad (5.51)$$

$$\theta_\nu = \frac{k^2\tau}{4}, \quad (5.52)$$

$$\sigma_\nu = \frac{2(1+6\gamma)k^2 R_\nu \tau^3 \omega}{3(2R_\nu+15)(4R_\nu+15)} + \frac{k^2\tau^2}{2(4R_\nu+15)}, \quad (5.53)$$

$$F_3 = \frac{(1+6\gamma)k^3 R_\nu \tau^4 \omega}{7(2R_\nu+15)(4R_\nu+15)} + \frac{k^3\tau^3}{7(4R_\nu+15)}, \quad (5.54)$$

$$h = \frac{k^2 R_b R_\nu \tau^3 \omega}{40R_\gamma} + \frac{R_\nu}{36(4R_\nu+15)}k^4\tau^4 - \left(\frac{R_b R_\nu \omega^2(2(1+6\gamma)R_b + (17\gamma+2)R_\gamma)}{256k^2R_\gamma^2}\right)k^4\tau^4, \quad (5.55)$$

$$\eta = -\frac{R_\nu k^2\tau^2}{6(4R_\nu+15)} + \frac{R_\nu}{6}k^2\tau^3\omega\left(\frac{5(1+6\gamma)}{(2R_\nu+15)(4R_\nu+15)} - \frac{R_b}{40R_\gamma}\right) \quad (5.56)$$

$$\delta\varphi = \frac{\gamma k^2 R_b R_\nu \tau^3 \omega \varphi_i}{32R_\gamma} - \frac{3\gamma k^2 R_b R_\nu \tau^4 \omega^2 \varphi_i}{64R_\gamma}\left(\frac{(1+4\gamma)}{4} + \frac{(1+6\gamma)R_b}{5R_\gamma}\right) \quad (5.57)$$

The comoving curvature perturbation, the Newtonian potentials and the gauge-invariant perturbation to the scalar field are given by:

$$\mathcal{R} = -\frac{R_\nu \tau\omega}{4(4R_\nu+15)}, \tag{5.58}$$

$$\Psi = \frac{R_\nu}{4R_\nu+15} + \frac{\tau\omega(2R_\nu^2-180\gamma R_\nu-15R_\nu)}{4(2R_\nu+15)(4R_\nu+15)}, \tag{5.59}$$

$$\Phi = -\frac{2R_\nu}{4R_\nu+15} - \frac{\tau\omega(2R_\nu^2-540\gamma R_\nu-75R_\nu)}{4(2R_\nu+15)(4R_\nu+15)}, \tag{5.60}$$

$$\delta\varphi_I = -\frac{3\gamma R_\nu \tau\omega\varphi_i}{2(4R_\nu+15)}. \tag{5.61}$$

Their behaviour is the same as in the usual NID in general relativity where $\Phi = -2\Psi$ [38, 34]. It is also interesting to note that at leading order they, as well as the comoving curvature perturbation that vanishes since it is an isocurvature mode, are completely independent on the IG model and differently from the previous isocurvature modes their leading order value is *exactly* the same as in general relativity.

Neutrino Velocity Mode (NIV)

The last mode, which has a counterpart in general relativity, is the neutrino velocity mode (NID). The mode is given by:

$$\delta_\gamma = \frac{4R_\nu}{3R_\gamma}k\tau - \frac{R_b R_\nu \omega(12\gamma+R_\gamma+2)}{4R_\gamma^2}k\tau^2, \tag{5.62}$$

$$\theta_\gamma = -\frac{kR_\nu}{R_\gamma} + \frac{3(1+6\gamma)R_b R_\nu\omega}{4R_\gamma^2}k\tau + \frac{R_\nu(8k^2R_\gamma^2-9(1+6\gamma)R_b\omega^2(3(1+6\gamma)R_b-R_\gamma))}{48R_\gamma^3}k\tau^2, \tag{5.63}$$

$$\delta_b = \frac{R_\nu}{R_\gamma}k\tau - \frac{3R_bR_\nu\omega(12\gamma + R_\gamma + 2)}{16R_\gamma^2}k\tau^2, \tag{5.64}$$

$$\delta_c = -\frac{3R_bR_\nu\omega}{16R_\gamma}k\tau^2, \tag{5.65}$$

$$\delta_\nu = -\frac{4}{3}k\tau - \frac{R_bR_\nu\omega}{4R_\gamma}k\tau^2, \tag{5.66}$$

$$\theta_\nu = k - \frac{(4R_\nu + 9)}{6(4R_\nu + 5)}k^3\tau^2, \tag{5.67}$$

$$\sigma_\nu = \frac{4}{3(4R_\nu + 5)}k\tau + \frac{4(1 + 6\gamma)R_\nu\omega}{(4R_\nu + 5)(4R_\nu + 15)}k\tau^2, \tag{5.68}$$

$$F_3 = \frac{4}{7(4R_\nu + 5)}k^2\tau^2, \tag{5.69}$$

$$h = \frac{3R_bR_\nu\omega}{8R_\gamma}k\tau^2, \tag{5.70}$$

$$\eta = -\frac{4R_\nu}{3(4R_\nu + 5)}k\tau - \frac{R_\nu\omega(R_b(4R_\nu + 5)(4R_\nu + 15) - 80(1 + 6\gamma)R_\gamma)}{16R_\gamma(4R_\nu + 5)(4R_\nu + 15)}k\tau^2, \tag{5.71}$$

$$\delta\varphi = \frac{\gamma R_bR_\nu\omega\varphi_i}{2R_\gamma}k\tau^2 - \frac{\gamma R_bR_\nu\omega^2\varphi_i(9(1 + 6\gamma)R_b + (72\gamma + 19)R_\gamma)}{96R_\gamma^2}k\tau^3. \tag{5.72}$$

The comoving curvature perturbation, the Newtonian potentials and the gauge-invariant perturbation to the scalar field at leading order are:

$$\mathcal{R} = -\frac{R_\nu\omega}{k(4R_\nu + 5)}, \tag{5.73}$$

$$\Psi = \frac{4R_\nu}{k(4R_\nu + 5)\tau}, \tag{5.74}$$

$$\Phi = -\frac{4R_\nu}{k(4R_\nu + 5)\tau}, \tag{5.75}$$

$$\delta\varphi_I = \frac{6\gamma R_\nu\omega\varphi_i}{k(4R_\nu + 5)}. \tag{5.76}$$

Note that, as in the NID mode, the Newtonian potentials Ψ and Φ, at most at the leading order, are exactly the same as in general relativity and also in this case have a singular behaviour in the synchronous gauge. Finally, it is interesting to note that the gauge-invariant perturbation to the scalar field is constant at leading order.

Scalar Field-Radiation Isocurvature Mode (RAD)

As already mentioned, the previous isocurvature modes that we have found solving the perturbed equations in IG are the extensions to the IG model of the well known isocurvature modes found in Einstein GR [38]. However, since in scalar-tensor theories an additional component takes part to the Universe evolution, i.e. the scalar field φ, we expect that this rise a new isocurvature mode [79, 47, 49].

Since this is entirely due to the presence of the scalar field it has no analogous with the isocurvature modes for the standard ΛCDM model. One might argue that this mode can be view as an extension of some quintessence isocurvature perturbation in the limit $\gamma \to 0$, since also in that case the quintessence field could rise new isocurvature mode [47] in addition to the standard ones from Ref.[38]. However, as we will see, this mode has not a finite limit for $\gamma \to 0$ as the previous ones, since it is strictly peculiar of the IG and Non-Minimally Coupled theories. For this reason this mode is peculiar of the IG theory. The perturbations are given by:

$$\delta_\gamma = -1 - \frac{2}{3}\omega\tau + \frac{1}{6}\omega\left(\frac{3(15\gamma+2)\omega}{4k} + \frac{k}{\omega}\right)k\tau^2 + \frac{\omega\left(-2k^2(3R_b(30\gamma+R_\gamma+5)-20R_\gamma) - 3(3\gamma(3\gamma(36\gamma+85)+58)+10)R_\gamma\omega^2\right)}{360R_\gamma}\tau^3, \tag{5.77}$$

$$\theta_\gamma = -\frac{1}{4}k^2\tau + \frac{1}{48}\omega\left(\frac{9(1+6\gamma)kR_b}{R_\gamma} - 4k\right)k\tau^2 + \frac{\omega\left(8k^2R_\gamma^2 + 3\omega^2\left(-27(6\gamma R_b+R_b)^2 + 21R_b(6\gamma R_\gamma+R_\gamma) + 2(15\gamma+2)R_\gamma^2\right)\right)}{576R_\gamma^2\omega}k^2\tau^3, \tag{5.78}$$

$$\delta_b = -\frac{\omega}{2}\tau + \frac{1}{8}\omega\left(\frac{3(15\gamma+2)\omega}{4k} + \frac{k}{\omega}\right)k\tau^2 + \frac{\omega\left(2k^2(3R_b(-30\gamma+R_\nu-6)+20R_\gamma) - 3(3\gamma(3\gamma(36\gamma+85)+58)+10)R_\gamma\omega^2\right)}{480R_\gamma}\tau^3, \tag{5.79}$$

$$\delta_c = -\frac{1}{2}\omega\tau + \frac{3}{32}(15\gamma+2)\omega^2\tau^2 + \frac{(k^2(80-18R_b)-9(3\gamma(3\gamma(36\gamma+85)+58)+10)\omega^2)}{1440}\omega\tau^3, \quad (5.80)$$

$$\delta_\nu = -1 - \frac{2\omega}{3}\tau + \frac{\omega\left(3(15\gamma+2)\omega^2+4k^2\right)}{24\omega}\tau^2 + \frac{1}{360}\left(k^2(40-6R_b)-3(3\gamma(3\gamma(36\gamma+85)+58)+10)\omega^2\right)\omega\tau^3, \quad (5.81)$$

$$\theta_\nu = -\frac{1}{4}k^2\tau - \frac{1}{12}\omega k^2\tau^2 + \frac{(4k^2(4R_\nu+11)+3(15\gamma+2)(4R_\nu+15)\omega^2)}{288(4R_\nu+15)}k^2\tau^3, \quad (5.82)$$

$$\sigma_\nu = \frac{1}{6(4R_\nu+15)}k^2\tau^2 - \frac{2\omega(1+6\gamma)(R_\nu+5)}{3(2R_\nu+15)(4R_\nu+15)}k^2\tau^3, \quad (5.83)$$

$$F_3 = \frac{1}{21(4R_\nu+15)}k^3\tau^3 - \frac{\omega(1+6\gamma)(R_\nu+5)}{7(2R_\nu+15)(4R_\nu+15)}k^3\tau^4, \quad (5.84)$$

$$h = \omega\tau - \frac{3}{16}(15\gamma+2)\omega^2\tau^2 + \frac{1}{720}\left(9(3\gamma(3\gamma(36\gamma+85)+58)+10)\omega^2+2k^2(9R_b-40)\right)\omega\tau^3, \quad (5.85)$$

$$\eta = -\frac{\omega}{6}\tau + \frac{(16k^2(R_\nu+5)+3(15\gamma+2)(4R_\nu+15)\omega^2)}{96(4R_\nu+15)\omega}\omega\tau^2 + \frac{-2k^2(3R_b(2R_\nu+15)(4R_\nu+15))}{1440(2R_\nu+15)(4R_\nu+15)}\omega\tau^3 + \frac{(-2k^2\left(-20\left(8R_\nu^2+60R_\nu+75\right)+3600\gamma(R_\nu+5)\right))}{1440(2R_\nu+15)(4R_\nu+15)}k\tau^3 + \\ - (3(3\gamma(3\gamma(36\gamma+85)+58)+10)\omega^2)\omega\tau^3, \quad (5.86)$$

$$\delta\varphi = -\frac{\varphi_i}{2} + \frac{3}{4}\gamma\varphi_i\omega\tau + \frac{\varphi_i\left(4k^2-3\gamma(27\gamma+8)\omega^2\right)}{48}\tau^2 + \frac{\varphi_i\left(9\gamma(3\gamma(180\gamma+83)+26)\omega^2+4k^2(9\gamma(R_b-4)-2)\right)}{1152}\omega\tau^3. \quad (5.87)$$

Before giving the expressions for the comoving curvature perturbation and for the Newtonian potentials, we analize the characteristics of the perturbations. In Einstein GR when one has an isocurvature mode this corresponds to a non vanishing relative entropy perturbations between two species. An example will be useful: in the NID (3.14) in general relativity, the relative entropy perturbation $\mathcal{S}_{\nu\gamma} = 3/4\delta_\nu - 3/4\delta_\gamma$ is different from zero. It can be easily seen that this in turn means that the two density perturbations cancels at leading order, that is $\delta\rho_\gamma + \delta\rho_\nu = 0$. Since in the scalar tensor theories the density perturbation of the scalar field is related in a very difficult way to the scalar field perturbation $\delta\varphi$ a naive criterion to understand the physics of isocurvature perturbations may be useful. In fact, expanding the perturbed equations in a Laurent series, it is easy to see that the isocurvature perturbations lead to terms singular in the conformal time τ. These terms have to vanish in order to find non-singular solutions for the perturbed field equations. Returning to the NID mode, it is easy to see that the only condition in order to make these terms vanish is the cancellation between the two radiation densities $\delta\rho_\gamma + \delta\rho_\nu = 0$.

With this in mind, it can be easily seen that for this mode not to have any singular term in the Laurent series expansion of the perturbed field equations we must have a cancellation, i.e. an isocurvature, between the next-to-leading term in the scalar field perturbation and the leading terms of the radiation density constrasts δ_ν and δ_γ in order to cancel the singular terms proportional to τ^{-2} in the perturbed Einstein equations. For this reason, from now on, we denote this mode with the label 'RAD', in fact, defining the scalar field energy density ρ_φ as in Eq.(4.20), it would be easy to check that this means that $\delta\rho_\varphi + \delta\rho_\gamma + \delta\rho_\nu = 0$, exactly as it happens for the Einstein GR isocurvature modes. It is also important to mention that the next-to-leading term in $\delta\varphi$ is determined through the Klein-Gordon equation (4.67) only by the constant leading term in $\delta\varphi$.

As a final comment we notice that this mode is really independent from the other previously mentioned, this can be easily seen since this is the only

mode that allows the scalar field perturbation in the synchronous gauge to have a constant leading order.

We now look at the comoving curvature perturbation, the Newtonian potentials and the gauge-invariant perturbation to φ. These quantities are given at leading order by:

$$\mathcal{R} = -\frac{5(R_\nu + 4)}{4(4R_\nu + 15)}\omega\tau, \tag{5.88}$$

$$\Psi = -\frac{(R_\nu + 5)}{(4R_\nu + 15)} - \frac{5\left(-180\gamma + 2R_\nu^2 - 36\gamma R_\nu + 17R_\nu + 30\right)}{4(2R_\nu + 15)(4R_\nu + 15)}\omega\tau, \tag{5.89}$$

$$\Phi = \frac{2(R_\nu + 5)}{(4R_\nu + 15)} + \frac{5\left(-540\gamma + 2R_\nu^2 - 108\gamma R_\nu + 5R_\nu - 30\right)}{4(2R_\nu + 15)(4R_\nu + 15)}\omega\tau, \tag{5.90}$$

$$\delta\varphi_I = -\frac{\varphi_i}{2} + \frac{3\varphi_i(5\gamma + 2\gamma R_\nu)}{4(4R_\nu + 15)}\omega\tau. \tag{5.91}$$

It is very interesting to note that the Newtonian potentials and the comoving curvature perturbations have the same expressions of the same quantities for the NID mode (5.58). The same holds for the next to leading term of the gauge-invariant quantity $\delta\varphi_I$, however the leading order in Eq.(5.91) is constant since $\delta\varphi$ has a constant term in the synchronous gauge description.

5.2 CMB Angular Power Spectra

We now present the results obtained for the CMB angular power spectrum with an extension of the modified public CLASS code [126, 127, 104] which we further extended to include the isocurvature modes for IG. The background evolution is given in Sec.4.5. The set of cosmological parameters used are given in the following table:

Quantity	Units
Ω_{b0}	0.02222
$\Omega_{\rm CDM0}$	0.1197
$T_{\rm CMB}$	$2.7255\,K$
n_s	0.9655
$\tau_{\rm reio}$	0.078

As mentioned in Sec.3.1, no known mechanisms can excite the NIV mode. For this reason we show only the results obtained for the BI, CDI, NID and RAD modes.

5.2.1 Temperature Power Spectra

In this section we give the results obtained for the CMB temperature power spectrum. Since the RAD mode is peculiar to scalar-tensor theories, we analyze its imprints separately from the other modes and start from them. In Figs.5.1, 5.2, 5.3 and 5.4 we show the power spectra of the adiabatic, BI, CDI and NID mode respectively for different values of γ. We remind that Planck constraint is $\gamma < 0.0017$ at 95% CL [104]. As we can see from Fig.5.1, where the C_ls are plotted in linear scale to evidence the differences with the ΛCDM model, the effect of the scalar field is to shift the peaks towards higher multipoles and to slightly change their amplitudes. This effect, first noticed in [126] is more pronounced for higher values of γ. From Figs.5.2, 5.3 and 5.4, we see that this occurs also for the isocurvature modes. We can also see that the BI and the CDI modes give exactly the same contributes to CMB temperature power spectrum, as we discussed in the previous section. For these modes, in addition to the shift of the peaks, we can see in Figs.5.2 and 5.3 a significant enhancement of the power spectrum at low multipoles. This can be stated more quantitatively if we look at the relative differences for these modes between the original CDI and BI modes in general relativity (see Figs.D.1, D.2 in Appendix D), from which we can see that there is a substantial enhancement of the low multipoles region of about 20%. This

does not happen for the NID mode in Fig.D.3.

We point out that, since these modes give very similair imprints on the CMB to those of Ref.[38], they obviously cannot lead to the structure formation as we have seen in Chapter 3.

We now show in Fig.5.5 the temperature power spectrum for the RAD mode and we compare it to the NID and CDI modes for the usual ΛCDM model in Fig.5.6. The shape of the angular power spectrum of this mode is totally different from the other ones. We can see from the different plots for $\gamma = 5 \cdot 10^{-3}$ and $\gamma = 5 \cdot 10^{-4}$ that the value of γ has a stronger impact on the amplitude of the peaks and their position with respect to the other modes. However, as we will see in the following sections, the main feature of this mode is that when we consider correlation with the adiabatic mode, it can appreciably lower the low multipoles region of the temperature power spectrum.

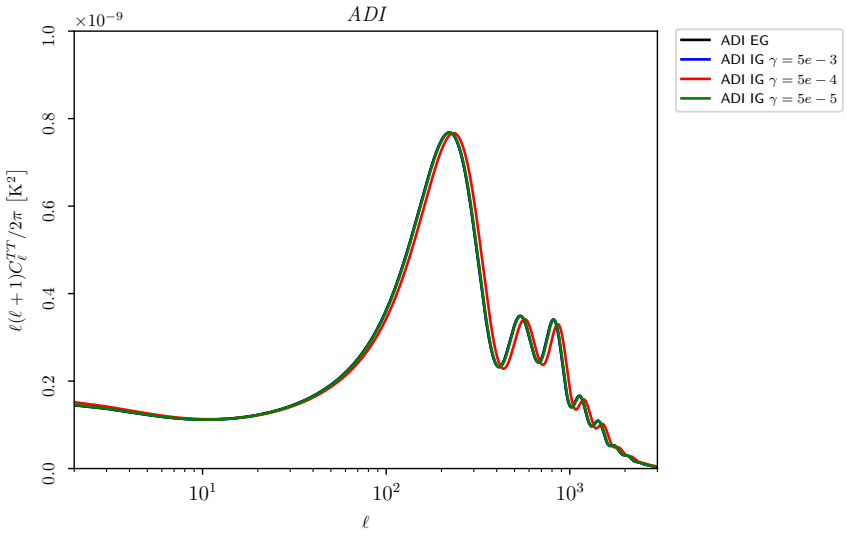

Figure 5.1: Adiabatic temperature power spectrum for three different values of γ, compared to the original ΛCDM model.

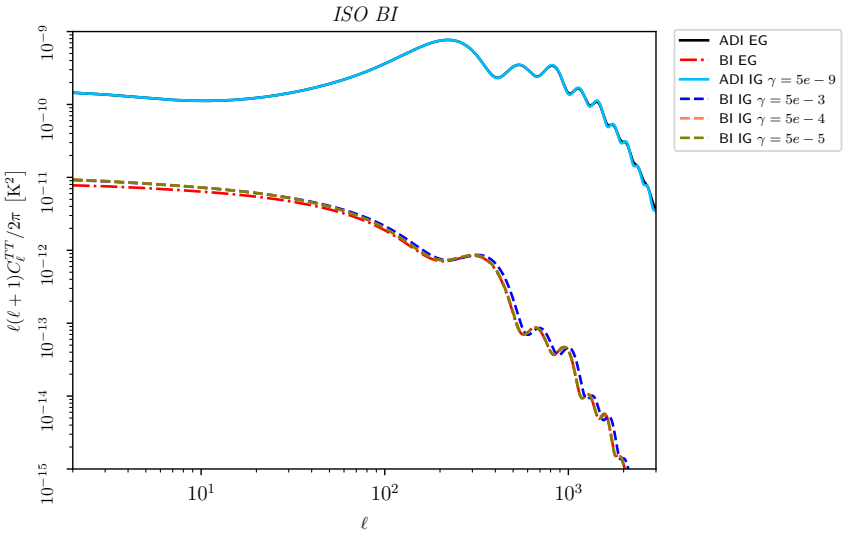

Figure 5.2: BI temperature power spectrum for three different values of γ, compared to the original ΛCDM model.

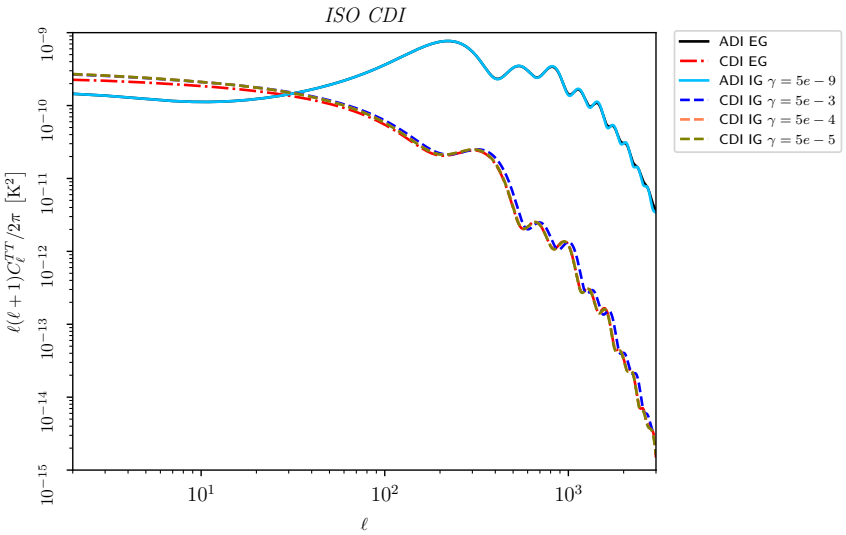

Figure 5.3: CDI temperature power spectrum for three different values of γ, compared to the original ΛCDM model.

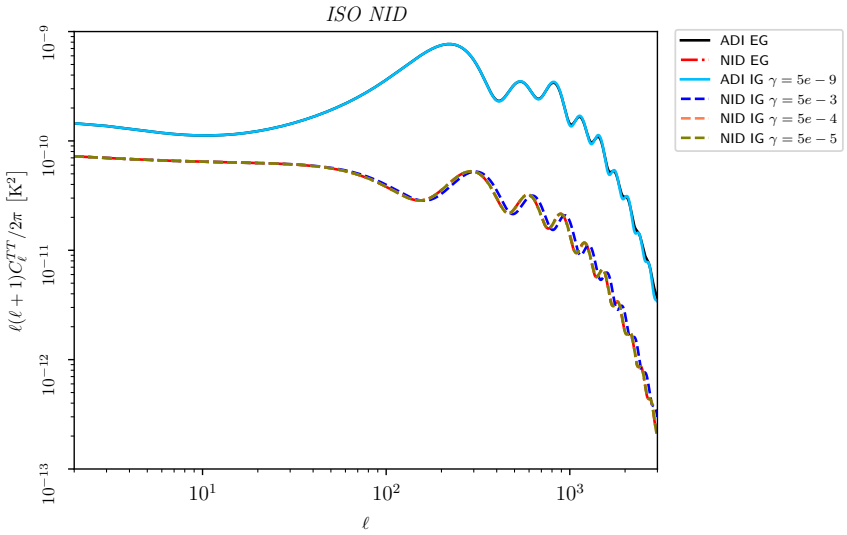

Figure 5.4: NID temperature power spectrum for three different values of γ, compared to the original ΛCDM model.

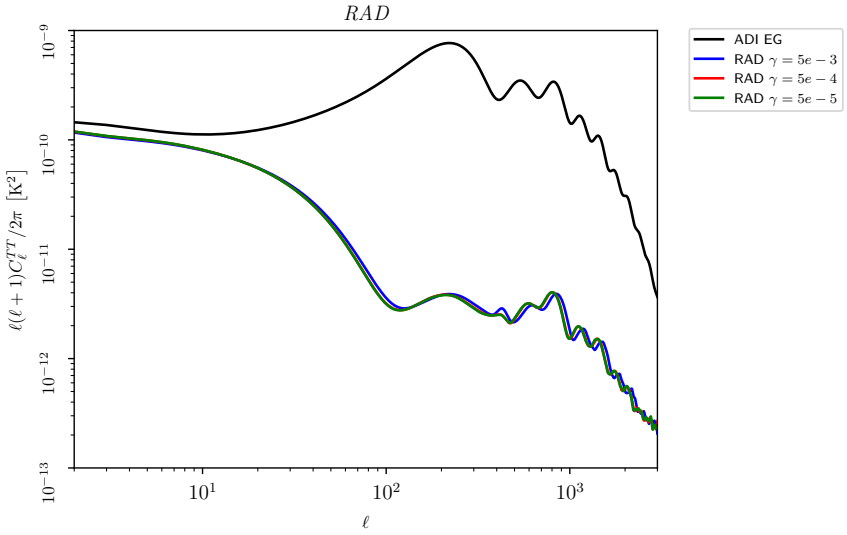

Figure 5.5: RAD temperature power spectrum for three different values of γ, compared to the original ΛCDM model.

5.2.2 EE polarization Spectra

We now show the E-mode polarization spectra for the initial conditions given in Sec.5.1. From now on, we plot only the isocurvature initial con-

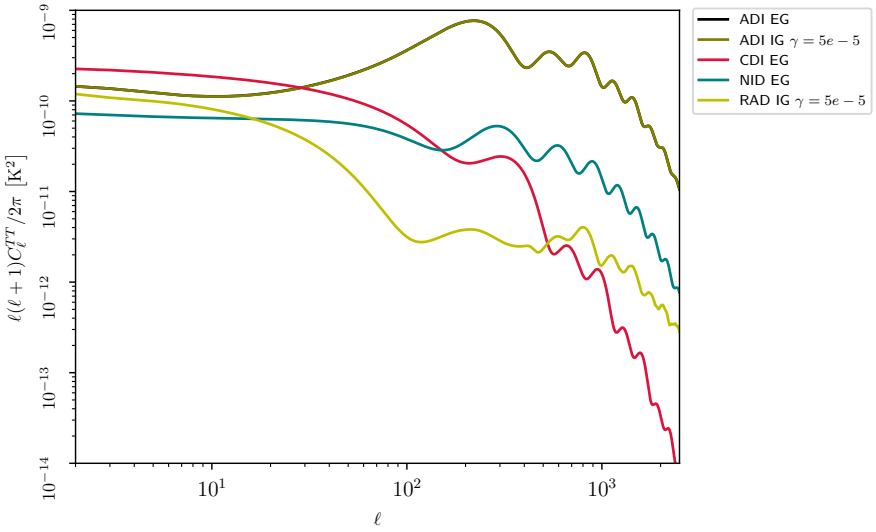

Figure 5.6: RAD temperature power spectrum for $\gamma = 0.00005$, compared to the NID and CDI ΛCDM model.

ditions, since an accurate analysis of the adiabatic mode has already been done in Ref.[126]. Nevertheless, we plot also the general relativity adiabatic mode and the adiabatic mode for a very low $\gamma = 5 \cdot 10^{-9}$ together with the isocurvature modes for a useful comparison. Since the CDI and the BI mode give the same imprints on the CMB power spectra with just different amplitudes, as we can see from Figs.5.2 and 5.3, from now on we give only the results from the CDI mode. The T-E cross-correlation spectra are given in Appendix C.

Also for the EE spectrum we can see that the CDI and NID modes give similair imprints to their Einstein GR counterparts and, as for the TT spectrum, the CDI mode differs from general relativity in an enhancement of the spectrum at low multipoles as we can see from Figs. 5.7 and D.4.

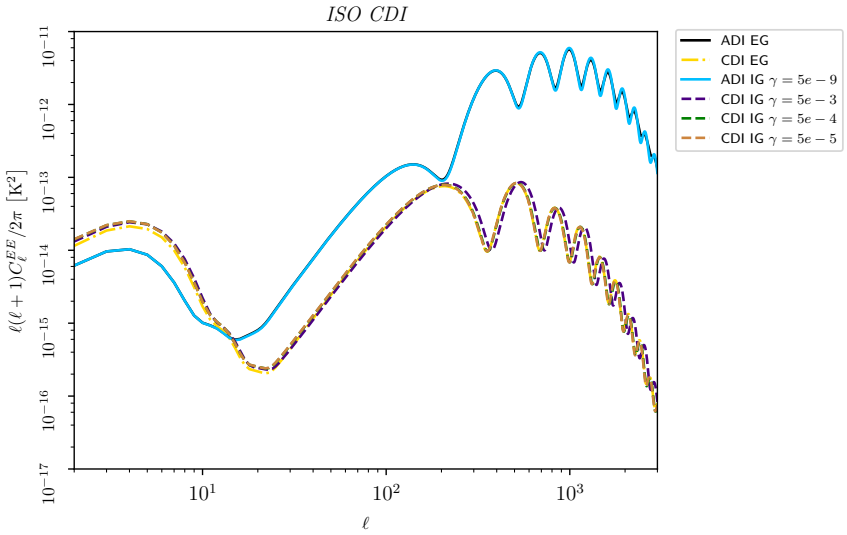

Figure 5.7: CDI EE power spectrum for three different values of γ, compared to the original ΛCDM model.

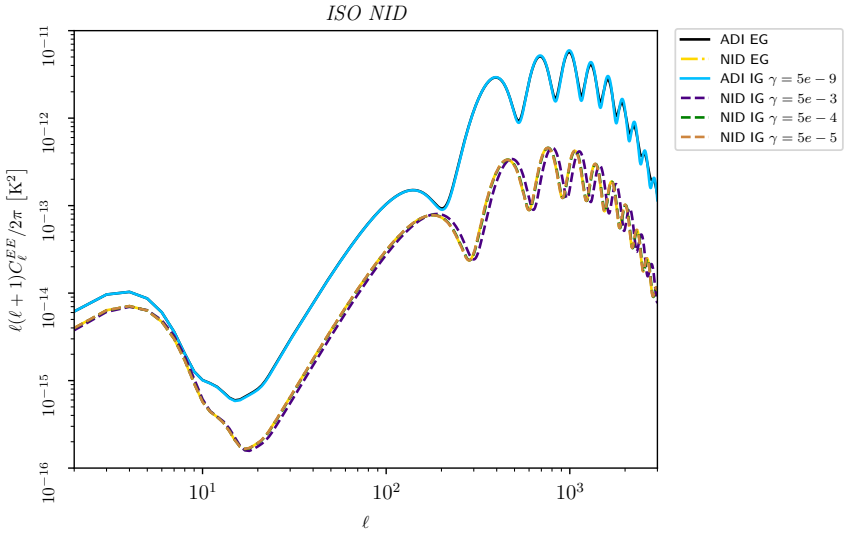

Figure 5.8: NIS EE power spectrum for three different values of γ, compared to the original ΛCDM model.

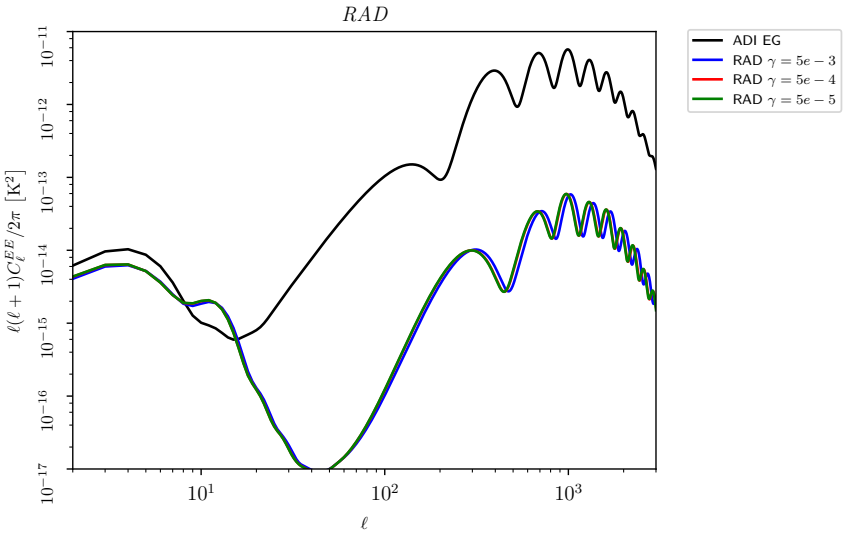

Figure 5.9: RAD EE spectrum for three different values of γ, compared to the original adiabatic mode for the ΛCDM model.

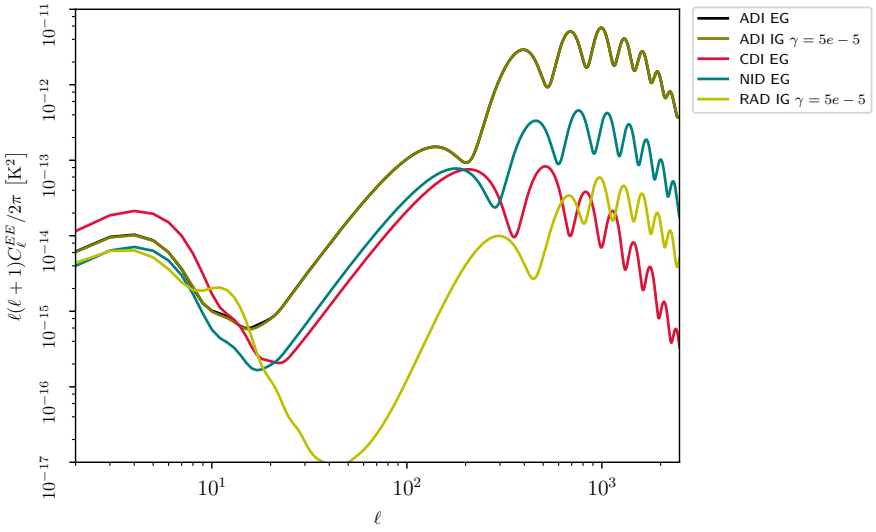

Figure 5.10: RAD temperature power spectrum for $\gamma = 0.00005$, compared to the NID and CDI ΛCDM model.

5.2.3 Lensing Power Spectrum

Another important quantity, which is worth showing, is the lensing power spectrum. As we mentioned in Sec.2.4, photons are deflected by the pres-

ence of gravitational potentials. The effect of this gravitational lensing is to smooth the acoustic peaks in temperature and to convert a fraction of the E polarization into B polarization. This effect is important especially on small angular scales $l \geq 1000$ [128] where the lensing B-modes peaks.

If we define the gravitational potential as [31, 128]:

$$\phi(\hat{n}) = -2 \int_0^{\chi^*} d\chi \, \frac{\chi^* - \chi}{\chi^* \chi} \Psi(\chi \hat{n}, \tau_0 - \tau), \tag{5.92}$$

where Ψ is the gravitational potential, τ_0 is the present conformal time and χ^* is the comoving distance to the last scattering surface, we can define the lensing power spectrum as

$$C_l^{\phi\phi} \equiv \langle \phi(\hat{n})^*_{lm} \phi(\hat{n})_{lm} \rangle, \tag{5.93}$$

where $\phi(\hat{n})_{lm}$ are the components of $\phi(\hat{n})$ in an spherical harmonics expansion. The reason for studying the lensing power spectrum is that it can be used to probe the matter power spectrum integrated back to the last scattering surface. Furthermore it correlates with the temperature anisotropies since they are influenced by the ISW effect and thus it can give important information about the dark energy domination at low redshift.

We now show the lensing power spectrum for the CDI, NID and RAD mode.

5.3 Correlated Adiabatic and Isocurvature Modes

We now analyze the correlation between the adiabatic and isocurvature modes with the formalism introduced in Sec.3.3. Following [74, 75] we are interested in finding a possible mechanism which can explain the lack of power in the low multipoles region of the CMB temperature power spectrum (see Sec.3.4). As we mentioned in the last section and we can see from Fig.D.3, the NID mode CMB imprints in the IG model are exactly the same as in general relativity. For this reason we only show the correlated isocurvature and adiabatic imprints for the RAD mode and for the effective CDI mode

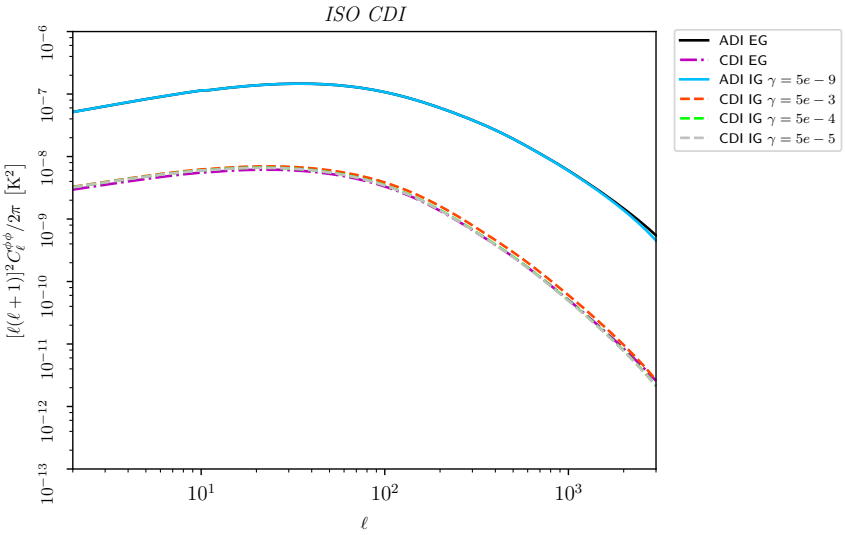

Figure 5.11: CDI $\phi\phi$ power spectrum for three different values of γ, compared to the original ΛCDM model.

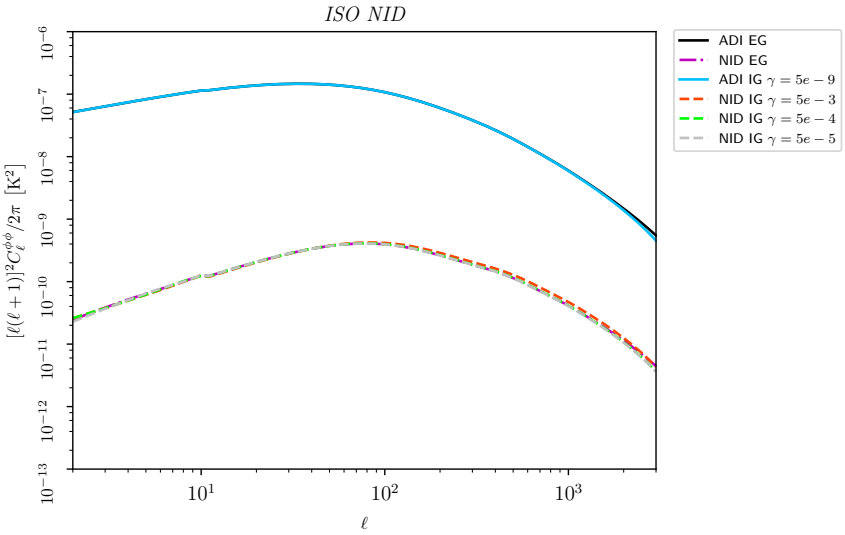

Figure 5.12: NID $\phi\phi$ power spectrum for three different values of γ, compared to the original ΛCDM model.

given by CDI + $\frac{R_c}{R_b}$BI [54], since, as we have seen, these two modes give practically the same CMB imprints. We denote the latter mode by MAT,

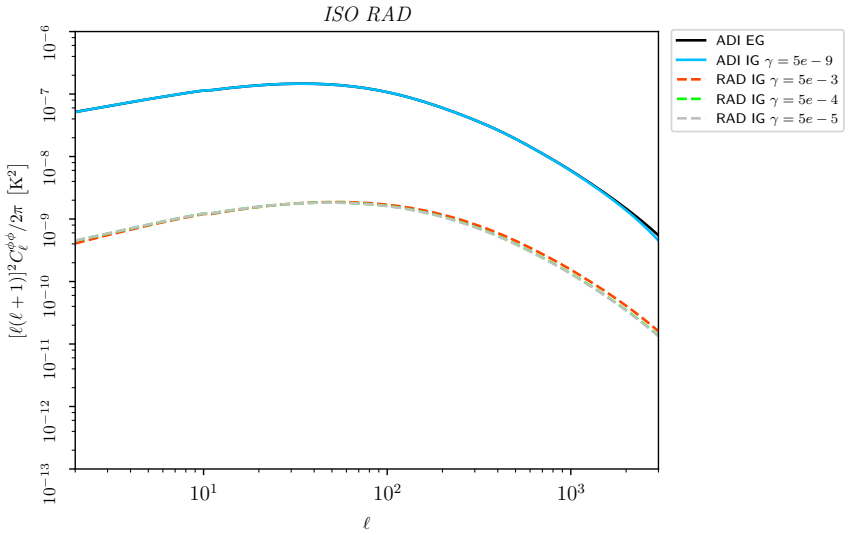

Figure 5.13: RAD $\phi\phi$ power spectrum for three different values of γ.

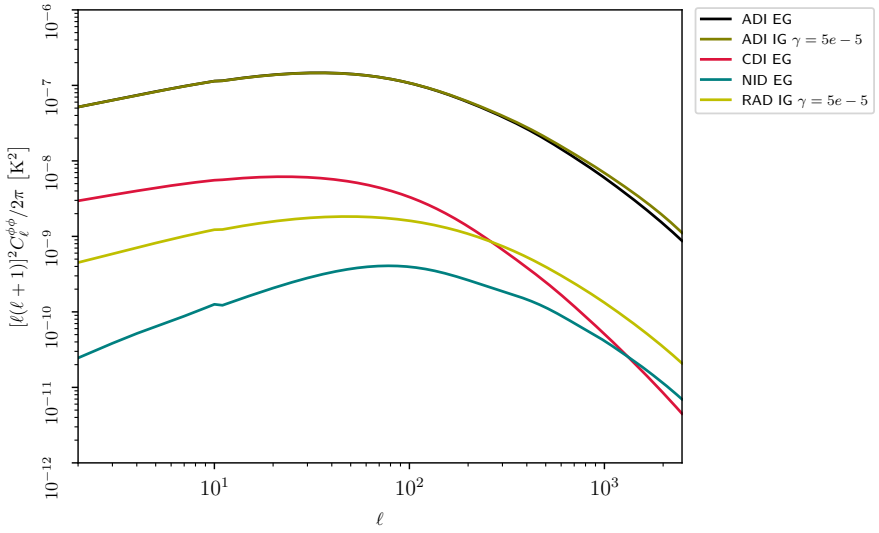

Figure 5.14: RAD temperature power spectrum for $\gamma = 0.00005$, compared to the NID and CDI ΛCDM model.

since it is due to isocurvature perturbations in the matter sector.

We show in Figs.5.15 and 5.16 this analysis for the IG model with $\gamma = 0.005$ for different values of the allowed isocurvature fraction $f_{\rm iso} = 0.1$, 0.5, 1

and for the three limit cases of totally correlated, totally anti-correlated and uncorrelated (with $\cos\theta = 1, -1, 0$ respectively) isocurvature and adiabatic mode for the RAD and MAT modes respectively. In these figures we have plotted the isocurvature, the adiabatic and the total power spectrum with the convention of Eq.(3.51). We also show the cross-correlation angular power spectra $C_l^{\rm corr}$ for the same values of $f_{\rm iso}$ and $\cos\theta$ in Figs.5.17 and 5.18.

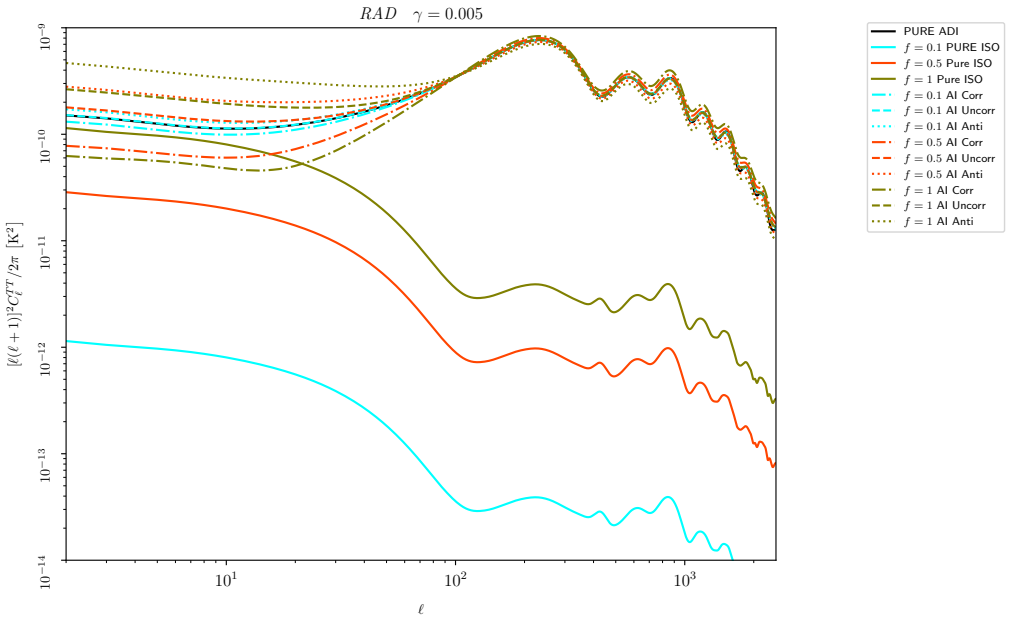

Figure 5.15: Temperature power spectrum for the RAD mode with different values of $f_{\rm iso}$ and $\cos\theta$.

As we can see from Figs.5.15 and 5.16 when isocurvature modes and adiabatic modes are correlated[†] the low multipoles region of the angular power spectrum can be significantly lowered as we discussed. However when the allowed fraction of isocurvature modes is too high the impact on the acoustic peaks is very strong and we thus can conclude that the allowed isocurvature fraction must be constrained to $0.1 \lesssim f_{\rm iso} \lesssim 0.5$ in order to lead to the observed large scale structures in the Universe.

[†]Note that in Ref.[75], due to different conventions, this holds when the modes are anti-correlated.

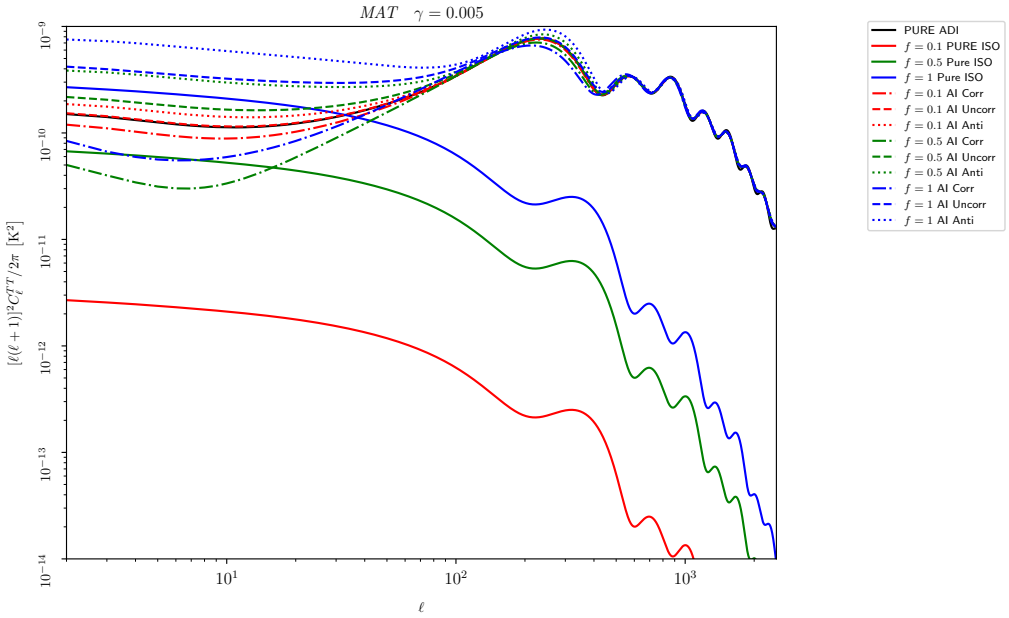

Figure 5.16: Temperature power spectrum for the MAT mode with different values of $f_{\rm iso}$ and $\cos\theta$.

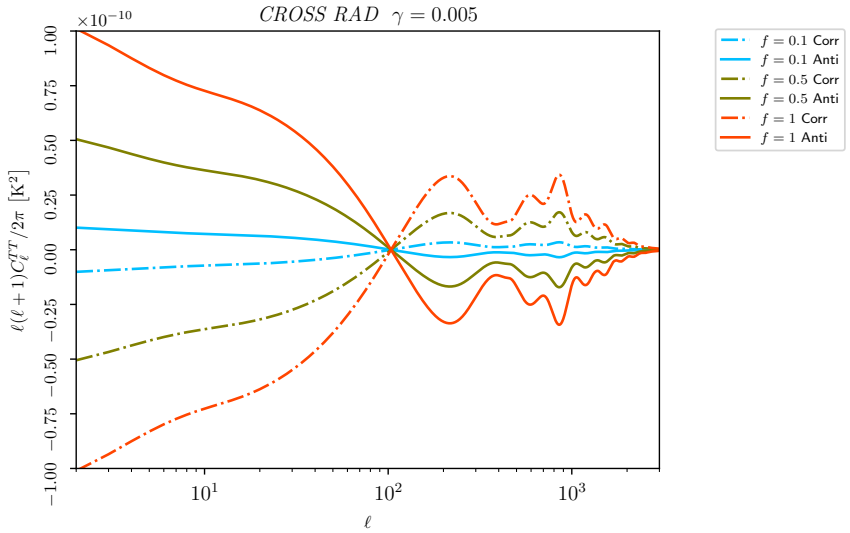

Figure 5.17: Temperature power spectrum for the correlated RAD and adiabatic mode with different values of $f_{\rm iso}$ and $\cos\theta$.

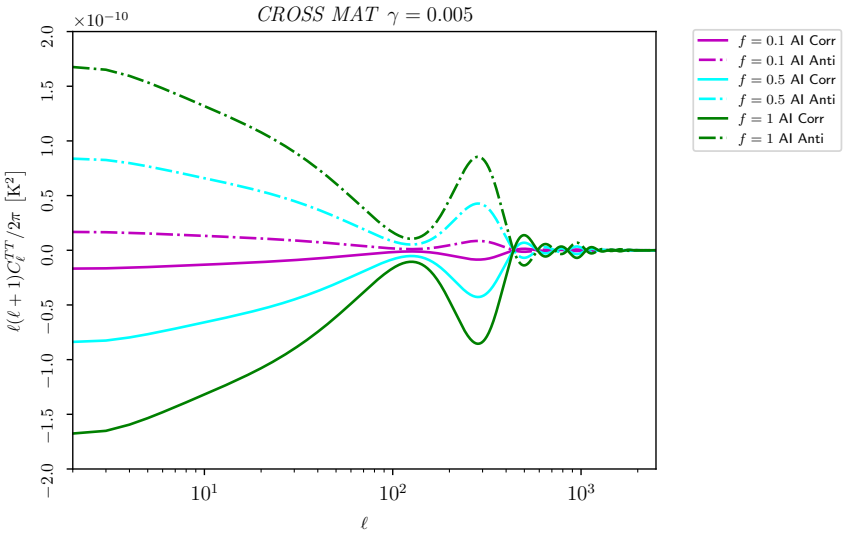

Figure 5.18: Temperature power spectrum for the correlated MAT and adiabatic mode with different values of $f_{\rm iso}$ and $\cos\theta$.

However, differently from what pointed out in Ref.[75] for the quintessence case, for the IG model we find that also the EE is lowered too in the case of correlation between adiabatic and isocurvature modes, while the TE cross correlation spectrum does not change as much as the EE. This could be useful in order to compare the a dynamical gravitational constant in the Einstein GR framework with scalar tensor theories. We can see these behaviour from Figs.5.19 and 5.20, where we plot the EE polarization and from Figs.5.21 and 5.22 where we plot the TE cross power spectrum. For a better understanding of the previous statement we plot the $f_{\rm iso} = 0.5$ case, for which these features are more emphasized.

5.4 Isocurvature Generation during Inflation

The generation of isocurvature perturbations in scalar-tensor theories has been examined by Starobinsky et al. in the context of the Jordan-Brans-Dicke model in Ref.[129] and then in the generalized Non-Minimally coupled model in Ref.[83]. We review here the main difference between the general

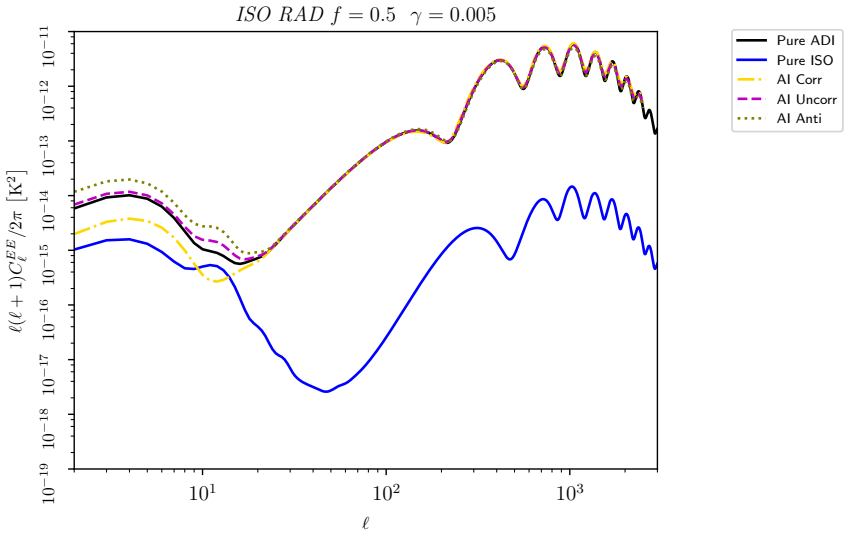

Figure 5.19: EE power spectrum for the correlated RAD and adiabatic mode with $f_{\rm iso} = 0.5$ and different values of $\cos\theta$.

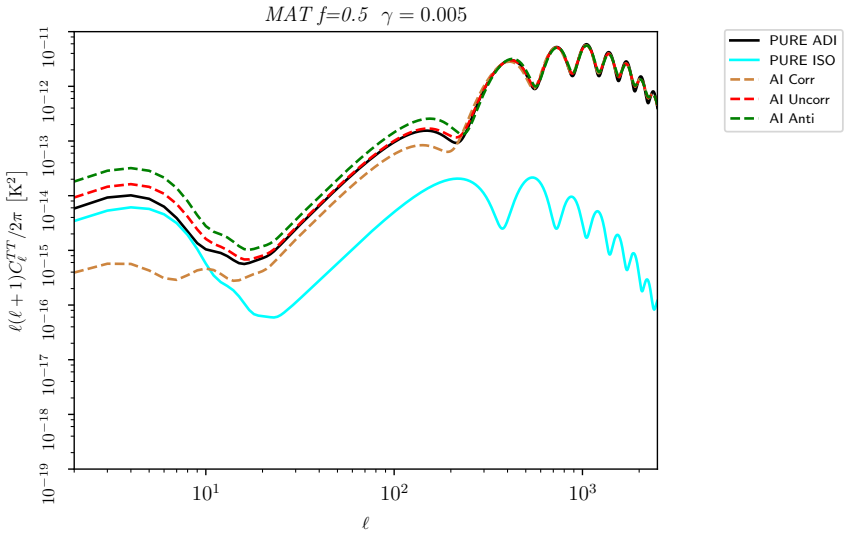

Figure 5.20: EE power spectrum for the correlated MAT and adiabatic mode with $f_{\rm iso} = 0.5$ and different values of $\cos\theta$.

relativity case explored in Sec.5.4 in the case of the IG model in order to connect the dynamics of the isocurvature modes found in the last sections,

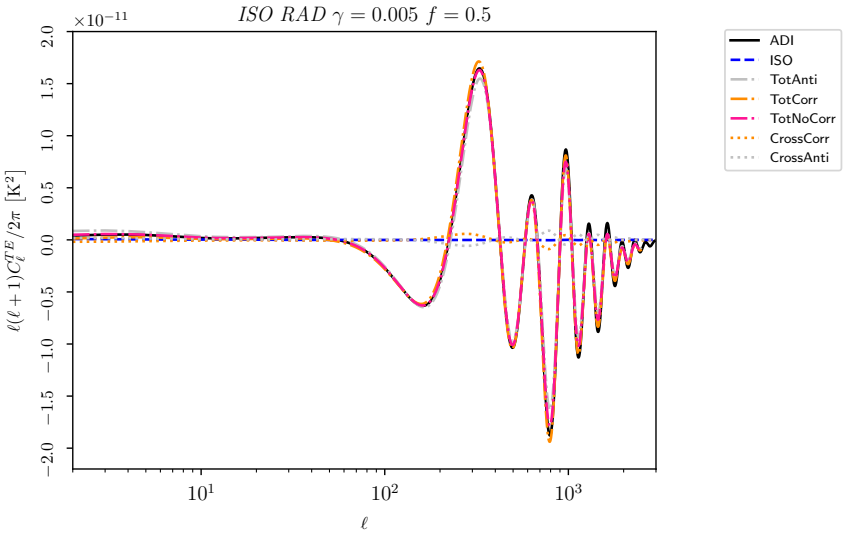

Figure 5.21: TE cross power spectrum for the correlated RAD and adiabatic mode with $f_{\rm iso} = 0.5$ and different values of $\cos\theta$.

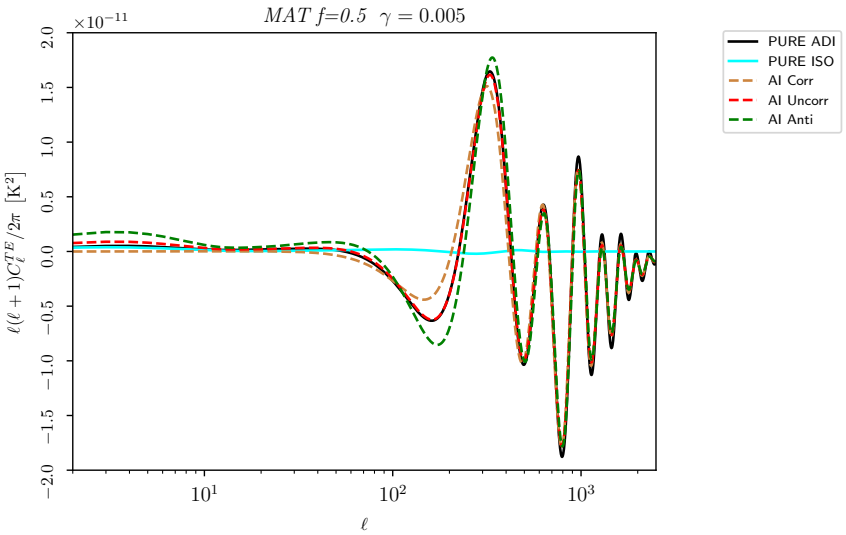

Figure 5.22: TE cross power spectrum for the correlated MAT and adiabatic mode with $f_{\rm iso} = 0.5$ and different values of $\cos\theta$.

with the primordial spectrum produced during inflation.

The idea is to do the calculations in the Einstein frame, where they are

easier, and then to make a conformal transformation to the Jordan frame that we consider the physical one in this case. Note that, however, one need to take care in charachterizing adiabatic and isocurvature perturbations in the different frames. In particular it has been proven that the notion of adiabacity is not invariant under conformal transformations [130]. In fact, although the curvature perturbation is invariant under conformal transformations for single-field inflation models, or for model that behave like an effective single-field inflation [131], generally this does not apply for inflation with two or more inflaton fields [130]. It is possible that isocurvature perturbations source the curvature perturbation in one conformal frame, even if the evolution is adiabatic in the other frame.

We denote the metric in the Jordan frame with $\hat{g}_{\mu\nu}$ and that in the Einstein frame with $g_{\mu\nu}$. We consider a simple model of inflation driven by two scalar field. The action in the Einstein frame is given by:

$$S = \int d^4x\sqrt{-g}\left[\frac{R}{2\kappa^2} - \frac{1}{2}g^{\mu\nu}\partial_\mu\chi\partial_\nu\chi - \frac{1}{2}e^{-\Gamma\kappa\chi}g^{\mu\nu}\partial_\mu\phi\partial_\nu\phi - U(\chi) - e^{-\beta\kappa\chi}V(\phi)\right], \tag{5.94}$$

where $\kappa^2 = 8\pi G$ and β and Γ are constants. It is straightforward to see that we can recover the action (5.94), from the action of the IG model together with an additional inflaton field ϕ

$$S = \int d^4x\sqrt{-\hat{g}}\left[\frac{\hat{R}\gamma\varphi^2}{2} - \frac{1}{2}\hat{g}^{\mu\nu}\partial_\mu\varphi\partial_\nu\varphi - \frac{1}{2}\hat{g}^{\mu\nu}\partial_\mu\phi\partial_\nu\phi - U(\varphi) - V(\phi)\right] \tag{5.95}$$

and making the conformal transformation:

$$g_{\mu\nu} = \Omega^2\hat{g}_{\mu\nu}, \tag{5.96}$$

$$\Omega^2 = \kappa^2\gamma\varphi^2 \equiv \exp\left(\kappa\chi\sqrt{\frac{4\gamma}{1+6\gamma}}\right), \tag{5.97}$$

with $\beta = 2\Gamma = 2\sqrt{\frac{4\gamma}{1+6\gamma}}$.

In the limit in which all the two fields in the Einstein frame are slowly

rolling, i.e. [129]

$$\max\{e^{-\beta\kappa\chi}\dot{\phi}^2,\, \dot{\chi}^2\} \ll e^{-\beta\kappa\chi}V, \tag{5.98}$$

$$|V_{,\phi}\,| \ll e^{-\frac{\Gamma\kappa\chi}{2}}V, \tag{5.99}$$

$$V_{,\phi\phi}\, e^{(\Gamma-\beta)\kappa\chi} \ll H^2, \tag{5.100}$$

the slow roll Klein-Gordon equations for the two fields and the 0-0 Friedmann equation in physical time are

$$3H\dot{\chi} = \beta\kappa e^{-\beta\kappa\chi}V, \tag{5.101}$$

$$3H\dot{\phi} = -e^{(\Gamma-\beta)\kappa\chi}V_{,\phi}\,, \tag{5.102}$$

$$H^2 = \frac{\kappa^2}{3}e^{-\beta\kappa\chi}V. \tag{5.103}$$

Note that these equations can be written in the following useful form:

$$\dot{\chi} = \frac{\beta}{\kappa}H, \tag{5.104}$$

$$\dot{\phi} = -H\frac{e^{\Gamma\kappa\chi}V_{,\phi}}{\kappa^2 V} \quad \text{and} \tag{5.105}$$

$$-\frac{\dot{H}}{H^2} = \frac{\beta^2}{2} + \frac{e^{\Gamma\kappa\chi}}{2\kappa^2}\left(\frac{V_{,\phi}}{V}\right)^2. \tag{5.106}$$

A solution for the slow-roll equations as a function of the scale factor is given by [132, 133]:

$$\chi = \frac{\beta}{\kappa}\ln a \equiv -\frac{\beta}{\kappa}N, \tag{5.107}$$

$$\kappa^2\int_{\phi_f}^{\phi} d\bar{\phi}\,\frac{V(\bar{\phi})}{V(\bar{\phi})_{,\bar{\phi}}} = \frac{1-e^{-\beta\Gamma N}}{\beta\Gamma}, \tag{5.108}$$

where ϕ_f is the value of the scalar field ϕ at the end of inflation where we set $a_f = 1$. If ϕ varies slowly with time we can approximate V as a constant and we have a power-law inflation, for which:

$$a(t) = \left[\frac{\beta^2\kappa\sqrt{V}}{2\sqrt{3}}\right]^{2/\beta^2}. \tag{5.109}$$

The Newtonian guage perturbed field equations on large scales ($k \ll aH$) in the slow-roll approximation are given by [129]:

$$\Phi = \frac{\beta\kappa}{2}\delta\chi - \frac{V_{,\phi}}{2V}\delta\phi, \tag{5.110}$$

$$3H\delta\dot{\chi} + (\beta\kappa)^2 e^{-\beta\kappa\chi}V\delta\chi - \beta\kappa e^{-\beta\kappa\chi}V_{,\phi}\,\delta\phi = 2\beta\kappa e^{-\beta\kappa\chi}V\Phi, \tag{5.111}$$

$$3H\delta\dot{\phi} + e^{(\Gamma-\beta)\kappa\chi}V_{,\phi\phi}\,\delta\phi + (\Gamma-\beta)\kappa V_{,\phi}\,e^{(\Gamma-\beta)\kappa\chi}\delta\chi = -2e^{(\Gamma-\beta)\kappa\chi}V_{,\phi}\,\Phi. \tag{5.112}$$

From Eq.(5.111), we can find the solution

$$\delta\chi = \frac{\beta}{\kappa}Q_1 = \text{const.} \tag{5.113}$$

We can insert the latter solution in Eqs.(5.110) and (5.112) and use the relation

$$3H\frac{d}{dt} = -e^{(\Gamma-\beta)\kappa\chi}V_{,\phi}\,\frac{d}{d\phi}, \tag{5.114}$$

to find the solution:

$$\delta\phi = -\frac{V_{,\phi}}{\kappa^2 V}(Q_1 e^{\Gamma\kappa\chi} - Q_2), \tag{5.115}$$

$$\Phi = \frac{\beta^2}{2}Q_1 + \frac{1}{2\kappa^2}\left(\frac{V_{,\phi}}{V}\right)^2(Q_1 e^{\Gamma\kappa\chi} - Q_2), \tag{5.116}$$

where Q_2 is another integration constant.

Using Eqs.(5.104), we can easily recast this solution in the form given in Eqs.(3.76) and (3.77) of Sec.3.5, with the difference that now we have a non-canonical kinetic term for the field ϕ, so that, defining $Q_1 = C_1 - C_3$ and $Q_2 = -C_3$, the right expressions are now:

$$\frac{\delta\chi}{\dot{\chi}} = \frac{C_1}{H} - \frac{C_3}{H}, \tag{5.117}$$

$$\frac{\delta\phi}{\dot{\phi}} = \frac{C_1}{H} + \frac{C_3}{H}(e^{-\Gamma\kappa\chi} - 1), \tag{5.118}$$

$$\Phi = -C_1\frac{\dot{H}}{H^2} + C_3\left[\frac{1}{2\kappa^2}(1 - e^{\Gamma\kappa\chi})\left(\frac{V_{,\phi}}{V}\right)^2 - \frac{\beta^2}{2}\right], \tag{5.119}$$

where, again, the terms with the constant C_1 represent the adiabatic mode, whereas those proportional to C_3 are the isocurvature ones. Exactly as we have done in Sec.3.5 we can match these perturbations with the amplitudes of quantum fluctuations generated during the inflationary stage. The only subtle difference is again due to the presence of the non-canonical kinetic term, so that we have at the end of inflation:

$$\delta\chi(\mathbf{k}) = \frac{H_k}{\sqrt{2k^3}}\epsilon_\chi(\mathbf{k}), \tag{5.120}$$

$$\delta\phi(\mathbf{k}) = \frac{H_k}{\sqrt{2k^3}}\epsilon_\phi(\mathbf{k})e^{\Gamma\kappa\chi_k/2}. \tag{5.121}$$

Using these expressions, the constant C_1 and C_3 are given by:

$$C_1 = \left[e^{\Gamma\kappa\chi}H\frac{\delta\phi}{\dot\phi} + (1-e^{\Gamma\kappa\chi})H\frac{\delta\chi}{\dot\chi}\right]_{t_k} = \frac{H_k^2}{\sqrt{2k^3}}\left[\frac{e^{3\Gamma\kappa\chi/2}}{\dot\phi}\epsilon_\phi(\mathbf{k}) + \frac{1-e^{-\Gamma\kappa\chi}}{\dot\chi}\epsilon_\chi(\mathbf{k})\right], \tag{5.122}$$

$$C_3 = \left[e^{\Gamma\kappa\chi}H\left(\frac{\delta\phi}{\dot\phi} - \frac{\delta\chi}{\dot\chi}\right)\right]_{t_k} = \frac{H_k^2}{\sqrt{2k^3}}\left[\frac{e^{3\Gamma\kappa\chi/2}}{\dot\phi}\epsilon_\phi(\mathbf{k}) - \frac{1}{\dot\chi}\epsilon_\chi(\mathbf{k})\right]. \tag{5.123}$$

So far we have done all the calculations in the Einstein frame, but we are interested in the quantities in the Jordan frame, so that we apply the conformal transformation (5.96). The variables in the Jordan frame, under the latter transformation, transform as [124]:

$$\hat\Phi = \Phi - \frac{\delta\Omega}{\Omega}, \tag{5.124}$$

$$\hat\Psi = \Psi + \frac{\delta\Omega}{\Omega}, \tag{5.125}$$

$$\hat a = a/\Omega, \tag{5.126}$$

$$d\hat t = dt/\Omega, \tag{5.127}$$

$$\hat H = \frac{\hat a_{\hat t}}{\hat a} = \Omega\left(H - \frac{\dot\Omega}{\Omega}\right), \tag{5.128}$$

where the subscript $\hat t$ denotes the derivative with respect to the physical time in the Jordan frame and $\delta\Omega = \Gamma\kappa\delta\chi\Omega/2$. Using these transformations we

obtain:

$$\frac{\delta\chi}{\dot{\chi}} = \Omega\frac{\delta\chi}{\chi_{\hat{t}}} = \frac{C_1 - C_3}{\hat{a}\Omega}\int^{\hat{t}} dt'\,\hat{\Omega}^2. \tag{5.129}$$

Since the scalar field φ varies very slowly in the post-inflationary universe as we have seen in Sec.4.5, Ω can be regarded as a constant and thus adiabatic and isocurvature perturbations are the same as in the Einstein frame, up to the constant Ω.

However, we are interested in the perturbations of the field φ, since we are searching for a phenomenological origin of the RAD mode. To this concern, we note from Eq.(5.97), that the following equalities hold:

$$\dot{\varphi} = \frac{\dot{\chi}}{\sqrt{1+6\gamma}}\exp\left(\kappa\chi\sqrt{\frac{4\gamma}{1+6\gamma}}\right), \tag{5.130}$$

$$\delta\chi = \frac{\delta\chi}{\sqrt{1+6\gamma}}\exp\left(\kappa\chi\sqrt{\frac{4\gamma}{1+6\gamma}}\right), \tag{5.131}$$

so that we have the important relation

$$\frac{\delta\chi}{\dot{\chi}} = \frac{\delta\varphi}{\dot{\varphi}}, \tag{5.132}$$

which translates, in the Einstein frame, to

$$\frac{\delta\chi}{\chi_{\hat{t}}} = \frac{\delta\varphi}{\varphi_{\hat{t}}}. \tag{5.133}$$

This means that the classification into isocurvature and adiabatic perturbations for the inflaton field χ is conformally invariant for this double inflation model. However, $\delta\chi$ and $\delta\varphi$ are not equal, in fact Eqs.(5.113),(5.128) and (5.131) imply that:

$$\delta\varphi = -4\varphi\frac{\gamma}{1+6\gamma}(C_1 - C_3), \tag{5.134}$$

and we thus see that isocurvature modes can be excited in this framework, although these are very small because of the small factor γ. After inflation the inflaton field ϕ is supposed to decay into the ordinary matter, while the IG field φ remains uncoupled to the ordinary matter and contribute to the gravitational sector as an unthermalized field. When a perturbation $\delta\varphi$,

which was stretched out of the Hubble radius during the inflationary stage, re-enters the Hubble radius during the radiation and matter dominated eras, the scalar field φ evolves as in Eq.(4.56) and from Eq.(5.134) we can see that it is possible to have a constant perturbation to the scalar field φ at the leading order. We thus expect that this could be a possible mechanism to excite the new RAD mode. However, it would be interesting to examine how the reheating era may affect these scalar field perturbations.

As a final comment, we stress that these results are not only specific of this model, but can be generalized to the Non-Minimally Coupled model. In this model, the perturbation to the scalar field produced during inflation are [134, 83]:

$$\delta\varphi = -4\varphi(C_1 - C_3)\frac{\xi\varphi(N_{\rm pl}^2 + \xi\varphi^2)}{N_{\rm pl}^2 + (1+6\xi)\xi\varphi}. \tag{5.135}$$

As pointed out in [134, 83] this can produce large isocurvature perturbation in the case when $\xi > 0$ due to the presence of $N_{\rm pl}^2$ even if ξ is small. We note that in the limit $N_{\rm pl}^2 \to 0$ Eq.(5.135) reduces to Eq.(5.134) and we recover the IG results.

Conclusions

The current cosmic concordance ΛCDM model explains the accelerated expansion of our Universe by the cosmological constant. However, it is important to investigate other models in which the effective cosmological constant may vary with time, in order to avoid the fine-tuning problems suffered by the cosmological constant. One possibility is to consider quintessence, a very light scalar field whose negative pressure drives the acceleration of the Universe. Another possibility is to consider modified gravity in which Einstein GR is abandoned. The simplest models of modified gravity are scalar-tensor theories in which the scalar field responsible for the acceleration of the Universe also mediates the gravitational strength.

In this work we focused on two of the simplest scalar-tensor theories in which a scalar field φ is non-minimally coupled to the Ricci scalar. These are the Induced Gravity theory (IG) in which the coupling is in the form $F(\varphi) = \gamma\varphi^2$ and the Non-Minimally Coupled (NMC) theory where $F(\varphi) = N_{\rm pl}^2 + \xi\varphi^2$.

We have derived the initial conditions for the cosmological perturbations and we found five regular independent isocurvature solutions for the perturbed field equations, in addition to the adiabatic solution. Among the isocurvature solutions, four are the generalization to Induced Gravity of the well known isocurvature modes in Einstein GR (which are the Baryon, CDM, Neutrino Density and Neutrino Velocity isocurvature modes), whereas the presence of the scalar field leads to a new mode, which is peculiar to this theory. Although we have focused on Induced Gravity theories, we have shown

how these results can be easily generalized to more general scalar-tensor theories as the Non-Minimally Coupled model. We then used these initial conditions to compute the CMB temperature, polarization and lensing power spectra with the modified CLASS code for Induced Gravity [126, 127, 104].

We summarize our results in the following:

- In scalar-tensor dark energy models in which the scalar field is quasi-static in the radiation era after neutrino decoupling, we have identified a new isocurvature regular mode (RAD). In this solution, the scalar field perturbation is constant in the synchronous gauge and the scalar field energy density compensates with the relativistic ones.

- In addition to this new solution we found the extension of the baryon, CDM, neutrino density and neutrino velocity isocurvature modes which are also present in Einstein GR.

- The imprints of the new RAD isocurvature mode on the CMB power spectra are completely new and they lead to interesting consequences, summarized in the following, when the RAD mode is correlated with the adiabatic one.

- The CMB angular power spectra of the latter four isocurvature modes are similair to those already known in Einstein GR. However for the baryon and CDM isocurvature modes the low multipoles region of the temperature power spectrum is enhanced of about 20%, making it interesting to study how a correlation with the adiabatic mode can affect the total angular power spectrum.

- Both the effective CDM (in which the Baryon and CDM modes are put together, since they lead to the same imprints on the CMB) and the RAD mode can lower the low multipoles region of the temperature power spectrum, if they are anti-correlated with the adiabatic modes. This could be an interesting mechanism which can explain the observed lack of power in that region of the CMB angular power spectrum. The

plots for the temperature power spectra suggest that the allowed fraction of these modes must be constrained by $0.1 \lesssim f_{\rm iso} \lesssim 0.5$ in order to not modify the acoustic peak structure.

- Simple models of inflation, within scalar tensor theories, where inflation is driven by two sclar fields, one of them being the Induced Gravity scalar field φ, could generate the RAD isocurvature mode.

As future perspectives, we plan to perform a Markov chain Monte Carlo exploration as in [127, 104] in order to constrain the model with the most recent cosmological data.

We also plan to study how the reheating era could affect the perturbation to the scalar field which generates the RAD mode.

Riassunto in Italiano

Una alternativa ai modelli di energia oscura in Relatività Generale sono i modelli di gravità modificata. Tra i modelli di gravità modificata una importante classe di modelli sono le teorie scalari-tensoriali, in cui un campo scalare accoppiato non minimalmente al tensore di Ricci guida l'espansione accelerata dell'Univero e causa una variazione del tempo della costante di Newton. In particolare in questo lavoro di tesi abbiamo considerato un modello di gravità indotta (Induced Gravity) nella quale il campo scalare φ possiede un accoppiamento col tensore di Ricci nella forma $F(\varphi) = \gamma\varphi^2$. Nonostante ciò, i risultati ottenuti non sono specifici di questa teoria, ma possono essere facilmente generalizzati a modelli più generali di teorie scalari-tensoriali.

Abbiamo derivato le condizioni iniziali per le perturbazioni cosmologiche in questo modello e trovato cinque soluzioni di isocurvatura regolari ed indipendenti oltre alla soluzione adiabatica. Di queste cinque, quattro sono generalizzazioni dei modi di isocurvatura in Relatività Generale, già conosciuti in isocurvatura, mentre il quinto è un nuovo modo caratterizzante delle teorie scalari-tensoriali, causato dalla presenza del campo scalare. Abbiamo poi usato queste condizioni iniziali per trovare gli spettri angolari della CMB in temperatura, polarizzazione e lensing, usando il codice pubblico CLASS, modificato per il modello di Induced Gravity [126].

I nostri risultati, per i quali rimandiamo al capitolo 5, possono essere riassunti nei seguenti punti:

- Nelle teorie scalari tensoriali in cui il campo scalare è quasi statico durante l'era della radiazione e dopo il disaccoppiamento dei neutrini,

il campo scalare porta ad un nuovo modo di isocurvatura (RAD). Per questo modo la perturbazione al campo scalare nel gauge sincrono è costante all'ordine dominante in $k\tau$ e la perturbazione alla densità di energia del campo scalare si compensa con quelle materia relativistica.

- Oltre a questa soluzione abbiao trovato le estensioni ad Induced Gravity dei modi di isocurvatura di Barioni, CDM, Neutrino Density e Neutrino Velocity già conosciuti in Relatività Generale.

- Gli effetti del nuovo modo di isocurvatura RAD sugli spettri di potenza angolari della CMB sono completamente originali e possono portare ad interessanti conseguenze nel caso in cui il modo RAD sia correlato con il modo adiabatico, come mostrato nei punti seguenti.

- Gli spettri di potenza angolari della CMB per i quattro modi con una controparte in Relatività Generale sono simili a quelli di quest'ultima. Nonostante questo, i modi di isocurvatura di Barioni e CDM mostrano un innalzamento dello spettro a bassi multipoli di circa il 20% e questo rende interessante studiare come una correlazione con il modo adiabatico possa modificare lo spettro di potenza angolare totale.

- Sia il modo di isocurvatura effettivo della CDM (in cui sono pesati i modi della CDM e quello dei Barioni dato che portano agli stessi imprint sulla CMB) che il nuovo modo RAD possono abbassare lo spettro di potenza angolare della CMB nella zona di bassi multipoli se correlati con il modo adiabatico. I grafici ottenuti suggeriscono che la frazione di isocurvatura permessa sia vincolata da $0.1 \lesssim f_{\rm iso} \lesssim 0.5$ per non modificare la zona dei picchi acustici. Questo può essere un interessante meccanismo per spiegare il problema della '*lack of power*' osservata nello spettro di potenza angolare della CMB.

- Abbiamo analizzato come il modo RAD possa essere generato in un semplice modello di doppia inflazione in cui uno dei due inflatoni è il campo scalare di Induced Gravity φ.

Appendix A

Newtonian Gauge Perturbed Equations for Scalar-Tensor model

In this appendix we give the perturbed Einstein and Klein-Gordon equations for the Induced Gravity and Non-Minimally coupled models in Newtonian Gauge in conformal time.

Induced Gravity

The perturbed Einstein equations are:

$$3\mathcal{H}(\Phi' + \mathcal{H}\Psi) + k^2\Phi + 3\frac{\varphi'}{\varphi}(\Phi' + 2\mathcal{H}\Psi) - \frac{\varphi'^2}{2\gamma\varphi^2}\Psi = \\ -\frac{1}{2\gamma\varphi^2}\left[3\varphi'\delta\varphi' - 6\mathcal{H}^2\gamma\varphi\delta\varphi - 6\mathcal{H}\gamma(\varphi\delta\varphi)' - 2\gamma k^2\delta\varphi + a^2\delta\rho_m + a^2V_{,\varphi}\,\delta\varphi\right], \tag{A.1}$$

$$k^2(\Phi'+\mathcal{H}\Psi) = \frac{a^2(\rho_m + P_m)\theta_m}{2\gamma\varphi^2} - \frac{k^2}{2\gamma\varphi^2}\left[2\gamma\varphi(\varphi'\Psi - \delta\varphi') - \delta\varphi(\varphi'(1+2\gamma) - 2\gamma\varphi\mathcal{H})\right], \tag{A.2}$$

$$\Phi'' + \mathcal{H}(\Psi + 2\Phi)' + \left(2\frac{a''}{a} - \mathcal{H}^2\right) + \frac{k^2}{3}(\Phi - \Psi) = \\ - \frac{a^2\delta\varphi}{\gamma\varphi^3}\left[P_m - V + \frac{\varphi'^2}{2a^2} + \frac{4\mathcal{H}\gamma\varphi\varphi'}{a^2} + \frac{2\gamma\varphi'^2}{a^2} + \frac{2\gamma\varphi\varphi''}{a^2}\right] + \\ + \frac{a^2}{2\gamma\varphi^2}(\delta P_m - V_{,\varphi}\,\delta\varphi) - \frac{\Psi}{\gamma\varphi^2}\left[\frac{\varphi'^2}{2} + 2\gamma(\mathcal{H}\varphi\varphi' + \varphi\varphi'' + \varphi'^2)\right] + \\ - \frac{\varphi'}{\varphi}(\Psi' + 2\Phi') + \frac{1}{\varphi}\delta\varphi'' + \frac{\delta\varphi'}{2\gamma\varphi^2}[(1+4\gamma)\varphi' + 2\gamma\varphi\mathcal{H}] + \\ + \frac{\delta\varphi}{6\gamma\varphi^2}[4\gamma k^2\varphi + 6\gamma\mathcal{H}\varphi' + 6\gamma\varphi''], \quad \text{(A.3)}$$

$$\Phi - \Psi = \frac{2\delta\varphi}{\varphi} + \frac{3a^2}{2k^2}\frac{(\rho_m + P_m)\sigma_m}{\gamma\varphi^2}. \quad \text{(A.4)}$$

The perturbed Klein-Gordon equation is

$$\delta\varphi'' = -2\delta\varphi'\left(\mathcal{H} + \frac{\varphi'}{\varphi}\right) - \delta\varphi\left[k^2 - \frac{\varphi'^2}{\varphi^2} + \frac{a^2(\rho_m - 3P_m)}{(1+6\gamma)\varphi^2}\right] + \\ + \frac{2a^2(\rho_m - 3P_m)}{(1+6\gamma)\varphi}\Psi + \frac{a^2(\delta\rho_m - 3\delta P_m)}{(1+6\gamma)\varphi} + \varphi'(3\Phi' + \Psi'). \quad \text{(A.5)}$$

The equations given above can be further simplified using the background Klein-Gordon equation found in Chapter 4.

Appendix B

Initial Conditions for General Non-Minimally Coupled Models

In this appendix we give explicit expressions for the leading terms of the isocurvature initial conditions in the Non-Minimally Coupled model considered in Sec.4.1.2. We used the background and perturbed field equations of Ref.[135] for the computations. Setting $N_{\rm pl}^2 = 0$ it is straightforward to recover the results of Chapter 5. The adiabatic mode has already been found in Ref.[135], thus we refer the reader to the latter reference for an explicit expression of it.

In the following the quantity named ω, altough we keep writing it with the same name, is different from which we used previously and is equal to [135]:

$$\omega_{\rm NMC} \equiv \omega = \frac{\rho_{\rm mat0}\sqrt{N_{\rm pl}^2 + \xi\varphi_i^2}}{\sqrt{3\rho_{\rm rad0}}\left(N_{\rm pl}^2 + \xi\varphi_i^2(1+6\xi)\right)}. \tag{B.1}$$

Baryon Isocurvature Mode

$$
\begin{aligned}
\delta_\gamma =& -\frac{2R_b}{3}\omega\tau + \frac{R_b\omega\left(\xi(1+6\xi)(15\xi+2)\varphi_i^2+2N_{\rm pl}^2\right)}{8\left(\xi(6\xi+1)\varphi_i^2+N_{\rm pl}^2\right)}\omega\tau^2,\\
\theta_\gamma =& -\frac{1}{12}R_b k^2\omega\tau^2 + \frac{{R_b}^2\omega^2\left(\xi(1+6\xi)\varphi_i^2+N_{\rm pl}^2\right)}{16R_\gamma\left(\xi\varphi_i^2+N_{\rm pl}^2\right)}k^2\tau^3+\\
&+\frac{R_b\omega^2\left(\xi(1+6\xi)(15\xi+2)\varphi_i^2+2N_{\rm pl}^2\right)}{96\left(\xi(1+6\xi)\varphi_i^2+N_{\rm pl}^2\right)}k^2\tau^3,\\
\delta_b =& 1-\frac{R_b}{2}\omega\tau + \frac{3R_b\omega^2\left(\xi(1+6\xi)(15\xi+2)\varphi_i^2+2N_{\rm pl}^2\right)}{32\left(\xi(6\xi+1)\varphi_i^2+N_{\rm pl}^2\right)}\tau^2,\\
\delta_c =& -\frac{R_b\omega}{2}\tau + \frac{3R_b\omega^2\left(\xi(1+6\xi)(15\xi+2)\varphi_i^2+2N_{\rm pl}^2\right)}{32\left(\xi(6\xi+1)\varphi_i^2+N_{\rm pl}^2\right)}\tau^2,\\
\delta_\nu =& -\frac{2R_b\omega}{3}\tau + \frac{R_b\omega^2\left(\xi(1+6\xi)(15\xi+2)\varphi_i^2+2N_{\rm pl}^2\right)}{8\left(\xi(6\xi+1)\varphi_i^2+N_{\rm pl}^2\right)}\tau^2,\\
\theta_\nu =& -\frac{1}{12}R_b\omega k^2\tau^2 + \frac{R_b\omega^2\left(\xi(1+6\xi)(15\xi+2)\varphi_i^2+2N_{\rm pl}^2\right)}{96\left(\xi(6\xi+1)\varphi_i^2+N_{\rm pl}^2\right)}k^2\tau^3,\\
\sigma_\nu =& -\frac{R_b\omega\left(\xi(1+6\xi)\varphi_i^2+N_{\rm pl}^2\right)}{6(2R_\nu+15)\left(\xi\varphi_i^2+N_{\rm pl}^2\right)}k^2\tau^3,\\
F_3 =& -\frac{R_b\omega\left(\xi(1+6\xi)\varphi_i^2+N_{\rm pl}^2\right)}{28(2R_\nu+15)\left(\xi\varphi_i^2+N_{\rm pl}^2\right)}k^3\tau^4,\\
h =& R_b\omega\tau - \frac{3R_b\omega^2\left(\xi(1+6\xi)(15\xi+2)\varphi_i^2+2N_{\rm pl}^2\right)}{16\left(\xi(1+6\xi)\varphi_i^2+N_{\rm pl}^2\right)}\tau^2,\\
\eta =& -\frac{R_b\omega}{6}\tau + \frac{R_b\omega^2\left(\xi(1+6\xi)(15\xi+2)\varphi_i^2+2N_{\rm pl}^2\right)}{32\left(\xi(1+6\xi)\varphi_i^2+N_{\rm pl}^2\right)}\tau^2,\\
\delta\varphi =& \frac{3}{2}\xi R_b\omega\varphi_i\tau - \frac{\xi R_b\omega^2\varphi_i\left(\xi(1+6\xi)(18\xi+5)\varphi_i^2+(5-12\xi)N_{\rm pl}^2\right)}{8\left(\xi(1+6\xi)\varphi_i^2+N_{\rm pl}^2\right)}\tau^2 - \frac{1}{8}\xi R_b\omega\varphi_i k^2\tau^3+\\
&-\frac{\xi R_b\omega^3\varphi_i\left(-2\xi^2(1+6\xi)^2(27\xi(9\xi+4)+11)\varphi_i^4-\left(54\xi^2-75\xi+22\right)N_{\rm pl}^4\right)}{96\left(\xi(6\xi+1)\varphi_i^2+N_{\rm pl}^2\right)^2}\tau^3+\\
&-\frac{\xi R_b\omega^3\varphi_i\left(-\xi\left(9\xi\left(-540\xi^2+4\xi+45\right)+44\right)N_{\rm pl}^2\varphi_i^2\right)}{96\left(\xi(6\xi+1)\varphi_i^2+N_{\rm pl}^2\right)^2}\tau^3.
\end{aligned}
$$

$$\begin{aligned}
\mathcal{R} =& -\frac{R_b\omega}{4}\tau,\\
\Psi =& -\frac{R_b\omega\left(-90\gamma^2\varphi_i^2+15\gamma\varphi_i^2+4N_{\rm pl}^2R_\nu+15N_{\rm pl}^2+4\gamma R_\nu\varphi_i^2\right)}{8(2R_\nu+15)\left(\gamma\varphi_i^2+N_{\rm pl}^2\right)}\tau,\\
\Phi =& \frac{R_b\omega\left(-270\gamma^2\varphi_i^2-15\gamma\varphi_i^2+4N_{\rm pl}^2R_\nu-15N_{\rm pl}^2+4\gamma R_\nu\varphi_i^2\right)}{8(2R_\nu+15)\left(\gamma\varphi_i^2+N_{\rm pl}^2\right)}\tau,\\
\delta\varphi_I =& \frac{3}{2}\gamma R_b\omega\varphi_i\tau.
\end{aligned}$$

CDM Isocurvature Mode

$$\begin{aligned}
\delta_\gamma =& -\frac{2R_c}{3}\omega\tau+\frac{R_c\omega\left(\xi(1+6\xi)(15\xi+2)\varphi_i^2+2N_{\rm pl}^2\right)}{8\left(\xi(6\xi+1)\varphi_i^2+N_{\rm pl}^2\right)}\omega\tau^2,\\
\theta_\gamma =& -\frac{1}{12}R_ck^2\omega\tau^2+\frac{{R_c}^2\omega^2\left(\xi(1+6\xi)\varphi_i^2+N_{\rm pl}^2\right)}{16R_\gamma\left(\xi\varphi_i^2+N_{\rm pl}^2\right)}k^2\tau^3+\\
&+\frac{R_c\omega^2\left(\xi(1+6\xi)(15\xi+2)\varphi_i^2+2N_{\rm pl}^2\right)}{96\left(\xi(1+6\xi)\varphi_i^2+N_{\rm pl}^2\right)}k^2\tau^3,\\
\delta_b =& -\frac{R_c}{2}\omega\tau+\frac{3R_c\omega^2\left(\xi(1+6\xi)(15\xi+2)\varphi_i^2+2N_{\rm pl}^2\right)}{32\left(\xi(6\xi+1)\varphi_i^2+N_{\rm pl}^2\right)}\tau^2,\\
\delta_c =& 1-\frac{R_c\omega}{2}\tau+\frac{3R_c\omega^2\left(\xi(1+6\xi)(15\xi+2)\varphi_i^2+2N_{\rm pl}^2\right)}{32\left(\xi(6\xi+1)\varphi_i^2+N_{\rm pl}^2\right)}\tau^2,\\
\delta_\nu =& -\frac{2R_c\omega}{3}\tau+\frac{R_c\omega^2\left(\xi(1+6\xi)(15\xi+2)\varphi_i^2+2N_{\rm pl}^2\right)}{8\left(\xi(6\xi+1)\varphi_i^2+N_{\rm pl}^2\right)}\tau^2,\\
\theta_\nu =& -\frac{1}{12}R_c\omega k^2\tau^2+\frac{R_c\omega^2\left(\xi(1+6\xi)(15\xi+2)\varphi_i^2+2N_{\rm pl}^2\right)}{96\left(\xi(6\xi+1)\varphi_i^2+N_{\rm pl}^2\right)}k^2\tau^3,\\
\sigma_\nu =& -\frac{R_c\omega\left(\xi(1+6\xi)\varphi_i^2+N_{\rm pl}^2\right)}{6(2R_\nu+15)\left(\xi\varphi_i^2+N_{\rm pl}^2\right)}k^2\tau^3,\\
F_3 =& -\frac{R_c\omega\left(\xi(1+6\xi)\varphi_i^2+N_{\rm pl}^2\right)}{28(2R_\nu+15)\left(\xi\varphi_i^2+N_{\rm pl}^2\right)}k^3\tau^4,
\end{aligned}$$

$$
\begin{aligned}
h =& R_c\omega\tau - \frac{3R_c\omega^2\left(\xi(1+6\xi)(15\xi+2)\varphi_i^2+2N_{\rm pl}^2\right)}{16\left(\xi(1+6\xi)\varphi_i^2+N_{\rm pl}^2\right)}\tau^2,\\
\eta =& -\frac{R_c\omega}{6}\tau + \frac{R_c\omega^2\left(\xi(1+6\xi)(15\xi+2)\varphi_i^2+2N_{\rm pl}^2\right)}{32\left(\xi(1+6\xi)\varphi_i^2+N_{\rm pl}^2\right)}\tau^2,\\
\delta\varphi =& \frac{3}{2}\xi R_c\omega\varphi_i\tau - \frac{\xi R_c\omega^2\varphi_i\left(\xi(1+6\xi)(18\xi+5)\varphi_i^2+(5-12\xi)N_{\rm pl}^2\right)}{8\left(\xi(1+6\xi)\varphi_i^2+N_{\rm pl}^2\right)}\tau^2 - \frac{1}{8}\xi R_c\omega\varphi_i k^2\tau^3 +\\
&- \frac{\xi R_c\omega^3\varphi_i\left(-2\xi^2(1+6\xi)^2(27\xi(9\xi+4)+11)\varphi_i^4-\left(54\xi^2-75\xi+22\right)N_{\rm pl}^4\right)}{96\left(\xi(6\xi+1)\varphi_i^2+N_{\rm pl}^2\right)^2}\tau^3 +\\
&- \frac{\xi R_c\omega^3\varphi_i\left(-\xi\left(9\xi\left(-540\xi^2+4\xi+45\right)+44\right)N_{\rm pl}^2\varphi_i^2\right)}{96\left(\xi(6\xi+1)\varphi_i^2+N_{\rm pl}^2\right)^2}\tau^3.
\end{aligned}
$$

$$
\begin{aligned}
\mathcal{R} =& -\frac{R_c\omega}{4}\tau,\\
\Psi =& -\frac{R_c\omega\left(-90\gamma^2\varphi_i^2+15\gamma\varphi_i^2+4N_{\rm pl}^2R_\nu+15N_{\rm pl}^2+4\gamma R_\nu\varphi_i^2\right)}{8(2R_\nu+15)\left(\gamma\varphi_i^2+N_{\rm pl}^2\right)}\tau,\\
\Phi =& \frac{R_c\omega\left(-270\gamma^2\varphi_i^2-15\gamma\varphi_i^2+4N_{\rm pl}^2R_\nu-15N_{\rm pl}^2+4\gamma R_\nu\varphi_i^2\right)}{8(2R_\nu+15)\left(\gamma\varphi_i^2+N_{\rm pl}^2\right)}\tau,\\
\delta\varphi_I =& \frac{3}{2}\gamma R_c\omega\varphi_i\tau.
\end{aligned}
$$

Neutrino Density Mode

$$
\begin{aligned}
\delta_\gamma &= -\frac{R_\nu}{R_\gamma} + \frac{k^2 R_\nu \tau^2}{6R_\gamma}, \\
\theta_\gamma &= -\frac{k^2 R_\nu \tau}{4R_\gamma} + \frac{3(1+6\xi)k^2 R_b R_\nu \tau^2 \omega}{16 R_\gamma^2}, \\
\delta_b &= \frac{k^2 R_\nu \tau^2}{8R_\gamma}, \\
\delta_c &= -\frac{k^2 R_b R_\nu \tau^3 \omega}{80 R_\gamma} + k^4 \tau^4 \frac{R_\nu}{72(4R_\nu + 15)}, \\
\delta_\nu &= 1 - \frac{k^2 \tau^2}{6}, \\
\theta_\nu &= \frac{k^2 \tau}{4}, \\
\sigma_\nu &= \frac{2(1+6\xi)k^2 R_\nu \tau^3 \omega}{3(2R_\nu + 15)(4R_\nu + 15)}, \\
F_3 &= \frac{(1+6\xi)k^3 R_\nu \tau^4 \omega}{7(2R_\nu + 15)(4R_\nu + 15)}, \\
h &= \frac{k^2 R_b R_\nu \tau^3 \omega}{40 R_\gamma}, \\
\eta &= -\frac{R_\nu k^2 \tau^2}{6(4R_\nu + 15)}, \\
\delta\varphi &= \frac{\xi k^2 R_b R_\nu \tau^3 \omega \varphi_i}{32 R_\gamma}.
\end{aligned}
$$

$$
\begin{aligned}
\mathcal{R} &= -\frac{R_\nu \tau \omega}{4(4R_\nu + 15)}, \\
\Psi &= \frac{R_\nu}{4R_\nu + 15}, \\
\Phi &= -\frac{2R_\nu}{4R_\nu + 15}, \\
\delta\varphi_I &= -\frac{3\xi R_\nu \tau \omega \varphi_i}{2(4R_\nu + 15)}.
\end{aligned}
$$

It is very interesting to note that the neutrino density mode is exactly the same as in the IG case provided the substitutions $\gamma \to \xi$ and $\omega \to \omega_{\rm NMC}$.

Neutrino Velocity Mode

$$
\begin{aligned}
\delta_\gamma =& \frac{4R_\nu}{3R_\gamma}k\tau - \frac{R_b R_\nu \omega \left(N_{\rm pl}^2(R_\gamma+2)+\xi\varphi_i^2(12\xi+R_\gamma+2)\right)}{4{R_\gamma}^2\left(\xi\varphi_i^2+N_{\rm pl}^2\right)}k\tau^2,\\
\theta_\gamma =& -\frac{kR_\nu}{R_\gamma} + \frac{3R_bR_\nu\omega\left(\xi(1+6\xi)\varphi_i^2+N_{\rm pl}^2\right)}{4{R_\gamma}^2\left(\xi\varphi_i^2+N_{\rm pl}^2\right)}k\tau\\
&+\left(\frac{kR_\nu}{6R_\gamma} - \frac{3R_bR_\nu\omega^2\left(\xi(1+6\xi)\varphi_i^2+N_{\rm pl}^2\right)\left(N_{\rm pl}^2(3R_b-R_\gamma)+\xi\varphi_i^2(3(1+6\xi)R_b-R_\gamma)\right)}{16k{R_\gamma}^3\left(\xi\varphi_i^2+N_{\rm pl}^2\right)^2}\right)k^2\tau^2\\
\delta_b =& \frac{R_\nu}{R_\gamma}k\tau - \frac{3R_bR_\nu\omega\left(N_{\rm pl}^2(R_\gamma+2)+\xi\varphi_i^2(12\xi+R_\gamma+2)\right)}{16{R_\gamma}^2\left(\xi\varphi_i^2+N_{\rm pl}^2\right)}k\tau^2,\\
\delta_c =& -\frac{3R_bR_\nu\omega}{16R_\gamma}k\tau^2,\\
\delta_\nu =& -\frac{4}{3}k\tau - \frac{R_bR_\nu\omega}{4R_\gamma}k\tau^2,\\
\theta_\nu =& k - \frac{(4R_\nu+9)}{6(4R_\nu+5)}k^3\tau^2\sigma_\nu =\\
F_3 =& \frac{4}{7(4R_\nu+5)}k^2\tau^2,\\
h =& \frac{3R_bR_\nu\omega}{8R_\gamma}k\tau^2,\\
\eta =& -\frac{4R_\nu}{3(4R_\nu+5)}k\tau - \frac{R_bR_\nu\omega}{16R_\gamma}\tau^2+,\\
&+\frac{5R_\nu\omega\left(\xi(1+6\xi)\varphi_i^2+N_{\rm pl}^2\right)}{(4R_\nu+5)(4R_\nu+15)\left(\xi\varphi_i^2+N_{\rm pl}^2\right)}k\tau^2,\\
\delta\varphi =& \frac{\xi R_bR_\nu\omega\varphi_i}{2R_\gamma}k\tau^2 - \frac{\xi^2N_{\rm pl}^2R_bR_\nu\omega^2\varphi_i^3(9(1+6\xi)R_b+(3\xi(72\xi+23)+19)R_\gamma)}{48{R_\gamma}^2\left(\xi\varphi_i^2+N_{\rm pl}^2\right)\left(\xi(1+6\xi)\varphi_i^2+N_{\rm pl}^2\right)},\\
&-\frac{\xi R_bR_\nu\omega^2\varphi_i\left(N_{\rm pl}^4(9R_b+(19-48\xi)R_\gamma)+\xi^2(1+6\xi)\varphi_i^4(9(6\xi R_b+R_b+8\xi R_\gamma)+19R_\gamma)\right)}{96{R_\gamma}^2\left(\xi\varphi_i^2+N_{\rm pl}^2\right)\left(\xi(1+6\xi)\varphi_i^2+N_{\rm pl}^2\right)}k\tau^3\\
\mathcal{R} =& \frac{R_\nu\omega}{k(4R_\nu+5)},\\
\Psi =& -\Phi = \frac{4R_\nu}{k(4R_\nu+5)\tau},\\
\delta\varphi_I =& \frac{6\xi R_\nu\omega\varphi_i}{k(4R_\nu+5)}.
\end{aligned}
$$

Scalar Field-Radiation Isocurvature Mode

$$
\begin{aligned}
\delta_\gamma =& -\frac{\left(\xi(1+6\xi)\varphi_i^2+N_{\rm pl}^2\right)}{(1+6\xi)\left(\xi\varphi_i^2+N_{\rm pl}^2\right)}-\frac{2\omega}{3}\tau+\\
&+\frac{1}{6}\omega\left(\frac{k\left(\xi(1+6\xi)\varphi_i^2+N_{\rm pl}^2\right)}{(1+6\xi)\omega\left(\xi\varphi_i^2+N_{\rm pl}^2\right)}-\frac{3\omega\left((15\xi-4)N_{\rm pl}^2-2\xi(1+6\xi)(15\xi+2)\varphi_i^2\right)}{8k\left(\xi(1+6\xi)\varphi_i^2+N_{\rm pl}^2\right)}\right)k\tau^2,\\
\theta_\gamma =& -\frac{\left(\xi(1+6\xi)\varphi_i^2+N_{\rm pl}^2\right)}{4(1+6\xi)\left(\xi\varphi_i^2+N_{\rm pl}^2\right)}k^2\tau+\omega\left(\frac{3kR_b\left(\xi(1+6\xi)\varphi_i^2+N_{\rm pl}^2\right)^2}{16(6\xi R_\gamma+R_\gamma)\left(\xi\varphi_i^2+N_{\rm pl}^2\right)^2}-\frac{k}{12}\right)k\tau^2,\\
\delta_b =& -\frac{\omega}{2}\tau+\frac{\omega}{8}\left(\frac{k\left(\xi(1+6\xi)\varphi_i^2+N_{\rm pl}^2\right)}{(1+6\xi)\omega\left(\xi\varphi_i^2+N_{\rm pl}^2\right)}-\frac{3\omega\left((15\xi-4)N_{\rm pl}^2-2\xi(1+6\xi)(15\xi+2)\varphi_i^2\right)}{8k\left(\xi(1+6\xi)\varphi_i^2+N_{\rm pl}^2\right)}\right)k\tau^2,\\
\delta_c =& -\frac{\omega}{2}\tau-\frac{3\omega^2\left((15\xi-4)N_{\rm pl}^2-2\xi(1+6\xi)(15\xi+2)\varphi_i^2\right)}{64\left(\xi(1+6\xi)\varphi_i^2+N_{\rm pl}^2\right)}\tau^2,\\
\delta_\nu =& -\frac{\left(\xi(1+6\xi)\varphi_i^2+N_{\rm pl}^2\right)}{(1+6\xi)\left(\xi\varphi_i^2+N_{\rm pl}^2\right)}-\frac{2\omega}{3}\tau+\\
&+\frac{\omega}{6}\left(\frac{k\left(\xi(1+6\xi)\varphi_i^2+N_{\rm pl}^2\right)}{(1+6\xi)\omega\left(\xi\varphi_i^2+N_{\rm pl}^2\right)}-\frac{3\omega\left((15\xi-4)N_{\rm pl}^2-2\xi(1+6\xi)(15\xi+2)\varphi_i^2\right)}{8k\left(\xi(1+6\xi)\varphi_i^2+N_{\rm pl}^2\right)}\right)k\tau^2,\\
\theta_\nu =& -\frac{\left(\xi(1+6\xi)\varphi_i^2+N_{\rm pl}^2\right)}{4(1+6\xi)\left(\xi\varphi_i^2+N_{\rm pl}^2\right)}k^2\tau-\frac{\omega}{12}k^2\tau^2,\\
\sigma_\nu =& \frac{\left(\xi(1+6\xi)\varphi_i^2+N_{\rm pl}^2\right)}{6(1+6\xi)(4R_\nu+15)\left(\xi\varphi_i^2+N_{\rm pl}^2\right)}k^2\tau^2,\\
F_3 =& \frac{\left(\xi(1+6\xi)\varphi_i^2+N_{\rm pl}^2\right)}{21(1+6\xi)(4R_\nu+15)\left(\xi\varphi_i^2+N_{\rm pl}^2\right)}k^3\tau^3,\\
h =& \omega\tau+\frac{3\omega^2\left((15\xi-4)N_{\rm pl}^2-2\xi(1+6\xi)(15\xi+2)\varphi_i^2\right)}{32\left(\xi(1+6\xi)\varphi_i^2+N_{\rm pl}^2\right)}\tau^2,\\
\eta =& -\frac{\omega}{6}\tau+\omega\left(\frac{\omega\left(2\xi(1+6\xi)(15\xi+2)\varphi_i^2+(4-15\xi)N_{\rm pl}^2\right)}{64k\left(\xi(1+6\xi)\varphi_i^2+N_{\rm pl}^2\right)}+\frac{k(R_\nu+5)\left(\xi(1+6\xi)\varphi_i^2+N_{\rm pl}^2\right)}{6(1+6\xi)(4R_\nu+15)\omega\left(\xi\varphi_i^2+N_{\rm pl}^2\right)}\right)
\end{aligned}
$$

$$
\begin{aligned}
\delta\varphi =& -\frac{\left(\xi(1+6\xi)\varphi_i^2+N_{\rm pl}^2\right)}{2\xi(1+6\xi)\varphi_i}+\frac{3\omega\left(\xi(1+6\xi)\varphi_i^2-N_{\rm pl}^2\right)}{4(1+6\xi)\varphi_i}\tau+\frac{\omega\left(\xi(1+6\xi)\varphi_i^2+N_{\rm pl}^2\right)}{12\xi(1+6\xi)\omega\varphi_i}k^2\tau^2+\\
&-\frac{\omega^2\left(\xi^2(1+6\xi)^2(27\xi+8)\varphi_i^4+(6\xi-2)N_{\rm pl}^4-3\xi(6\xi+1)(19\xi-2)N_{\rm pl}^2\varphi_i^2\right)}{16(1+6\xi)\varphi_i\left(\xi(1+6\xi)\varphi_i^2+N_{\rm pl}^2\right)}\tau^2.
\end{aligned}
$$

$$
\begin{aligned}
\mathcal{R} =& -\frac{\omega\tau}{4(4R_\nu+15)}\left(\frac{6\xi N_{\rm pl}^2(R_\gamma-6)}{(1+6\xi)\left(\xi\varphi_i^2+N_{\rm pl}^2\right)}-R_\gamma+4R_\nu+21\right),\\
\Psi =& -\frac{\omega(R_\nu+5)\left(\xi(1+6\xi)\varphi_i^2+N_{\rm pl}^2\right)}{(1+6\xi)(4R_\nu+15)\omega\left(\xi\varphi_i^2+N_{\rm pl}^2\right)},\\
\Phi =& \frac{2\omega(R_\nu+5)\left(\xi(1+6\xi)\varphi_i^2+N_{\rm pl}^2\right)}{(1+6\xi)(4R_\nu+15)\omega\left(\xi\varphi_i^2+N_{\rm pl}^2\right)}\\
\delta\varphi_I =& -\frac{\omega\left(\xi(1+6\xi)\varphi_i^2+N_{\rm pl}^2\right)}{2\xi\omega(6\xi\varphi_i+\varphi_i)}.
\end{aligned}
$$

Appendix C

CMB Cross Correlation Power Spectra

In this appendix we show sequentially the T-E cross-correlation power spectra for the CDI, NID and RAD modes. We do not show the BI contribution since, apart from a different amplitude, they are the same of the CDI mode. We note that the contribution of the RAD mode to these cross-correlation spectra is an order of magnitude smaller than which of the CDI and NID modes.

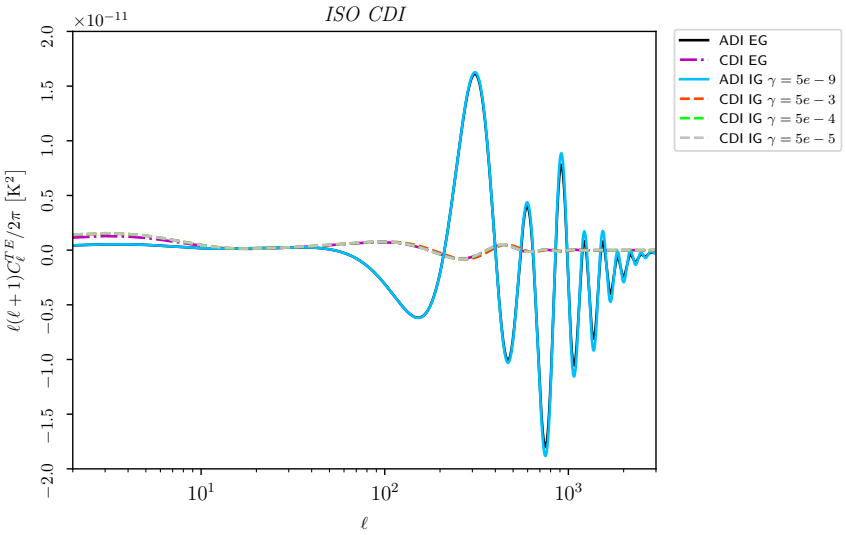

Figure C.1: CDI T-E cross power spectrum for three different values of γ, compared to the original ΛCDM model.

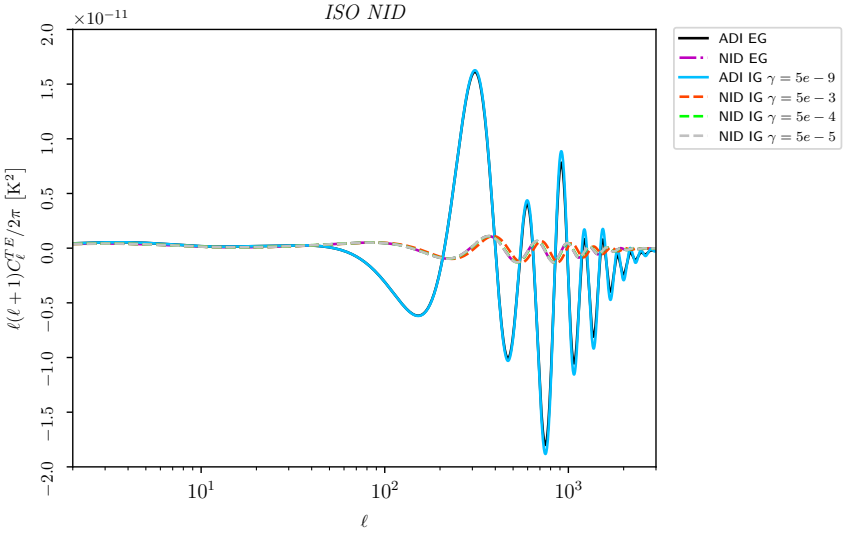

Figure C.2: NID T-E cross power spectrum for three different values of γ, compared to the original ΛCDM model.

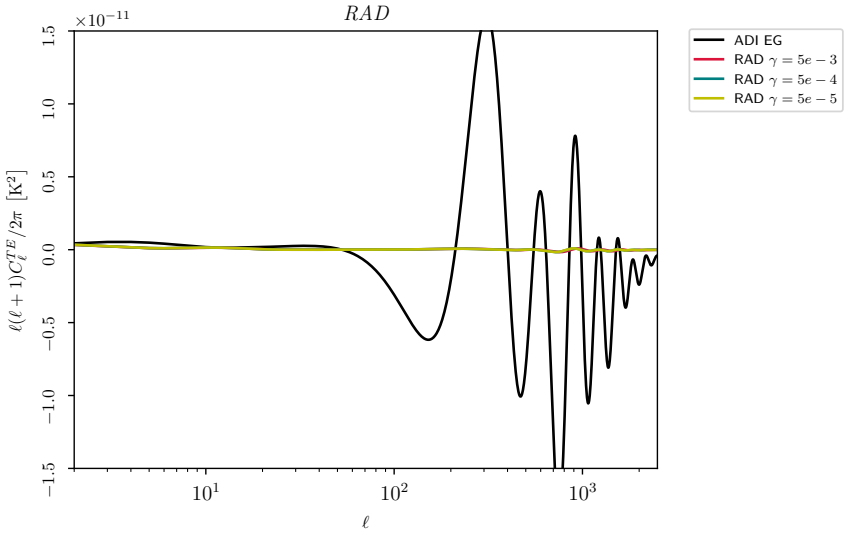

Figure C.3: RAD T-E cross spectrum for three different values of γ, compared to the original adiabatic mode for the ΛCDM model.

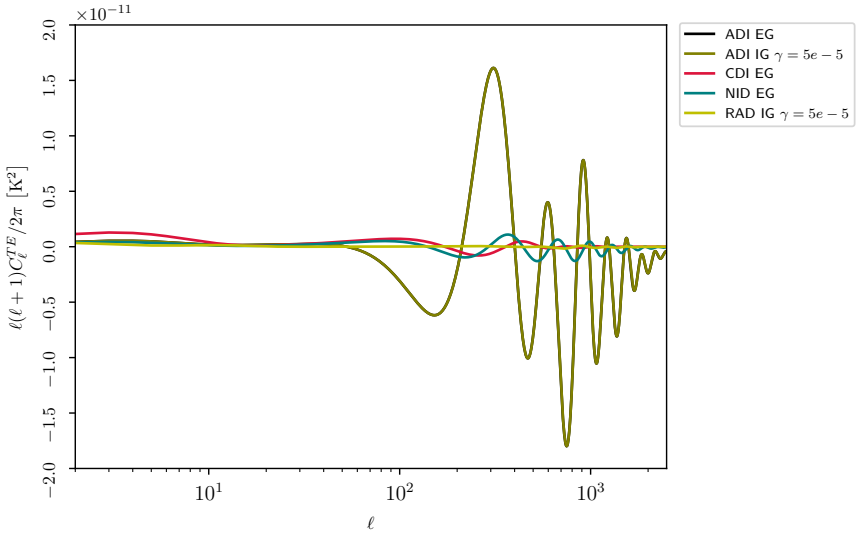

Figure C.4: RAD temperature power spectrum for $\gamma = 0.00005$, compared to the NID and CDI ΛCDM model.

Appendix D

CMB Angular Power Spectra Relative Differences

In this appendix we show the relative differences between the BI, CDI and NID modes of Sec.5.1 and their EG counterparts from Ref.[38]. We show the TT, EE, TE and $\phi\phi$ power spectra sequentially. For TT, EE and $\phi\phi$ we plot the quantities

$$\frac{C_l^{ii} - C_{l\,\mathrm{EG}}^{ii}}{C_{l\,\mathrm{EG}}^{ii}} \equiv \frac{\Delta C_l^{ii}}{C_{l\,\mathrm{EG}}^{ii}}, \tag{D.1}$$

where the subscript EG denotes the original Einstein Gravity mode and $i = T, E, \phi$, whereas for the cross-correlation power spectra we plot the quantities

$$\frac{\Delta C_l^{iT}}{\sqrt{C_{l\,\mathrm{EG}}^{ii} C_{l\,\mathrm{EG}}^{TT}}}. \tag{D.2}$$

Since the BI and CDI have almost the same behaviour we show both their relative differences only for the TT power spectrum and we plot only the CDI mode for the other spectra.

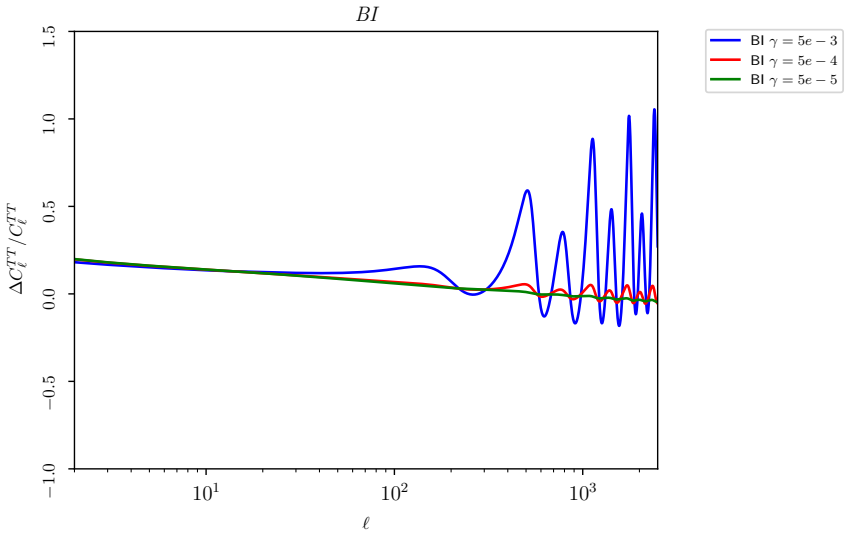

Figure D.1: BI relative temperature power spectrum for three different values of γ, compared to the original ΛCDM model.

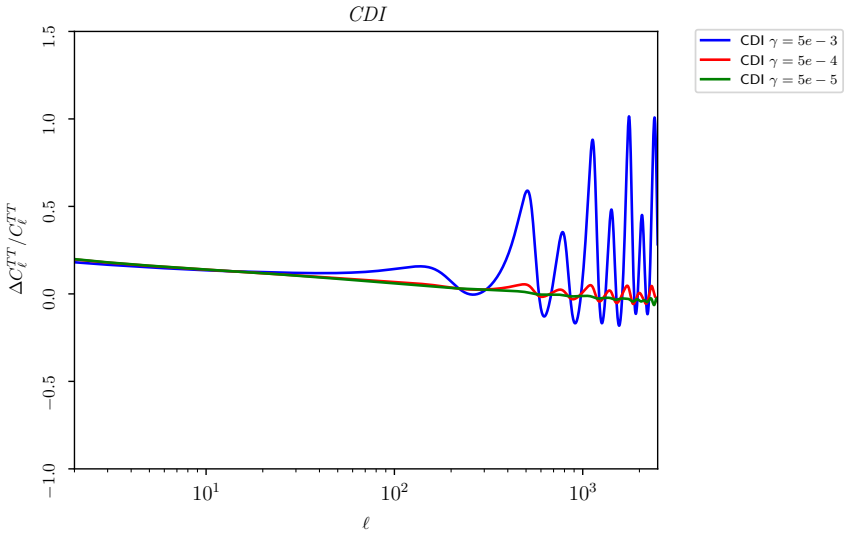

Figure D.2: CDI relative temperature power spectrum for three different values of γ, compared to the original ΛCDM model.

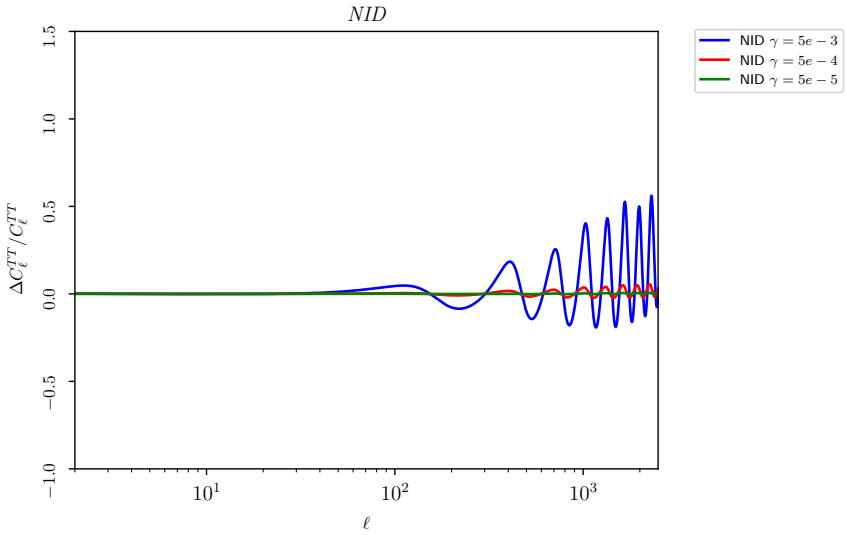

Figure D.3: NID relative temperature power spectrum for three different values of γ, compared to the original ΛCDM model.

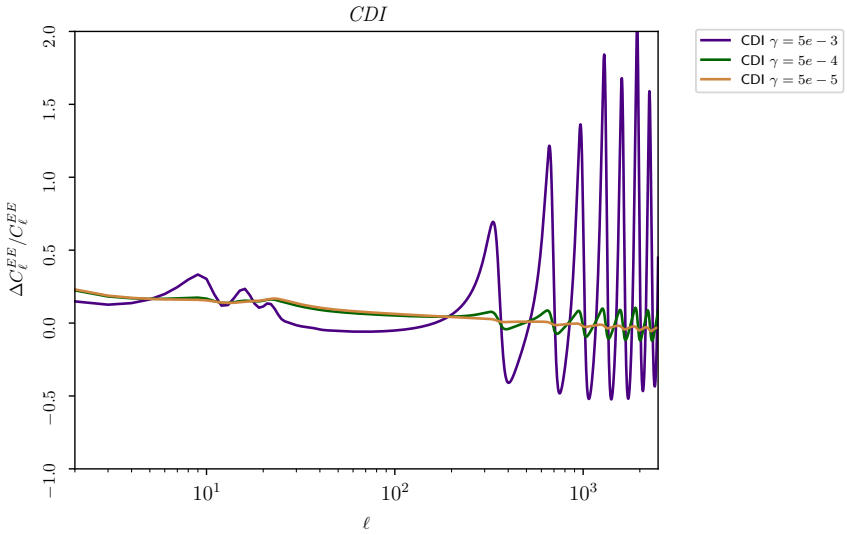

Figure D.4: CDI relative EE power spectrum for three different values of γ, compared to the original ΛCDM model.

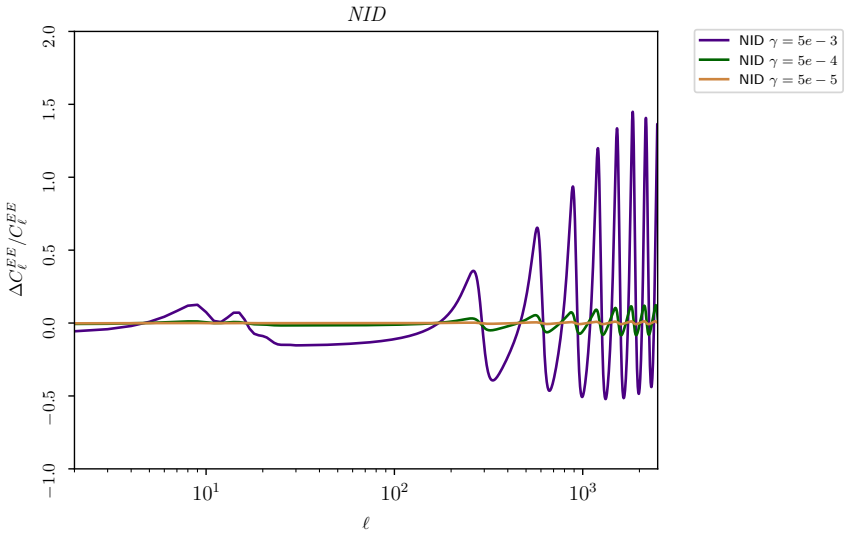

Figure D.5: NID relative EE power spectrum for three different values of γ, compared to the original ΛCDM model.

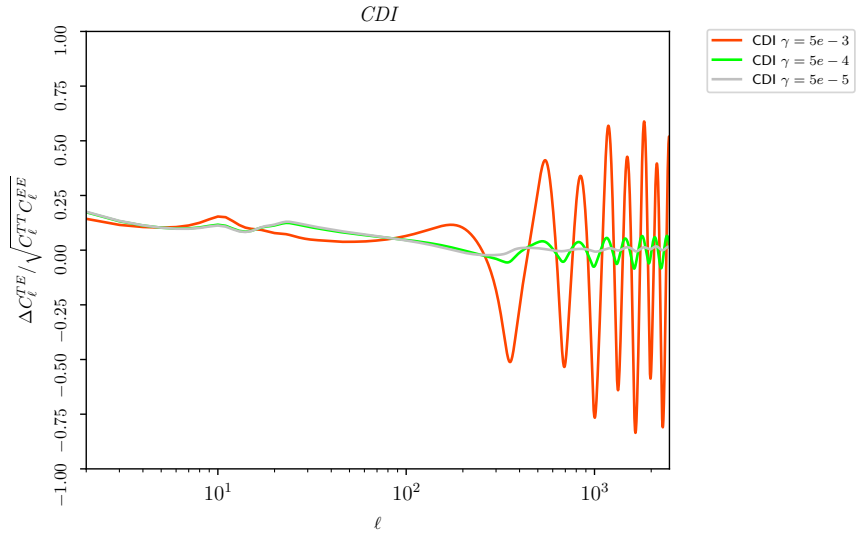

Figure D.6: CDI relative ET power spectrum for three different values of γ, compared to the original ΛCDM model.

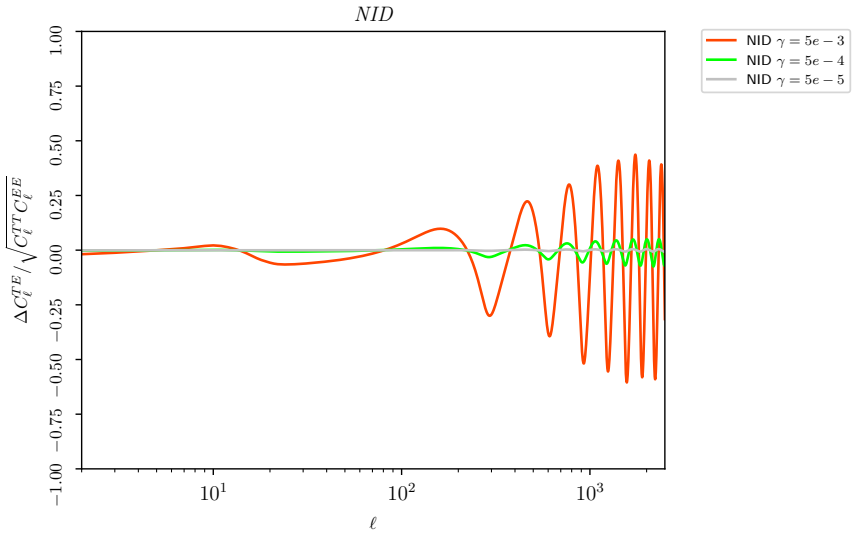

Figure D.7: NID relative ET power spectrum for three different values of γ, compared to the original ΛCDM model.

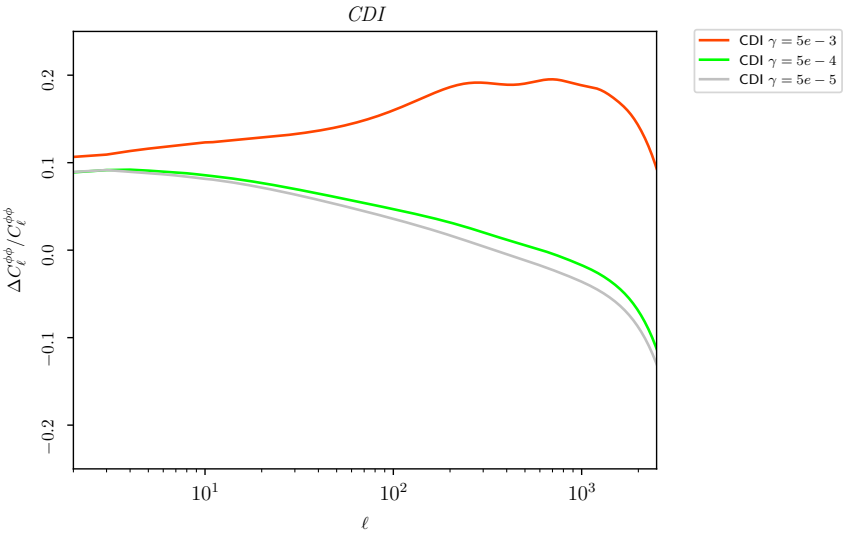

Figure D.8: CDI relative $\phi\phi$ power spectrum for three different values of γ, compared to the original ΛCDM model.

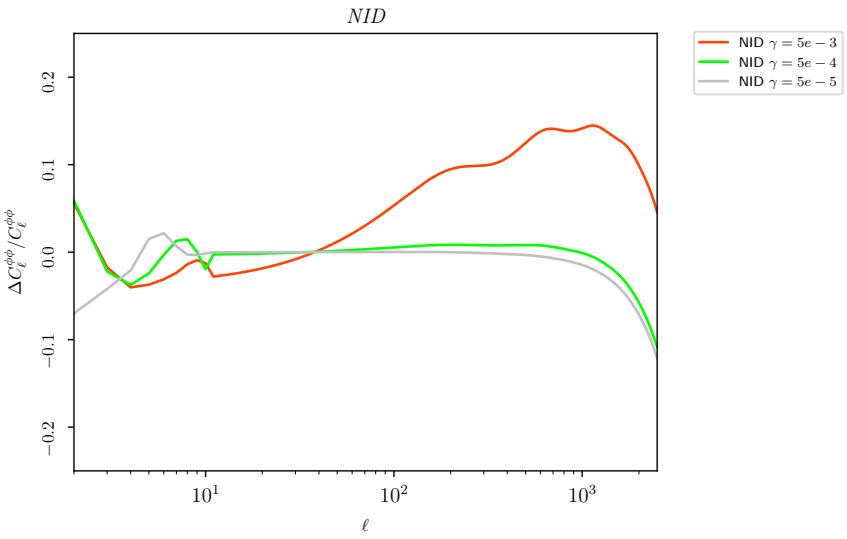

Figure D.9: NID relative $\phi\phi$ power spectrum for three different values of γ, compared to the original ΛCDM model.

Acknowledgements

At the end of this work, I think some thanks are due.

First of all I would like to thank Prof. Roberto Balbinot for rising in me the interest in cosmology, for his supervision to this work and for all the useful advices he gave me.

I must then express my gratitude to the two persons who made this work possible and who made the time I passed at INAF beautiful. I thank Dr. Fabio Finelli for the interest he showed in having me as a student and for taking always the right decision, even when I could not understand them. I am grateful to Dr. Daniela Paoletti, has always been available for asking me about my doubts, even when they were stupid, giving me interesting points of view. I also thank Daniela for her priceless help with the CLASS code, I could not have done it on my own.

I would like to thank Dr. Mario Ballardini for welcoming it at INAF and for useful advices out of the scope of my thesis.

I also have to thank Prof. Alexei Starobinsky for useful comments on the last part of my thesis.

Nevertheless, this work has been accompanied by all the things happened in these months out of its context. For this reason I would like to thank my parents and my family, for giving me the opportunity to arrive at this point and who sustained me during these years.

I also express my gratitude to Elisa for being always present for me, even if I often am not.

Finally, thanks to my grandmother, for everything.

Bibliography

[1] A. Friedmann. Über die Krümmung des Raumes. *Zeitschrift fur Physik*, 10:377–386, 1922.

[2] G. Lemaître. Un Univers homogène de masse constante et de rayon croissant rendant compte de la vitesse radiale des nébuleuses extra-galactiques. *Annales de la Societe Scietifique de Bruxelles*, 47:49–59, 1927.

[3] E. Hubble. *A Relation Between Distance and Radial Velocity Among Extra-Galactic Nebulae*, page 9. 1988.

[4] A. G. Riess, A. V. Filippenko, P. Challis, A. Clocchiatti, A. Diercks, P. M. Garnavich, R. L. Gilliland, C. J. Hogan, S. Jha, R. P. Kirshner, B. Leibundgut, M. M. Phillips, D. Reiss, B. P. Schmidt, R. A. Schommer, R. C. Smith, J. Spyromilio, C. Stubbs, N. B. Suntzeff, and J. Tonry. Observational Evidence from Supernovae for an Accelerating Universe and a Cosmological Constant. *AJ*, 116:1009–1038, September 1998.

[5] S. Weinberg. Gravitation and Cosmology: Principles and Applications of the General Theory of Relativity. *American Journal of Physics*, 41:598–599, April 1973.

[6] R. A. D'Inverno. *Introducing Einstein's relativity*. 1992.

[7] C. W. Misner, K. S. Thorne, and J. A. Wheeler. *Gravitation*. 1973.

[8] V. Mukhanov. *Physical Foundations of Cosmology*. March 2001.

[9] S. Weinberg. *Cosmology*. Oxford University Press, 2008.

[10] D. Baumann. *Cosmology*. 2013.

[11] Planck Collaboration, P. A. R. Ade, N. Aghanim, M. Arnaud, M. Ashdown, J. Aumont, C. Baccigalupi, A. J. Banday, R. B. Barreiro, J. G. Bartlett, and et al. Planck 2015 results. XIII. Cosmological parameters. *A&A*, 594:A13, September 2016.

[12] G. Gamow. Erratum: Expanding Universe and the Origin of Elements [. *Physical Review*, 71:273–273, February 1947.

[13] A. M. Boesgaard and G. Steigman. Big bang nucleosynthesis - Theories and observations. *ARA&A*, 23:319–378, 1985.

[14] D. Baumann. *The Physics of Inflation*. 2012.

[15] M. E. Peskin and D. V. Schroeder. *An Introduction to Quantum Field Theory*. Westview Press, 1995.

[16] D. J. Fixsen. The Temperature of the Cosmic Microwave Background. *ApJ*, 707:916–920, December 2009.

[17] G. Bertone. *Particle Dark Matter : Observations, Models and Searches*. Cambridge University Press, 2010.

[18] A. Einstein. Kosmologische Betrachtungen zur allgemeinen Relativitätstheorie. *Sitzungsberichte der Königlich Preußischen Akademie der Wissenschaften (Berlin), Seite 142-152.*, 1917.

[19] G. Lemaitre. Evolution of the Expanding Universe. *Proceedings of the National Academy of Science*, 20:12–17, January 1934.

[20] D. Janzen. Einstein's cosmological considerations. *ArXiv e-prints*, February 2014.

[21] A. S. Eddington. The cosmological controversy. *Science Progress*, 34:225–236, 1939.

[22] Y. B. Zel'Dovich. Cosmological Constant and Elementary Particles. *ZhETF Pisma Redaktsiiu*, 6:883, November 1967.

[23] P. J. E. Peebles and B. Ratra. Cosmology with a time-variable cosmological 'constant'. *ApJL*, 325:L17–L20, February 1988.

[24] S. M. Carroll. The Cosmological Constant. *Living Reviews in Relativity*, 4:1, February 2001.

[25] P. J. Peebles and B. Ratra. The cosmological constant and dark energy. *Reviews of Modern Physics*, 75:559–606, April 2003.

[26] S. Tsujikawa. Quintessence: a review. *Classical and Quantum Gravity*, 30(21):214003, November 2013.

[27] C. Wetterich. Cosmology and the fate of dilatation symmetry. *Nuclear Physics B*, 302:668–696, June 1988.

[28] I. Zlatev, L. Wang, and P. J. Steinhardt. Quintessence, Cosmic Coincidence, and the Cosmological Constant. *Physical Review Letters*, 82:896–899, February 1999.

[29] A. R. Liddle and R. J. Scherrer. Classification of scalar field potentials with cosmological scaling solutions. *PRD*, 59(2):023509, January 1999.

[30] C.-P. Ma and E. Bertschinger. Cosmological Perturbation Theory in the Synchronous and Conformal Newtonian Gauges. *ApJ*, 455:7, December 1995.

[31] S. Dodelson and G. Efstathiou. Modern Cosmology. *Physics Today*, 57:60–61, July 2004.

[32] J. M. Bardeen. Gauge-invariant cosmological perturbations. *PRD*, 22:1882–1905, October 1980.

[33] V. F. Mukhanov, H. A. Feldman, and R. H. Brandenberger. Theory of cosmological perturbations. *Phys.Rep.*, 215:203–333, June 1992.

[34] M. Giovannini. Theoretical Tools for CMB Physics. *International Journal of Modern Physics D*, 14:363–510, 2005.

[35] Antony Lewis. CAMB Notes. `http://cosmologist.info/notes/CAMB.pdf`.

[36] J. R. Bond and A. S. Szalay. The collisionless damping of density fluctuations in an expanding universe. *ApJ*, 274:443–468, November 1983.

[37] A. Kosowsky. Cosmic microwave background polarization. *Annals of Physics*, 246:49–85, February 1996.

[38] M. Bucher, K. Moodley, and N. Turok. General primordial cosmic perturbation. *PRD*, 62(8):083508, October 2000.

[39] J. C. Mather, E. S. Cheng, D. A. Cottingham, R. E. Eplee, Jr., D. J. Fixsen, T. Hewagama, R. B. Isaacman, K. A. Jensen, S. S. Meyer, P. D. Noerdlinger, S. M. Read, L. P. Rosen, R. A. Shafer, E. L. Wright, C. L. Bennett, N. W. Boggess, M. G. Hauser, T. Kelsall, S. H. Moseley, Jr., R. F. Silverberg, G. F. Smoot, R. Weiss, and D. T. Wilkinson. Measurement of the cosmic microwave background spectrum by the COBE FIRAS instrument. *ApJ*, 420:439–444, January 1994.

[40] N. Aghanim, S. Majumdar, and J. Silk. Secondary anisotropies of the CMB. *Reports on Progress in Physics*, 71(6):066902, June 2008.

[41] R. K. Sachs and A. M. Wolfe. Perturbations of a Cosmological Model and Angular Variations of the Microwave Background. *ApJ*, 147:73, January 1967.

[42] D. J. Eisenstein, I. Zehavi, D. W. Hogg, R. Scoccimarro, M. R. Blanton, R. C. Nichol, R. Scranton, H.-J. Seo, M. Tegmark, Z. Zheng, S. F. An-

derson, J. Annis, N. Bahcall, J. Brinkmann, S. Burles, F. J. Castander, A. Connolly, I. Csabai, M. Doi, M. Fukugita, J. A. Frieman, K. Glazebrook, J. E. Gunn, J. S. Hendry, G. Hennessy, Z. Ivezić, S. Kent, G. R. Knapp, H. Lin, Y.-S. Loh, R. H. Lupton, B. Margon, T. A. McKay, A. Meiksin, J. A. Munn, A. Pope, M. W. Richmond, D. Schlegel, D. P. Schneider, K. Shimasaku, C. Stoughton, M. A. Strauss, M. SubbaRao, A. S. Szalay, I. Szapudi, D. L. Tucker, B. Yanny, and D. G. York. Detection of the Baryon Acoustic Peak in the Large-Scale Correlation Function of SDSS Luminous Red Galaxies. *ApJ*, 633:560–574, November 2005.

[43] W. Hu and S. Dodelson. Cosmic Microwave Background Anisotropies. *ARA&A*, 40:171–216, 2002.

[44] M. Abramowitz and I. A. Stegun. *Handbook of mathematical functions : with formulas, graphs, and mathematical tables*. 1970.

[45] A. Challinor and H. Peiris. Lecture notes on the physics of cosmic microwave background anisotropies. In M. Novello and S. Perez, editors, *American Institute of Physics Conference Series*, volume 1132 of *American Institute of Physics Conference Series*, pages 86–140, May 2009.

[46] M. Bucher. Physics of the cosmic microwave background anisotropy. *International Journal of Modern Physics D*, 24:1530004–303, January 2015.

[47] D. Langlois. Perturbations cosmologiques isocourbures et le CMB. *Comptes Rendus Physique*, 4:953–959, October 2003.

[48] A. R. Liddle and D. H. Lyth. *Cosmological Inflation and Large-Scale Structure*. June 2000.

[49] S. Weinberg. Adiabatic modes in cosmology. *PRD*, 67(12):123504, June 2003.

[50] N. Deruelle and V. F. Mukhanov. Matching conditions for cosmological perturbations. *PRD*, 52:5549–5555, November 1995.

[51] H. Kodama and M. Sasaki. Cosmological Perturbation Theory. *Progress of Theoretical Physics Supplement*, 78:1, 1984.

[52] D. Wands. Multiple Field Inflation. In M. Lemoine, J. Martin, and P. Peter, editors, *Inflationary Cosmology*, volume 738 of *Lecture Notes in Physics, Berlin Springer Verlag*, page 275, 2008.

[53] L. Amendola and F. Finelli. Effects of a Decaying Cosmological Fluctuation. *Physical Review Letters*, 94(22):221303, June 2005.

[54] C. Gordon and A. Lewis. Observational constraints on the curvaton model of inflation. *PRD*, 67(12):123513, June 2003.

[55] P. J. E. Peebles and J. T. Yu. Primeval Adiabatic Perturbation in an Expanding Universe. *ApJ*, 162:815, December 1970.

[56] P. J. E. Peebles. Origin of the large-scale galaxy peculiar velocity field - A minimal isocurvature model. *Nature*, 327:210, May 1987.

[57] R. Cen, J. P. Ostriker, and P. J. E. Peebles. A Hydrodynamic Approach to Cosmology: The Primeval Baryon Isocurvature Model. *ApJ*, 415:423, October 1993.

[58] G. Efstathiou and J. R. Bond. Isocurvature cold dark matter fluctuations. *MNRAS*, 218:103–121, January 1986.

[59] G. Efstathiou and J. R. Bond. Microwave anisotropy constraints on isocurvature baryon models. *MNRAS*, 227:33P–38P, August 1987.

[60] Planck Collaboration, P. A. R. Ade, N. Aghanim, C. Armitage-Caplan, M. Arnaud, M. Ashdown, F. Atrio-Barandela, J. Aumont, C. Baccigalupi, A. J. Banday, and et al. Planck 2013 results. XXII. Constraints on inflation. *A&A*, 571:A22, November 2014.

[61] Planck Collaboration, P. A. R. Ade, N. Aghanim, M. Arnaud, F. Arroja, M. Ashdown, J. Aumont, C. Baccigalupi, M. Ballardini, A. J. Banday, and et al. Planck 2015 results. XX. Constraints on inflation. *A&A*, 594:A20, September 2016.

[62] K. Enqvist, H. Kurki-Suonio, and J. Väliviita. Open and closed CDM isocurvature models contrasted with the CMB data. *PRD*, 65(4):043002, February 2002.

[63] D. Langlois. Correlated adiabatic and isocurvature perturbations from double inflation. *PRD*, 59(12):123512, June 1999.

[64] D. Langlois and A. Riazuelo. Correlated mixtures of adiabatic and isocurvature cosmological perturbations. *PRD*, 62(4):043504, August 2000.

[65] L. Amendola, C. Gordon, D. Wands, and M. Sasaki. Correlated Perturbations from Inflation and the Cosmic Microwave Background. *Physical Review Letters*, 88(21):211302, May 2002.

[66] D. Wands, K. A. Malik, D. H. Lyth, and A. R. Liddle. New approach to the evolution of cosmological perturbations on large scales. *PRD*, 62(4):043527, August 2000.

[67] M. Beltrán, J. García-Bellido, J. Lesgourgues, and M. Viel. Squeezing the window on isocurvature modes with the Lyman-α forest. *PRD*, 72(10):103515, November 2005.

[68] L. R. Abramo and F. Finelli. Attractors and isocurvature perturbations in quintessence models. *PRD*, 64(8):083513, October 2001.

[69] P. Brax, J. Martin, and A. Riazuelo. Exhaustive study of cosmic microwave background anisotropies in quintessential scenarios. *PRD*, 62(10):103505, November 2000.

[70] C. Skordis and A. Albrecht. Planck-scale quintessence and the physics of structure formation. *PRD*, 66(4):043523, August 2002.

[71] M. Kawasaki, T. Moroi, and T. Takahashi. Isocurvature fluctuations in tracker quintessence models. *Physics Letters B*, 533:294–301, May 2002.

[72] J. M. Bardeen, P. J. Steinhardt, and M. S. Turner. Spontaneous creation of almost scale-free density perturbations in an inflationary universe. *PRD*, 28:679–693, August 1983.

[73] M. Kawasaki, T. Moroi, and T. Takahashi. Cosmic microwave background anisotropy with cosine-type quintessence. *PRD*, 64(8):083009, October 2001.

[74] T. Moroi and T. Takahashi. Correlated Isocurvature Fluctuation in Quintessence and Suppressed Cosmic Microwave Background Anisotropies at Low Multipoles. *Physical Review Letters*, 92(9):091301, March 2004.

[75] C. Gordon and W. Hu. Low CMB quadrupole from dark energy isocurvature perturbations. *PRD*, 70(8):083003, October 2004.

[76] K. Karwan. A model of large quintessence isocurvature fluctuations and a low cosmic microwave background quadrupole. *JCAP*, 7:009, July 2007.

[77] A. Rassat, J.-L. Starck, P. Paykari, F. Sureau, and J. Bobin. Planck CMB anomalies: astrophysical and cosmological secondary effects and the curse of masking. *JCAP*, 8:006, August 2014.

[78] A. A. Starobinskiĭ. Multicomponent de Sitter (inflationary) stages and the generation of perturbations. *ZhETF Pisma Redaktsiiu*, 42:124, August 1985.

[79] D. Polarski and A. A. Starobinsky. Isocurvature perturbations in multiple inflationary models. *PRD*, 50:6123–6129, November 1994.

[80] A. D. Linde. Generation of isothermal density perturbations in the inflationary universe. *Physics Letters B*, 158:375–380, August 1985.

[81] D. Polarski and A. A. Starobinsky. Spectra of perturbations produced by double inflation with an intermediate matter-dominated stage. *Nuclear Physics B*, 385:623–650, October 1992.

[82] P. J. E. Peebles and A. Vilenkin. Quintessential inflation. *PRD*, 59(6):063505, March 1999.

[83] A. A. Starobinsky, S. Tsujikawa, and J. Yokoyama. Cosmological perturbations from multi-field inflation in generalized Einstein theories. *Nuclear Physics B*, 610:383–410, September 2001.

[84] F. di Marco, F. Finelli, and R. Brandenberger. Adiabatic and isocurvature perturbations for multifield generalized Einstein models. *PRD*, 67(6):063512, March 2003.

[85] F. di Marco and F. Finelli. Slow-roll inflation for generalized two-field Lagrangians. *PRD*, 71(12):123502, June 2005.

[86] C. Gordon, D. Wands, B. A. Bassett, and R. Maartens. Adiabatic and entropy perturbations from inflation. *PRD*, 63(2):023506, January 2001.

[87] A. A. Starobinsky. Dynamics of phase transition in the new inflationary universe scenario and generation of perturbations. *Physics Letters B*, 117:175–178, November 1982.

[88] M. Sasaki. Large Scale Quantum Fluctuations in the Inflationary Universe. *Progress of Theoretical Physics*, 76:1036–1046, November 1986.

[89] V. F. Mukhanov. The quantum theory of gauge-invariant cosmological perturbations. *Zhurnal Eksperimentalnoi i Teoreticheskoi Fiziki*, 94:1–11, July 1988.

[90] P. Jordan. *Schwerkraft und Weltall: Grundlagen der theoretischen Kosmologie*. Die Wissenschaft. F. Vieweg, 1955.

[91] C. Brans and R. H. Dicke. Mach's Principle and a Relativistic Theory of Gravitation. *Physical Review*, 124:925–935, November 1961.

[92] Gregory Walter Horndeski. Second-order scalar-tensor field equations in a four-dimensional space. *Int. J. Theor. Phys.*, 10:363–384, 1974.

[93] T. Clifton, P. G. Ferreira, A. Padilla, and C. Skordis. Modified gravity and cosmology. *Phys.Rep.*, 513:1–189, March 2012.

[94] C. Charmousis, E. J. Copeland, A. Padilla, and P. M. Saffin. General Second-Order Scalar-Tensor Theory and Self-Tuning. *Physical Review Letters*, 108(5):051101, February 2012.

[95] T. Damour and K. Nordtvedt. General relativity as a cosmological attractor of tensor-scalar theories. *Physical Review Letters*, 70:2217–2219, April 1993.

[96] Y. Fujii and K.-i. Maeda. *The Scalar-Tensor Theory of Gravitation*. July 2007.

[97] R. Gannouji, D. Polarski, A. Ranquet, and A. A. Starobinsky. Scalar tensor models of normal and phantom dark energy. *JCAP*, 9:016, September 2006.

[98] S. Tsujikawa. Matter density perturbations and effective gravitational constant in modified gravity models of dark energy. *PRD*, 76(2):023514, July 2007.

[99] B. Bertotti, L. Iess, and P. Tortora. A test of general relativity using radio links with the Cassini spacecraft. *Nature*, 425:374–376, September 2003.

[100] J. García-Bellido and D. Wands. Constraints from inflation on scalar-tensor gravity theories. *PRD*, 52:6739–6749, December 1995.

[101] T. Chiba, N. Sugiyama, and J. Yokoyama. Imprints of the metrically coupled dilaton on density perturbations in inflationary cosmology. *Nuclear Physics B*, 530:304–324, October 1998.

[102] V. Faraoni. *Cosmology in Scalar-Tensor Gravity.* Kluwer Academic Publishers, 2004.

[103] F. S. Accetta, D. J. Zoller, and M. S. Turner. Induced-gravity inflation. *PRD*, 31:3046–3051, June 1985.

[104] M. Ballardini, F. Finelli, C. Umiltà, and D. Paoletti. Cosmological constraints on induced gravity dark energy models. *JCAP*, 5:067, May 2016.

[105] A. Zee. Broken-symmetric theory of gravity. *Physical Review Letters*, 42:417–421, February 1979.

[106] A. Zee. Spontaneously generated gravity. *Phys. Rev. D*, 23:858–866, Feb 1981.

[107] Stephen L. Adler. Einstein Gravity as a Symmetry Breaking Effect in Quantum Field Theory. *Rev. Mod. Phys.*, 54:729, 1982. [Erratum: Rev. Mod. Phys.55,837(1983)].

[108] F. Cooper and G. Venturi. Cosmology and broken scale invariance. *PRD*, 24:3338–3340, December 1981.

[109] G. Turchetti and G. Venturi. Gravitation and broken scale invariance. *Nuovo Cimento A Serie*, 66:221–228, November 1981.

[110] F. Finelli, A. Tronconi, and G. Venturi. Dark energy, induced gravity and broken scale invariance. *Physics Letters B*, 659:466–470, January 2008.

[111] C. Baccigalupi, S. Matarrese, and F. Perrotta. Tracking extended quintessence. *PRD*, 62(12):123510, December 2000.

[112] T. Chiba. Quintessence, the gravitational constant, and gravity. *PRD*, 60(8):083508, October 1999.

[113] J. Ehlers. Examples of Newtonian limits of relativistic spacetimes. *Classical and Quantum Gravity*, 14:A119–A126, January 1997.

[114] K. Schwarzschild. Über das Gravitationsfeld einer Kugel aus inkompressibler Flüssigkeit nach der Einsteinschen Theorie. In *Sitzungsberichte der Königlich Preussischen Akademie der Wissenschaften zu Berlin, Phys.-Math. Klasse, 424-434 (1916)*, March 1916.

[115] A. Loinger. Revisiting the Einstein field of a mass point. *ArXiv General Relativity and Quantum Cosmology e-prints*, August 1999.

[116] R. W. Hellings, P. J. Adams, J. D. Anderson, M. S. Keesey, E. L. Lau, E. M. Standish, V. M. Canuto, and I. Goldman. Experimental test of the variability of G using Viking lander ranging data. *Physical Review Letters*, 51:1609–1612, October 1983.

[117] D. F. Torres. Quintessence, superquintessence, and observable quantities in Brans-Dicke and nonminimally coupled theories. *PRD*, 66(4):043522, August 2002.

[118] S. Chandrasekhar. The Post-Newtonian Equations of Hydrodynamics in General Relativity. *ApJ*, 142:1488, November 1965.

[119] C. M. Will. The Confrontation between General Relativity and Experiment. *Living Reviews in Relativity*, 9:3, March 2006.

[120] K. Nordtvedt, Jr. Post-Newtonian Metric for a General Class of Scalar-Tensor Gravitational Theories and Observational Consequences. *ApJ*, 161:1059, September 1970.

[121] R. M. Wald. *General relativity*. 1984.

[122] S. Capozziello, R. de Ritis, and A. A. Marino. Some aspects of the cosmological conformal equivalence between the 'Jordan frame' and the 'Einstein frame'. *Classical and Quantum Gravity*, 14:3243–3258, December 1997.

[123] V. Faraoni and E. Gunzig. Einstein frame or Jordan frame ? *ArXiv Astrophysics e-prints*, October 1999.

[124] J.-c. Hwang. Cosmological perturbations in generalized gravity theories: conformal transformation. *Classical and Quantum Gravity*, 14:1981–1991, July 1997.

[125] J. Lesgourgues. The Cosmic Linear Anisotropy Solving System (CLASS) I: Overview. *ArXiv e-prints*, April 2011.

[126] C. Umiltà. Cosmological predictions for a scalar tensor dark energy model by a dedicated Einstein-Boltzmann code. *Master Thesis*, 2014.

[127] C. Umiltà, M. Ballardini, F. Finelli, and D. Paoletti. CMB and BAO constraints for an induced gravity dark energy model with a quartic potential. *JCAP*, 8:017, August 2015.

[128] Planck Collaboration, P. A. R. Ade, N. Aghanim, C. Armitage-Caplan, M. Arnaud, M. Ashdown, F. Atrio-Barandela, J. Aumont, C. Baccigalupi, A. J. Banday, and et al. Planck 2013 results. XVII. Gravitational lensing by large-scale structure. *A&A*, 571:A17, November 2014.

[129] A. A. Starobinsky and J. Yokoyama. Density fluctuations in Brans-Dicke inflation. *ArXiv General Relativity and Quantum Cosmology e-prints*, February 1995.

[130] J. White, M. Minamitsuji, and M. Sasaki. Curvature perturbation in multi-field inflation with non-minimal coupling. *JCAP*, 7:039, July 2012.

[131] J.-O. Gong, J.-c. Hwang, W. I. Park, M. Sasaki, and Y.-S. Song. Conformal invariance of curvature perturbation. *JCAP*, 9:023, September 2011.

[132] A. Linde. Extended chaotic inflation and spatial variations of the gravitational constant. *Physics Letters B*, 238:160–165, April 1990.

[133] A. L. Berkin and K.-I. Maeda. Inflation in generalized Einstein theories. *PRD*, 44:1691–1704, September 1991.

[134] S. Tsujikawa and H. Yajima. New constraints on multifield inflation with nonminimal coupling. *PRD*, 62(12):123512, December 2000.

[135] M. Rossi. Dark energy as a scalar field non-minimally coupled to gravity. *Master Thesis*, 2017.